2015-09-03

Exploring the Role of FUS Mutants from Stress Granule Incorporation to Nucleopathy in Amyotrophic Lateral Sclerosis: A Dissertation

Hae Kyung Ko
University of Massachusetts Medical School

EXPLORING THE ROLE OF FUS MUTANTS FROM STRESS GRANULE INCORPORATION TO NUCLEOPATHY IN AMYOTROPHIC LATERAL SCLEROSIS

A Dissertation Presented

By

HAE KYUNG KO

Submitted to the Faculty of the

University of Massachusetts Graduate School of Biomedical Sciences, Worcester

in partial fulfillment of the requirements for the degree of

DOCTOR OF PHILOSOPHY

SEPTEMBER, 3, 2015

PROGRAM IN CELL AND DEVELOPMENTAL BIOLOGY

EXPLORING THE ROLE OF FUS MUTANTS FROM STRESS GRANULE INCORPORATION TO NUCLEOPATHY IN AMYOTROPHIC LATERAL SCLEROSIS

A Dissertation Presented By
HAE KYUNG KO

The signatures of the Dissertation Defense Committee signify completion and approval as to style and content of the Dissertation

---

Lawrence J. Hayward, MD, Ph.D., Thesis Advisor

Daryl A. Bosco, Ph.D., Member of Committee

Fen-Biao Gao, Ph.D., Member of Committee

Jeffrey A. Nickerson, Ph.D., Member of Committee

Benjamin Wolozin, MD, Ph.D., Member of Committee

The signature of the Chair of the Committee signifies that the written dissertation meets the requirements of the Dissertation Committee

---

Charles G. Sagerström, Ph.D., Chair of Committee

The signature of the Dean of the Graduate School of Biomedical Sciences signifies that the student has met all graduation requirements of the school.

Anthony Carruthers, Ph.D.,
Dean of the Graduate School of Biomedical Sciences

Department of Cell and Developmental Biology
September, 3, 2015

Acknowledgments

I would like to first thank my advisor, Dr. Lawrence Hayward for his support on my graduate study over the past years. His broad knowledge and huge literature searches not only in the ALS field but also in new science technology always inspired me and made my narrow view of science stretch into much larger scopes. I also give my sincere thanks my great committee members, Dr. Daryl Bosco, Dr. Fen-Biao Gao, Dr. Jeffrey Nickerson, and Dr. Charles Sagerstrom for their valuable suggestions and helpful discussions. I also thank Dr. Benjamin Wolozin for serving as part of my dissertation examination committee. Without all of their encouragement and guidance, I could not have achieved this accomplishment.

My special thanks is also given to Dr. Fumihiko Urano, Dr. David Weaver, and Dr. Kendall Knight for their friendly supports when I needed to find a new lab just after I transferred from University of Florida. I appreciate Dr. Anthony Imbalzano for his helpful suggestions and guidance throughout my graduate studies.

Thank you all in the Hayward lab, formal and current for their support on my project. Especially, thank you, Hongru for help mouse tissue preparation and immunostaining. You were always available whenever I needed your help in the lab. Thank you, Shuwen. I really enjoyed having you as a lab company, though it was just for one year.

I also thank Dr. Wolfe, Dr. Lawson, Ankit, Amy and Tom for their suggestions and help on the project for zinc finger nucleases, Jennifer for her suggestions on the photo-cross-linking project, and Dr. Lokireddy and Dr. Goldberg for analyzing proteasome activity assay for the PML-NB paper. What is more, I would like thank Dr. Robert H. Brown Jr. and all in the Brown lab for their suggestions and discussions during the Brown lab meeting beginning at 8 AM every Wednesdays. I also appreciate people in the Bosco lab, Gao lab, and Landers lab for sharing their reagents and equipments.

Thank you, my friends in Massachusetts, Florida, and Korea. Margaret Hampshire, Paster Kohl, Marta, Paster Soto, Lucy, and all church family for their love and prayers. Thank you, Ok Hyun and Ji Hae for friendship and encouragement-I will miss our chatting breaks over coffees. Thank you, Soo Jung for being a graduate study buddy at UF, and continuous friendship since then. Thank you, Hee Jung and Sun Hae. I really miss you all.

My husband, Young Seok Kim, deserves my special thanks. Whenever I needed to work in the lab at night time, he always gave me a ride and waited my work done, which made me feel safe. I would like to thank my family; parents, sister Yu Kyung and brother Seoung Il for their love, support, and dedication. Thank you, my little girl Lumi! Your smile and love make me happy all the time. I also thank my in-law family for their prayers. I know this moment would not be achieved without their love, encouragement, support, and prayers.

Finally, I would like to thank God for his guidance and encouragement all the time. I always keep his word in my mind, “Be strong and courageous. Do not be afraid; do not be discouraged, for the Lord your God will be with you wherever you go (Joshua 1:9)”. I tried to keep this word when I prepared the graduate school application. Obviously, I know his word will hold me tightly until my dissertation defense is complete. I am very excited to open the next door that he has already prepared for me. Thank you, Lord!

Abstract

Amyotrophic lateral sclerosis (ALS) is a progressive neurodegenerative disease characterized by preferential motor neuron death in the brain and spinal cord. The rapid disease progression results in death due to respiratory failure, typically within 3-5 years after disease onset. While ~90% of cases occur sporadically, remaining 10% of ALS cases show familial inheritance, and the number of genes linked to ALS has increased dramatically over the past decade.

FUS/TLS (Fused in Sarcoma/ Translocated to liposarcoma) is a nucleic acid binding protein that may regulate several cellular functions, including RNA splicing, transcription, DNA damage repair and microRNA biogenesis. More than 50 mutations in the FUS gene are linked to 4% of familial ALS, and many of these may disrupt the nuclear localization signal, leading to variable amounts of FUS accumulation in the cytoplasm. However, the mechanism by which FUS mutants cause motor neuron death is still unknown.

The studies presented in this dissertation focused on investigating the properties of FUS mutants in the absence and presence of stress conditions. We first examined how ALS-linked FUS mutants behaved in response to imposed stresses in both cell culture and zebrafish models of ALS. We found that FUS mutants were prone to accumulate in stress granules in proportion to their degree of cytoplasmic mislocalization under conditions of oxidative stress, ER stress, and heat shock.

However, many FUS missense mutants are retained predominantly in the nucleus, and this suggested the possibility that these mutants might also perturb one or more nuclear functions. In a human cell line expressing FUS variants and in human fibroblasts from an ALS patient, mutant FUS expression was associated with enlarged promyelocytic leukemia nuclear bodies (PML-NBs) under basal condition. Upon oxidative insult with arsenic trioxide (ATO), PML-NBs in control cells increased acutely in size and were turned over within 12-24 h, as expected. However, PML-NBs in FUS mutant cells did not progress through the expected turnover but instead continued to enlarge over 24 h. We also observed a persistent accumulation of the transcriptional repressor Daxx and the 11S proteasome regulator in association with these enlarged PML-NBs. Furthermore, the peptidase activities of the 26S proteasome were decreased in FUS mutant cells without any changes in the expression of proteasome subunits.

These results demonstrate that FUS mutant expression may alter cellular stress responses as manifested by (i) accumulation of mutant FUS into stress granules and (ii) inhibition of PML-NB dynamics. These findings suggest a novel nuclear pathology specific to mutant FUS expression that may perturb nuclear homeostasis and thereby contribute to ALS pathogenesis.

Table of Contents

List of Tables

List of Figures

List of Abbreviations

ALS: Amyotrophic lateral sclerosis (ALS)

ATO: Arsenic trioxide

CB: Cajal bodies

ER: Endoplasmic reticulum

fALS: familial ALS (fALS)

FTD: Frontotemporal Dementia

FUS/TLS: Fused in Sarcoma/Translocated in Liposarcoma

GEMs: Gemini of coiled bodies

HEK293: Human embryonic kidney 293

NLS: Nuclear localization signal

LMN: lower motor neuron

P-bodies: processing bodies

PML-NBs: Promyelocytic leukemia bodies

PBS: Phosphate-buffered saline

RFU: relative fluorescence unit

ROS: reactive oxygen species

sALS: sporadic ALS

SMA: spinal muscular atrophy

SMN: survival of motor neuron

snRNP: small nuclear ribonucleoprotein

SOD1: Cu/Zn superoxide dismutase 1

SUMO: small ubiquitin-like modifier

TDP-43: TAR DNA binding protein 43

UMN: Upper motor neuron

WT: wild type

Preface

Part of this dissertation is published as:

Mutant FUS proteins that cause amyotrophic lateral sclerosis incorporate into stress granules

Daryl A. Bosco, Nathan Lemay, Hae Kyung Ko, Hongru Zhou, Chris Burke, Thomas J. Kwiatkowski Jr, Peter Sapp, Diane McKenna-Yasek, Robert H. Brown Jr, and Lawrence J. Hayward

(2010) Human Molecular Genetics 19(21): 4160-4175.

Chapter I

Introduction to Amyotrophic Lateral Sclerosis

I.1 Amyotrophic Lateral Sclerosis

Amyotrophic lateral sclerosis (ALS) or motor neuron disease (MND) is a progressive neurodegenerative condition characterized by loss of motor neurons in the cerebral cortex, brainstem and spinal cord. The term ALS encompasses the pathological features of patients in that “amyotrophic” refers to the muscle atrophy caused by lower motor neuron degeneration and “lateral sclerosis” describes the fibrotic changes in the lateral columns of the spinal cord (Rowland and Shneider 2001). ALS was initially described by the French physician Jean-Marin Charcot in 1869, but we still do not understand the disease mechanisms underlying preferential degeneration of motor neurons. The mean age of onset is 55 years old but rare juvenile onset also occurs. ALS is classified as familial (fALS) and sporadic (sALS) forms. Ninety percent of ALS cases occur sporadically, and the remaining ten percent of ALS cases show familial inheritance that may be linked to specific gene mutations. Death occurs due to respiratory failure in most cases, typically within 3 to 5 years after symptom onset. At present, no treatment exists to significantly slow the course of this disease.

I.1.1 Epidemiology

ALS affects 2.16 individuals per 100,000 per year in the general European population (Logroscino, Traynor et al. 2010), and this rate is consistent with the study based on US population (McGuire, Longstreth et al. 1996). Males are affected more frequently than females (Logroscino, Traynor et al. 2010, Mehta, Antao et al. 2014). The

lifetime risk of ALS is 1:350 for men and 1:400 for women (Johnston, Stanton et al. 2006). Incidence rate gradually increases with advanced age, but it decreases considerably after the age of 80 years (Logroscino, Traynor et al. 2010).

The incidence rate in certain areas including Guam, Japan's Kii Peninsula, and western New Guinea is much higher (Gajdusek and Salazar 1982, Kuzuhara and Kokubo 2005). For instance, the incidence rate of Guam ALS was 7.5/100,000/year during the period of 1980-1989 (Okumura 2003). Several theories have been proposed to explain the high frequency of disease in this region. Khabazian *et al.* reported that this higher incidence rate is caused by exposure to neurotoxins such as sterol glucosides and β-methylamino-L-alanine (BMAA) (Khabazian, Bains et al. 2002), suggesting environmental risk factors may contribute to disease pathogenesis (Al-Chalabi and Hardiman 2013). In addition to cyanotoxins, proposed potential risk factors include smoking, exercise, football play, heavy metal and pesticides exposure, and armed services (Al-Chalabi and Hardiman 2013). According to the gene-time-environment (GTE) model, accumulated exposure to environmental risk factors is able to approach the threshold for disease, and certain types of mutations in genes can shorten the duration to reach the threshold (Al-Chalabi and Hardiman 2013).

I.1.2 Clinical phenotypes, diagnosis and treatment

ALS is the most common motor neuron disease and affects both upper and lower motor neurons in the spinal cord, brain stem, and cortex. Some individuals exhibit

restricted phenotypes involving either lower motor neuron (LMN) signs or upper motor neuron (UMN) signs only, and they are diagnosed with progressive spinal muscular atrophy or primary lateral sclerosis, respectively. The symptoms for LMN loss include fasciculation, cramps, and muscle atrophy, and those in UMN degeneration show spasticity and hyperreflexia (Gordon 2013). The signs of ALS usually begin in a single limb in about two-thirds of patients (limb-onset ALS) (Kiernan, Vucic et al. 2011). Bulbar-onset ALS, affecting ~25% of patients, causes difficulties in speaking and swallowing, and limb features are developed later (Kiernan, Vucic et al. 2011). With disease progression, most patients develop problems in swallowing and eating food.

There is no single biomarker for the diagnosis of ALS. Clinicians examine the combination of UMN and LMN signs developed in the same body region and identify subsequent evidence of disease progression to other regions (Kiernan, Vucic et al. 2011). The El Escorial diagnostic criteria were developed in 1994 for ALS diagnosis by the World Federation of Neurology for research and clinical trial purposes. This guideline line has been modified several times to improve sensitivity and diagnostic certainty (Miller, Munsat et al. 1999), but a 9-12 month delay usually occurs before clinicians are able to confirm diagnosis (Al-Chalabi and Hardiman 2013). As ALS progresses rapidly and the median survival of patients is about 2 to 3 years from symptom onset, it is critical to develop a marker to provide more rapid diagnosis so that appropriate therapies can be initiated earlier in the course.

No cure is yet available for ALS. Riluzole is the only drug shown to provide even a modest benefit of 2 to 3 months for survival (Miller, Mitchell et al. 2012). Riluzole exhibits anti-glutamatergic properties, which has been proposed to reduce excitotoxicity in ALS (Stevenson, Yates et al. 2009), but it may also affect other components such as sodium channels (Sierra Bello, Gonzalez et al. 2012). Its side effects can include diarrhea, fatigue, and dizziness. In the U.S, more than 50% of patients take this medicine (Gordon 2013).

I.2 Causative Genes and pathological Mechanisms

While most cases of ALS are sporadic, about 5 to 10 percent of ALS patients are affected by autosomal dominant inheritance. To date, more than 20 genetic loci have been identified accounting for most fALS and a small portion of sALS cases (Renton, Chio et al. 2014) (Table 1-1). Important cellular processes influenced by these gene products include vesicle trafficking, RNA metabolism, cytoskeletal dynamics, and protein degradation (Renton, Chio et al. 2014). Mutations in four major ALS genes, including superoxide dismutase 1 (*SOD1*), TAR DNA-binding protein (*TARDBP*), fused in sarcoma (*FUS*) and chromosome 9 open reading frame 72 (*C9ORF72)* account for over 50% of fALS cases (Rosen, Siddique et al. 1993, Sreedharan, Blair et al. 2008, Kwiatkowski, Bosco et al. 2009, DeJesus-Hernandez, Mackenzie et al. 2011, Renton, Majounie et al. 2011). Mutations in several other genes including ubiquilin2 (*UBQLN2*), profilin1 (*PFN1*), optineurin (*OPTN*), and valosin-containing protein (*VCP*) are also identified in

Subtype	Gene symbols	Gene name	Chromosome	Inheritance	Onset	Function
ALS1	*SOD1*	Superoxide dismuatse 1	21q22.1	Dominant	Adult	Enzyme
ALS2	*Alsin*	ALS2	2q33	Recessive	Juvenile	GEF signaling
ALS3	*unknown*	unknown	18q21	Dominant	Adult	unknown
ALS4	*SETX*	Senataxin	9q34	Dominant	Juvenile	RNA metabolism
ALS5	*SPAST*	Spatascin	15q15-q21	Recessive	Juvenile	unknown
ALS6	*FUS*	Fused in sarcoma	16p11	Dominant	Adult	RNA metabolism
ALS7	*unknown*	unknown	20p13	Dominant	Adult	unknown
ALS8	*VAPB*	VAMP (vesicle-associated membrane protein)-associated protein B and C	20q13.3	Dominant	Adult	Vesicle Tracfficking
ALS9	*ANG*	Angionenin	14q11.2	Dominant	Adult	Vascularization
ALS10	*TARDBP*	TAR DNA-binding protein	1p36.22	Dominant	Adult	RNA metabolism
ALS11	*FIG4*	FIG4 homologue	6q21	Dominant	Adult	Vesicle Tracfficking
ALS12	*OPTN*	Optineurin	10p13	Recessive	Adult	Vesicle Tracfficking
ALS13	*ATXN2*	Ataxin 2	12q23-q24.1	Dominant	Adult	RNA metabolism
ALS14	*VCP*	Valosin-contaning protein	9p13	Dominant	Adult	Vesicle Tracfficking
ALS15	*UBQLN2*	Ubiquilin 2	xp11.21	Dominant	Both	Protein degradation
ALS16	*SIGMAR1*	Sigma non-opioid intracelular receptor 1	9p13	Recessive	Juvenile	Calcium signaling
ALS18	*PFN1*	Profilin 1	17p13.3	Dominant	Adult	Cytoskeletal movement
ALS21	*MATR3*	Matrin 3	5q31.2	Dominant	Adult	RNA metabolism
ALS-FTD	*C9ORF72*	Chromosome 9 open reading frame 72	9p21.2	Dominant	Adult	unknown
ALS-FTD	*CHCHD10*	Coiled-coil-helix-coiled-coil-helix domain containing 10	22q11.23	Dominant	Adult	Oxidative phosphorylation
ALS-FTD	*TBK1*	TANK-binding kinase 1	12q14.2	Dominant	Adult	Protein degradation

Table 1-1 Causative genes identified in ALS

ALS but they are less prevalent (Johnson, Mandrioli et al. 2010, Maruyama, Morino et al. 2010, Deng, Chen et al. 2011, Wu, Fallini et al. 2012). Recently, new ALS genes are identified including matrin 3 (*MATR3*), coiled-coil-helix-coiled-coil-helix domain containing 10 (*CHCHD10*), and TANK-binding kinase 1 (*TBK1*) (Bannwarth, Ait-El-Mkadem et al. 2014, Johnson, Pioro et al. 2014, Cirulli, Lasseigne et al. 2015, Freischmidt, Wieland et al. 2015).

The dominant missense mutations in SOD1 were the first reported in 1993 following genetic linkage to chromosome 21q22.1 in 1993 (Rosen, Siddique et al. 1993). Over one hundred mutations have been found in SOD1, and they account for ~20 percent of fALS and ~3 percent of sALS (Andersen 2006). The most frequent variant of SOD1 mutations in North America is the A4V mutation (Cudkowicz, McKenna-Yasek et al. 1997). Individuals harboring SOD1-A4V have an aggressive course, and death can occur within a year after symptom onset (Cudkowicz, McKenna-Yasek et al. 1997). Transgenic mouse models expressing mutant SOD1 have been developed that have contributed the most insights regarding possible pathogenic mechanisms in ALS (McGoldrick, Joyce et al. 2013). Proposed mechanisms include misfolded mutant SOD1 aggregates, axonal transport defects, non-cell autonomous toxicity, impairment of the ubiquitin-proteasome system, and the disruption of mitochondria function.

The mutations in gene *TARDBP*, which encodes TAR DNA binding protein 43 (TDP-43) were identified in 2008 (Sreedharan, Blair et al. 2008). Initially, TDP-43 was identified as the major component of ubiquitin positive inclusions in frontotemporal lobar

degeneration (FTLD) (Neumann, Sampathu et al. 2006). The mutations in TDP-43 affect ~4 % of fALS and ~1% of sALS (Chio, Calvo et al. 2012). TDP-43 is composed of two RNA recognition motifs, a nuclear localization signal, a nuclear export signal and a C-terminal glycine-rich domain. While TDP-43 is expressed predominantly in the nucleus, it shuttles between the nucleus and cytoplasm (Ayala, Zago et al. 2008). More than 50 mutations of TDP-43 are identified, and most of them are clustered at the C-terminal glycine-rich regions that may serve as a low complexity or prion-like domain (Cushman, Johnson et al. 2010, Robberecht and Philips 2013). The normal function of TDP-43 is thought to regulate RNA splicing, trafficking, transcription, and miRNA biogenesis (Lee, Lee et al. 2012). Several pathological properties of TDP-43 have been discovered, including abnormal hyper-phosphorylation and ubiquitination of TDP-43, sarkosyl-insoluble TDP-43 inclusion, formation of the truncated 20-25 kDa TDP-43 C-terminal fragments (CTFs), translocation of TDP-43 into cytoplasm and lack of normal expressions in the nucleus (Lee, Lee et al. 2012).

The locus of FUS/TLS (fused in sarcoma/translocated in liposarcoma) was mapped on chromosome 16p11 from three independent studies analyzing European and North American pedigrees affected with autosomal dominant ALS (Abalkhail, Mitchell et al. 2003, Ruddy, Parton et al. 2003, Sapp, Hosler et al. 2003). Mutations in FUS were identified in 2009 by sequencing analysis of affected families (Kwiatkowski, Bosco et al. 2009, Vance, Rogelj et al. 2009). In common with TDP-43, FUS contains nucleic acid binding motifs and an intrinsically disordered region, but the two proteins are organized

differently. The discovery of the mutations in TDP-43 and FUS provided a rationale for considering altered RNA metabolism as a major contributor to motor neuron degeneration (Ling, Polymenidou et al. 2013). The pathological features include abnormal FUS-positive cytoplasmic inclusions in motor neurons of patients (Kwiatkowski, Bosco et al. 2009, Vance, Rogelj et al. 2009). Interestingly, these inclusions are TDP-43-negative (Kwiatkowski, Bosco et al. 2009, Vance, Rogelj et al. 2009). More than 50 mutations in FUS account for ~4% of fALS and ~1% of sALS (Deng, Gao et al. 2014). Most FUS mutations cluster within a nuclear localization signal (NLS) at the C-terminus, and these are thought be disrupt the NLS, which impairs transportin-1 mediated nuclear import of FUS (Dormann, Rodde et al. 2010). It is still unknown whether FUS causes motor neuron degeneration by a loss-of function mechanism, a toxic gain-of-function mechanism, or both.

A hexanucleotide repeat expansion $(GGGGCC)_n$ in C9ORF72 indicated that a large intronic repeat expansion could contribute to ALS (DeJesus-Hernandez, Mackenzie et al. 2011, Renton, Majounie et al. 2011). This expansion located in chromosome 9p21 may account for the majority of fALS (~40 percent) and ~25 percent of FTD, strongly supporting the concept of a pathological overlap between ALS and FTD (Majounie, Renton et al. 2012). The C9ORF72 repeat expansion may affect ~7 percent of sALS in people of European ancestry (Majounie, Renton et al. 2012). The normal function of this gene is unknown. The pathological length of the expanded repeats is still unclear, but several hundreds or thousands of repeats may contribute to disease (Robberecht and

Philips 2013). Pathological features include TDP-43-positive inclusions in the spinal cord, cortex, and hippocampus and TDP-43-negative but p62/SQSTM1-ubiquitin-positive inclusions in the hippocampus and cerebellum (Al-Sarraj, King et al. 2011, DeJesus-Hernandez, Mackenzie et al. 2011). In addition, the neuronal cells from the frontal cortex and spinal cord in patients with C9ORF72 mutations contain abnormal RNA foci (DeJesus-Hernandez, Mackenzie et al. 2011). Interestingly, though this gene with abnormal expansion does not contain an AUG start codon, it can direct the production of insoluble dipeptides (poly GA, poly GP, and poly GR) by repeat-associated non-ATG (RAN) translation. Therefore, at least three hypotheses have been proposed to explain the pathogenesis associated with C9ORF72 repeats: (1) C9ORF72 haploinsufficiency, (2) repeat-associated RNA toxicity, and (3) toxic RAN protein species (Ling, Polymenidou et al. 2013).

Clearly, ALS pathology is very complex. Several molecular mechanisms based on the nature of causative genes have been proposed, including oxidative stress, mitochondria dysfunction, excitotoxicity, protein aggregation, dysregulated endosomal trafficking, impaired axonal transport, neuroinflammation, and altered RNA metabolism (Ferraiuolo, Kirby et al. 2011).

I.3 ALS Links to Frontotemporal Dementia (FTD)

Frontotemporal dementia (FTD) or frontotemporal lobar degeneration (FTLD) is a progressive neuronal degeneration in the frontal and temporal cortices. It is the second

most common dementia after Alzheimer's disease and affected individuals change their personality and behavior with gradual defects in language skills (Van Langenhove, van der Zee et al. 2012). Mutations in genes encoding the microtubule-associated protein tau (*MAPT*) and progranulin (*PGRN*) account for 20% of FTD (Hutton, Lendon et al. 1998, Baker, Mackenzie et al. 2006). FTDs are classified pathologically based on the type of neuronal inclusions in the cortex (Lillo and Hodges 2009). TDP-43 has been found as the main component of the ubiquitin positive inclusions in the large portion of FTD patients and most ALS patients (Neumann, Sampathu et al. 2006). ~15% of FTD patients become affected with ALS and ~15% of ALS patients develop FTD with TDP-43 positive inclusions in cortical neurons (Ringholz, Appel et al. 2005, Lillo and Hodges 2009). These results suggest that ALS shares several clinical and pathological features with FTD. Supporting this notion, ALS-linked mutations in C9ORF72 genes are identified in FTD as well (DeJesus-Hernandez, Mackenzie et al. 2011).

In addition to TDP-43 inclusions in FTD, FUS-positive inclusions are also identified and account for ~9% of FTD (Ling, Polymenidou et al. 2013). In contrast to ALS-FUS, which is caused by mutations in FUS, cytoplasmic FUS in FTD harbors rare or no genetic alternation (Neumann, Rademakers et al. 2009, Van Langenhove, van der Zee et al. 2010). We still do not know how one protein contributes to the disease pathogenesis in both ALS and FTD.

I.4 Molecular Mechanisms of FUS

I.4.1 The normal function of FUS

FUS was initially identified as a component in human myxoid liposarcomas where the N-terminal portion of FUS fused with CCAAT enhancer-binding homologus protein (CHOP) as a consequence of a chromosome translocation t(12;16)(q13.3;p11.2) (Crozat, Aman et al. 1993). FUS is expressed ubiquitously in human tissues and cultured cell lines but is absent in cardiac muscle cells and melanocytes (Andersson, Stahlberg et al. 2008). FUS localizes predominately in the nucleus but also shuttles rapidly between nucleus and cytoplasm (Zinszner, Sok et al. 1997). FUS comprises several domains including a Q/G/S/Y-rich domain, RGG-rich regions, an RNA recognition motif (RRM), a zinc finger motif and a PY-type nuclear localization signal (PY-NLS) recognized by the nuclear import receptor, Transportin 1 (Figure 1). Both the QGSY-rich domain and glycine rich region (amino acids 1-239) have a disordered prion-like property that may facilitate the self-aggregation of FUS (Cushman, Johnson et al. 2010). With TAF15 (TATA-binding protein associated factor 15) and EWS (Ewing sarcoma protein), FUS belongs to the FET family. TAF15 and EWS have domain structures similar to FUS, and they are also associated with FTD and ALS (Law, Cann et al. 2006, Tan and Manley 2009, Mackenzie and Neumann 2012).

FUS binds RNA, single-stranded DNA with lower affinity, and double stranded DNA and regulates RNA biogenesis including splicing, transcription, and mRNA transport (reviewed in (Lagier-Tourenne, Polymenidou et al. 2010, Ling, Polymenidou et al. 2013)).

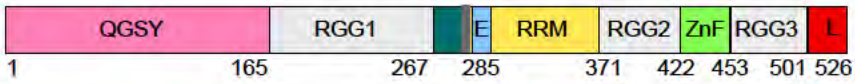

Figure 1 Domain structure of FUS

FUS contains several domains including a Gln-Gly-Ser-Tyr (QGSY)-rich region (pink), three Arg-Gly-Gly (RGG)-rich regions (grey), an RNA recognition motif (RRM; yellow), a zinc-finger motif (ZnF; green) and a PY-type of nuclear localization signal (L; red).

Transcription FUS was found in a complex of RNA polymerase II and its general transcription factor TFIID (Bertolotti, Melot et al. 1998). Later, FUS binding to the C-terminal domain of RNA polymerase II (RNAPII) is observed (Schwartz, Ebmeier et al. 2012). This interaction can prevent premature hyperphosphorylation of Ser2 at the C-terminal domain of RNAPII. Further analysis of this interaction demonstrated that FUS binding to RNA can serve as a seed that recruits RNA-free FUS to form a fibrous assembly, and RGG-Zn-RGG and prion-like domain of FUS can contribute to this assembly (Schwartz, Wang et al. 2013). While FUS promotes RNAPII transcription, FUS can inhibit RNAPIII transcription through direct interaction with the transcription factor TATA-binding protein (TBP) in HeLa cells (Tan and Manley 2010). In addition, FUS can regulate target gene transcription through binding on the specific single-stranded DNA sequences containing three copies of the TCCCCGT, AAAGTGTC, or AGGTTCTA located within their promotor regions (Tan, Riley et al. 2012).Transcriptions of cyclin D1 and Manganese superoxide dismutase (MnSOD) may be regulated by FUS (Wang, Arai et al. 2008, Dhar, Zhang et al. 2014). In addition, Ishigaki *et al.* found that binding FUS to antisense RNA strands at the promotor regions decreased transcription of the coding strand, indicating that FUS regulates both transcription and alternative splicing (Ishigaki, Masuda et al. 2012). Consistent with this finding, a recent study reveals that FUS should be present during the transcription reaction to effect splicing events through an interaction between RNAP II and U1 snRNP (Yu and Reed 2015).

Splicing Previously, FUS was identified in H complex as heterogeneous nuclear ribonucleoparticles (hnRNP) P2 (Calvio, Neubauer et al. 1995), and FUS immunoprecipitation experiment reveals that FUS interacts with splicing factors such as polypyrimidine tract-binding protein (PTB or hnRNPI), SRm160 and SR proteins (SC35 and SRp75) (Meissner, Lopato et al. 2003). This indicates that FUS plays a role in splicing and spliceosome assembly. More recently, FUS interaction with essential splicing factor U1 snRNP has been found in several studies (Sun, Ling et al. 2015, Yu, Chi et al. 2015, Yu and Reed 2015).

The CLIP-seq approaches have identified that FUS targets more than 5,500 RNAs in human brains and more than 6,800 in various cell lines (Ishigaki, Masuda et al. 2012, Lagier-Tourenne, Polymenidou et al. 2012, Orozco, Tahirovic et al. 2012, Rogelj, Easton et al. 2012). These RNAs have exceptionally long introns and multiple binding sites. FUS binding across the pre-mRNA displays a sawtooth-like pattern in both mouse and human brains because FUS is clustered at the beginning of long introns (>100kb) and decreases gradually toward the 3’ end (Lagier-Tourenne, Polymenidou et al. 2012, Rogelj, Easton et al. 2012). This binding pattern also implicates the role of FUS in the stabilization of nascent RNA during transcriptional elongation. FUS binding occurs with preference for a GUGGU motif (Lagier-Tourenne, Polymenidou et al. 2012).

The microtubule-associated protein Tau (MAPT) is reported as the first physiological splice target of FUS in neurons (Orozco, Tahirovic et al. 2012). In the mouse brain, FUS binds to Tau pre-mRNA directly, and the depletion of FUS in the rat hippocampal

neurons enhances the expression of Tau exons 3 and 10, which results in impaired cytoskeletal organization. Another study using high-throughput sequencing in mouse primary cortical neurons with FUS knockdown demonstrated that FUS mediated alternative splicing in genes such as *Mapt*, *Camk2a* and *Fmr1* (Ishigaki, Masuda et al. 2012).

The splicing targets of FUS also include the gene coding for RNA-binding proteins (RBP) in human brains and mouse neurons, and FUS regulates the splicing of these genes through binding to their highly conserved introns (Nakaya, Alexiou et al. 2013). Interestingly, the authors found that FUS bound to the two conserved introns between exon 6 and exon 8 of human and mouse FUS itself.

Previous studies showed that FUS prefers to bind to GGUG-containing RNA (Lerga, Hallier et al. 2001, Iko, Kodama et al. 2004) and the major RNA binding sites within FUS localize at the RGG2-ZnF-RGG3 domains (Iko, Kodama et al. 2004). Recent study revealed that FUS binding was targeted to the whole length of pre-mRNAs with limited sequence preference to GGU (Rogelj, Easton et al. 2012). Others found that FUS binds to RNA through AU-rich stem-loops (Hoell, Larsson et al. 2011).

All together, these studies support the idea that FUS regulates splicing on nascent transcripts and target RNAs contain long introns. Moreover, proteins translated from these target RNAs play an important role in neuronal development and synaptic maintenance. However, these studies couldn’t reveal a defined FUS binding motif.

RNA transport Although FUS expresses predominantly in the nucleus (Andersson, Stahlberg et al. 2008), FUS is able to shuttle between nucleus and cytoplasm (Zinszner, Sok et al. 1997). This property of FUS may contribute to RNA transport and local translation. For instance, FUS is able to translocate to dendritic spines through microtubules and actin filaments concomitant with increased RNA content in the spine of cultured hippocampal neurons (Fujii, Okabe et al. 2005). FUS depletion in hippocampal pyramidal neurons showed abnormal spine morphology and attenuated spine density. Furthermore, FUS mediates the transport of mRNA encoding an actin-stabilizing protein Nd1-L for its local translation in dendritic spines of mouse hippocampal neurons through the stimuli with the glutamate receptor mGluR5 (Fujii and Takumi 2005).

miRNA production FUS is found in the large Drosha complex with TDP-43 and can bind to Drosha and pri-miRNA such as pri-miR-9-2 and 15a (Gregory, Yan et al. 2004, Morlando, Dini Modigliani et al. 2012). While FUS mutants (R521C and P525L) do not alter Drosha binding, FUS depletion in neuronal cells alters the large class of miRNA expression including specific neuronal miRNA, which is critical for neuronal function, activity, and differentiation. This result suggests that insufficient FUS expression in nucleus by FUS mutants may participate in ALS pathogenies through the alternation of miRNA biogenies.

DNA damage response FUS is initially identified as a target of ATM (ataxia-telangiectasia mutated) which catalyses FUS phosphorylation at Ser^{42} when cells are exposed to ionizing radiation (IR) to cause DNA double-strand break (Gardiner, Toth et

al. 2008). The rapid recruitment of FUS to the sites of laser-induced DNA double-strand breaks is mediated by the poly (ADP-ribose) polymerase (PARP), and the prion-like domain of FUS promotes accumulation at sites of DNA damage (Mastrocola, Kim et al. 2013, Rulten, Rotheray et al. 2014). In addition, the interaction between FUS and histone deacetylase 1 (HDAC1) in response to DNA damage is discovered, and this complex could work for DNA repair in neurons (Wang, Pan et al. 2013). The authors found that cultured motor neurons expressing ALS-linked FUS mutants R244C, R514S, H1517Q, and R521C fail to recruit FUS at the site of DNA damage as well as diminish FUS interaction with HDAC1. Moreover, motor cortex tissues from ALS patients expressing FUS-R521C or P525L exhibit increased γH2AX positive staining that indicates increased DNA damage, suggesting ALS with FUS mutants has deficits in DNA repair (Wang, Pan et al. 2013).

I.4.2 FUS animal models of ALS

I.4.2.1 Rodent model

Before the discovery of ALS-linked mutations in FUS, two FUS knockout mouse lines were generated. FUS null mice having inbred C57BL/6 background died within 16 hours after birth because of chromosome instability and abnormal lymphocyte development suggesting FUS may play a critical role in genome maintenance (Hicks, Singh et al. 2000). Another FUS knockout mouse model was generated from an outbred background (CD1 with 129/SvEv) and showed male sterility and enhanced sensitivity to

irradiation (Kuroda, Sok et al. 2000). However, these mouse models were not examined for defects in motor function. Recently, FUS knockout outbred homozygous mice were generated using a mixed background of B6 and ICR strains to analyze motor phenotypes (Kino, Washizu et al. 2015). Surprisingly, FUS knockout did not develop ALS-like symptoms. Instead of motor neuron degeneration, FUS knockout mice developed vacuolation in the hippocampus and exhibited hyperactivity and reduced anxiety-related behaviors, suggesting that the phenotype of FUS knockout is more like FTLD.

To investigate the toxic gain of FUS function, several transgenic rodent lines expressing FUS variants have been developed. So far, two rat and six mouse models expressing either FUS-WT, mutants (R521C, R521G, or R495X), or truncated forms (1-359 or 1-478) have been generated (Table 1-2). The detailed information about these transgenic models will be discussed below.

The first transgenic rat models expressing human FUS-WT and FUS-R521C were generated in 2011 (Huang, Tong et al. 2012). Overexpression of FUS-R521C in rats resulted in progressive paralysis with loss of neurons in cortex and hippocampus. These affected neurons contained ubiquitin aggregates. However, these rats did not develop obvious motor phenotypes. Over expression of FUS-WT also induced neuron death at one year of age and showed a deficit in learning and memory more indicative of an FTLD-like phenotype.

Table 1-2 Summary for FUS rodent models. Y, yes; N, no; -, not addressed.

Reference	Species	Promotor	Type of FUS	Protein expression (fold)	Symptom onset	Life span	Motor impairment	Motor neuron loss	Muscle atrophy	NMJ denervation	Neuro-inflammation	Inclusion	Findings
Huang et al., PLoS Genet, 2011	Rat	TRE	h-FUS-WT	-	12 months	-	N	N	N	N	N	Ubiquitin	cognitive dysfunction, neuronal loss in frontal cortex
			h-FUS-R521C	-	5 weeks	6 weeks	Y	N	Y	Y	Yes in the brain and spinal cord	Ubiquitin	-
Verbeeck et al., Mol Neurodegener. 2012	Mouse	Cloned into AAV-1 vector	V5-hFUS-WT	-	-	-	N	N	-	-	N	N	-
			V5-hFUS-R521C	-	-	-	N	N	-	-	N	N	-
			V5-hFUS	-	-	-	N	N	-	-	N	FUS/ Ubiquitin	-
Mitchell et al., Acta Neuropathol. 2013	Mouse	mouse prion	HA-hFUS-WT (+/+)	1 9	1 month	10-13 weeks	Gait impairment Limb paralysis	~60%	Y	Y	in the spinal cord	FUS	-
Shelkovnikova et al., JBC, 2013	Mouse	Thy-1	Truncated form of hFUS 1-359 (Hemizygous)	Lower than the levels of endogenous mouse FUS	2.5-4.5 months	2 weeks after onset < 5 months	Gait impairment Limb paralysis	~50% loss in the spinal cord	Y	Y	In anterior horns of the spinal cord	FUS	sequestration of endogenous FUS in aggregates of FUS 1-359
Qiu et al, JCI, 2014	Mouse	Syrian hamster prion	Flag-tagged R521C	similar to the level of endogenous mouse FUS	-	4-6 weeks after onset	abnormal gaits, motor coordination problems	~55% loss at the age of 1-3 months	-	Y	In anterior horns of the spinal cord	-	mutant interact with normal FUS/Bdnf splicing defect/signs for DNA damage/RNA Seq/splicing defect
Sephton et al,, PNAS, 2014	mouse	cyto megalovirus immediate early enhancer-chicken β-actin hybrid (CAG)	R521G	similar to the level of endogenous mouse FUS	10-14 days	early lethality before 30 days	Y	N	less severe	Y	yes, In the brain and spinal cord	N	decreased the number and density of mature spines
			R521G-escaped early lethality	similar to the level of endogenous mouse FUS	2 month	30% survived at 300 days	Y	N	-	-	N	-	changes in social interactions altered dendritic branching in spinal cord a reduction in the number and density of mature spines
Tibshirani et al, HMG 2015 (mice from Hayward lab)	Mouse	mouse prion	WT	<2	-	-	N	-	-	-	-		nuclear PRMT1 localization
			R495X	3-5	8-12 month	-	N	-	-	-	-	-	abnormal cytoplamic PRMT1 localization

The first transgenic mouse lines expressing HA-tagged human FUS-WT were generated by the Shaw group, and both hemizygous and homozygous mouse lines were examined (Mitchell, McGoldrick et al. 2013). While hemizygous mice (expression level 1.6x control) showed no motor pathology, homozygous transgenic mice (expression level 1.9x control) developed motor neuron degeneration with globular and skein-like-FUS and ubiquitin-negative inclusions in motor neurons. Somatic brain transgenic (SBT) mice were generated by bilateral intracerebroventricular injection of recombinant adeno-associated virus (rAAV) expressing V5-tagged human FUS-wild type, R521C, or p.G466VfsX14 (FUS$\triangle_{14}$) (Verbeeck, Deng et al. 2012). Mice expressing the FUS$\triangle_{14}$ mutant exhibit neuronal cytoplasmic inclusions recognized by antibodies to ubiquitin, p62, α-internexin, and the poly-adenylate(A)-binding protein 1 (PABP-1) at 3 months of age. Despite FUS$\triangle_{14}$ mice harboring ubiquitin positive FUS inclusions, this mouse line did not develop a motor phenotype or degeneration. In 2013, FUS transgenic mice expressing a truncated human FUS construct, which contains only the region of 1-359 amino acid, lacking nuclear localization signals and major RNA binding motifs, were generated and displayed severe motor phenotypes with FUS cytoplasmic aggregation (Shelkovnikova, Peters et al. 2013). These mice developed motor neuron degeneration at the age of 2.5 to 4.5 months, and death occurred within several days after onset, indicating that FUS aggregation in neurons may be sufficient to cause ALS-like phenotypes. The other transgenic mouse model expressing FUS-R521C exhibited evidence of DNA damage in cortical and spinal motor neurons as well as dendritic and

synaptic defects in the spinal motor neurons (Qiu, Lee et al. 2014). The authors observed that an interaction between HDAC1 and endogenous FUS was diminished in the FUS-R521C mice. Furthermore, FUS-521C mice displayed splicing defects in 5' noncoding exons of the brain-derived neurotrophic factor (Bdnf) gene and impaired transportation of Bdnf mRNA into distal dendrites. Recently, transgenic mouse models expressing either FUS-WT or FUS-R521G showed severe motor defects with neuroinflammation, denervated neuromuscular junctions, and premature death (Sephton, Tang et al. 2014). However, the disease onset in these mouse models was 10 to 14 days old, and there was no control for global EGFP over expression in these models. Interestingly, the R521G mouse that escaped from early lethality exhibits defects in motor function and social interactions. Although these mouse models do not show the pathological features including FUS mislocalization, aggregation and motor neuron loss, the FUS-R521G mouse exhibits a reduction of dendritic branches and mature spines suggesting that the FUS mutant might disrupt synaptic homeostasis through a toxic gain of function (Sephton, Tang et al. 2014).

I.4.2.2 Other animal models

In addition to rodent models, zebrafish (Danio reio), *Caenorhabditis elegans*, and *Drosophila melanogaster* have been used to investigate the pathological role of FUS in ALS. The zebrafish (Danio rerio) has several advantages for the study of human disease because of its genetic homology to mammals, external fertilization, large egg production,

rapid development, and transparency of embryo. It has been used widely in biomedical research, including ALS (Patten, Armstrong et al. 2014). The knockdown of endogenous FUS or over expression of mutant FUS (R521H) showed abnormal motor phenotypes including swimming defects, axon shortening, and abnormal branchings (Kabashi, Bercier et al. 2011, Armstrong and Drapeau 2013). These results suggest that both gain and loss of FUS function are involved in motor neuron degeneration. Consistent with this finding, the overexpression or loss of the Drosophila homologue Cabeza (Caz) exhibits motor neuron degeneration, neuromuscular junction disruption, reduced viability, and shortened lifespan (Sasayama, Shimamura et al. 2012, Xia, Liu et al. 2012). Furthermore, FUS mutant expressions in C. *elegant* causes progressive motor dysfunction and reduced lifespan by a dominant gain-of-function (Murakami, Yang et al. 2012). Taken together, these animal models suggest loss of FUS function and gain-of-toxicity may act together to participate in FUS mediated pathology.

I.4.3 The pathological role of FUS in ALS

All FUS mutations reported to date are dominant except for one recessive mutation, H517Q, found in the index Cape Verdian family (Kwiatkowski, Bosco et al. 2009). Most FUS mutations localize within the PY-NLS region and may affect translocation into the cytoplasm upon disruption of the interaction with Transportin 1 (Bosco, Lemay et al. 2010, Dormann, Rodde et al. 2010, Ito, Seki et al. 2011, Kino, Washizu et al. 2011). The most aggressive FUS mutations, such as P525L and R495X, contain disrupted nuclear

localization signals, localize mostly to the cytoplasm, and cause juvenile onset with short survival of 1 to 2 years (Baumer, Hilton et al. 2010, Huang, Zhang et al. 2010). Motor neurons from these patients contain basophilic inclusions, whereas individuals harboring FUS-R521C mutations show tangle-like cytoplasmic inclusions in both neurons and glial cells (Baumer, Hilton et al. 2010, Huang, Zhang et al. 2010, Mackenzie, Ansorge et al. 2011). While several roles of FUS in altered stress responses, protein aggregate formation, and altered RNA metabolism have been proposed, we still do not fully understand which molecular mechanisms are most relevant to motor neuron toxicity in mutant FUS mediated ALS.

I.4.3.1 Stress granules

Upon stress exposure, eukaryotic cells stall translation and form cytoplasmic RNA-protein complexes, referred to as ribonucleoprotein (RNP) granules, including processing bodies (P-bodies) and stress granules (Anderson and Kedersha 2008, Buchan and Parker 2009). Stress granules are dynamic structures and may protect cells from insults with oxidative stress, heat shock, or glucose deprivation by conserving energy and producing the essential proteins for survival and recovery (Kedersha, Ivanov et al. 2013).

Initial findings showed that oxidative stress induced localization of endogeneous or GFP-tagged FUS to stress granules in HeLa cells (Andersson, Stahlberg et al. 2008). Later, mutant TDP-43 associated with ALS is accumulated into stress granules following oxidative stress (Colombrita, Zennaro et al. 2009). This result suggests that impaired

stress responses may contribute to ALS pathogenesis. Therefore, we investigated cellular localizations of FUS variants under stress conditions in a cell culture and zebrafish model of ALS (in chapter II). Further discussion related to stress granules in ALS pathogenesis appears in chapter IV.

I.4.3.2 Altered RNA metabolism and Gem loss

CLIP/exon array with depletion of FUS expression revealed that FUS deficiency altered the levels or splicing of target mRNAs, suggesting that insufficient expression of FUS in the nucleus by ALS-linked FUS mutants may participate in pathological effects through alteration on RNA metabolism (Lagier-Tourenne, Polymenidou et al. 2012, Rogelj, Easton et al. 2012, Ling, Polymenidou et al. 2013). For instance, the depletion of FUS expression in human neurons derived from stem cells or mouse brain decreases the expression of *Csma1*, *Nrxn3*, *Nlgnl*, *Smyd3* and *Kenip4*, which are essential for axonogenesis, cytoskeleton organization, and synaptic formation and function (Lagier-Tourenne, Polymenidou et al. 2012).

FUS mutants are found to accumulate the essential components for splicing in cytoplasmic aggregates and reduce their activity (Gerbino, Carri et al. 2013, Sun, Ling et al. 2015, Yu, Chi et al. 2015). Patient fibroblasts harboring FUS mutant R514G or R521C show the mislocalization of U1 snRNP, such as SmB and U1 snRNA in cytoplasm (Yu, Chi et al. 2015). Moreover, SmB showed co-localization with cytosolic FUS mutants. Knockdown of U1 snRNP such as U1-70K or U1 in zebrafish showed motor neuron

defect, indicating that U1 snRNP is important to motor neuron homeostasis. In addition, Sun *et al*. found that snRNA levels are changed in ALS patient fibroblasts harboring FUS mutants, and reduced interaction with U1-70K and Sm-B/D are also observed in HeLa cells expressing GFP tagged FUS-R495X or P525L (Sun, Ling et al. 2015). There results indicate that FUS play an important role for splicing regulation in HeLa cells and patient fibroblasts. The RNA-mediated oligonucleotide annealing, selection, and ligation with next-generation sequencing (RASL-seq) analysis in ALS patient fibroblasts with R521G, H517Q, and M511Nfs*6 (△NLS) mutations in FUS revealed altered splicing events compared to fibroblasts from three control individuals. FUS mutant fibroblasts showed 57 splicing events had an increased long isoform and 53 splicing events had an enhanced short isoform. These changes in snRNPs result in loss of Gems, one of subnuclear organelles, supporting the notion that defects in RNA metabolism and Gem assembly may contribute to motor neuron death in ALS.

In addition to Gems, expression of FUS mutants has been reported to alter the assembly of other nuclear bodies including speckles and paraspeckles (Nishimoto, Nakagawa et al. 2013, Shelkovnikova, Robinson et al. 2014, Takanashi and Yamaguchi 2014). Therefore, the roles of nuclear bodies and possible toxic effects of FUS mutants on nuclear body assembly will be discussed in the following section.

I.5 Possible toxic effects of FUS on nuclear bodies

Mammalian cell nuclei contain several subnuclear organelles including nucleoli, nuclear speckles and paraspeckles, Cajal bodies, nuclear Gems, histone locus bodies, and promyelocytic leukemia bodies (PML-NBs) (Mao, Zhang et al. 2011). These nuclear bodies are membrane-less and highly dynamic. Dysfunction of these assemblies has been linked to conditions including neurodegenerative diseases and cancers (Zimber, Nguyen et al. 2004, Woulfe 2008, de The, Le Bras et al. 2012) (Table 1-3).

Nucleolus The Nucleolus is assembled around the cluster of tandemly repeated ribosomal DNA genes and plays a role in ribosomal RNA synthesis and nascent ribosome assembly (Pederson 2011). These events occur in three distinct subnucleolar compartments termed the fibrillar center (FC), dense fibrillar component (DFC) and granular component (GC) (Boulon, Westman et al. 2010). The FCs contain rDNA and transcription factor UBF. The transcription by RNA Pol I machinery produces pre-rRNA, 45S rRNA. This event occurs either in the FCs or at the border between the FC and the DFC. The DFC contains pre-rRNA processing factors including the small nucleolar ribonucleoproteins (snoRNP), and fibrillarin. The GC encloses the FC and the DFC and works for pre-ribosome subunit assembly. In addition to the role in rRNA biogenesis, the nucleolus also regulates cellular stress responses. Under stress conditions including transcription inhibition, viral infection, or DNA damage, nucleolus re-organizes its structure and protein composition (Boulon, Westman et al. 2010). A recent proteome database for human nucleolus reveals that more than 4,500 proteins can accumulate in nucleolus transiently or persistently (Ahmad, Boisvert et al. 2009).

Name	Number per cell	Size (μm)	Components	Proposed Functions	Findings in ALS research
Nucleolus	1-4	0.5-8.0	Fibrillarin,Nucleolin, B23/NPM	rRNA biogenesis	Toxic dipeptides (GR and PR) accumulation in ALS-C9ORF72
Speckles	20-50	0.8-1.8	SC35, Malat1	storage/assembly/modification of pre-mRNA splicing factors	Decreased the number of poly (A) foci in ALS-FUS
Paraspeckles	5-20	0.5	PSP1, PSF, p54nrb/ NONO	nuclear retention of adenosine to inosine hyperedited mRNAs	FUS interacts with p54nrb Cytoplasmic p54nrb inclusions in ALS-FUS
Cajal bodies/Gems	0-10	0.1-2.0	p80 coilin/SMN	assembly and trafficking of snRNP and snoRNP	Gem loss in ALS-FUS and ALS-TDP43
PML-NB	1-30	0.3-1.0	PML, Daxx, Sp100	cellular stress response, nuclear protein quality control	PML-positive intranuclear inclusion

Table 1-3 Nuclear bodies

Nucleolar dysfunction is found in ALS (Hetman and Pietrzak 2012). The polymers of arginine-rich dipeptides (GR and PR) translated from the ALS associated gene C9ORF72 repeat expansion, translocate to the nucleus, and accumulate in the nucleolus causing deficits in rRNA biogenesis, concomitant with cell death (Kwon, Xiang et al. 2014).

Speckles Nuclear speckles or SC35 domains are enriched with components for pre-mRNA splicing and locate in the inter chromatin regions of the nucleoplasm (Spector and Lamond 2011). Pre-mRNA splicing factors include small nuclear ribonucleoproteins (snRNPs) and serine-arginine rich (SR) proteins. SR proteins contain the arginine/serine-rich dipeptide domain (RS domain) and the RNA-recognition motif. In addition to pre-mRNA splicing factors, several RNAs including metastasis-associated lung adenocarcinoma transport 1 (MALAT1) long non-conding RNA, and a population of poly(A)$^+$ RNAs also accumulate in nuclear speckles. Transcription inhibition either by the drug treatment or as the result of heat shock exposure increases the size of speckles concomitant with accumulation of splicing factors indicating that nuclear speckles may regulate storage, assembly, and modification of splicing factors (Spector and Lamond 2011). In SH-SY5Y cells expressing FUS mutants poly (A) mRNA and SMN1 are sequestered in the cytoplasm and decreased the number of nuclear speckles (Takanashi and Yamaguchi 2014).

Paraspeckles Paraspeckles were recently discovered in 2002 and are distinct from nuclear speckles, although they are located adjacent to speckles in the inter chromatin space (Fox, Lam et al. 2002). Only mammalian cells contain typically 10 to 20

paraspeckles that are formed by the complex of the RNA-protein structure. The paraspeckle proteins include PSF/SFPQ, P54NRB/NONO, and PSPC1 (paraspeckle protein 1), which are the members of the DBHS (Drosophila melanogaster Behavior, Human Splicing) family. These proteins along with a long nuclear non-coding RNA (lncRNA) NEAT1 (also known as Men ε/β), can form paraspeckles (Fox and Lamond 2010). Paraspeckles may control gene expression through the nuclear retention of adenosine to inosine hyperedited mRNAs harboring double stranded RNA regions. HeLa cells treated with Actinomycin D (1 μg/ml) to inhibit RNA Pol transcription show that paraspeckles move to the perinucleolar cap region with other RNA Pol factors suggesting paraspeckles are involved in the cellular stress response (Fox and Lamond 2010).

While the level of NEAT1 is low in the nervous tissues and paraspeckles are absent in neurons under basal condition, NEAT1_2 lncRNA levels in the patient spinal motor neurons are up-regulated abnormally during the early stage of ALS (Nishimoto, Nakagawa et al. 2013). Moreover, FUS is identified as an essential component of paraspeckles through binding to either NEAT1_2 long non-coding RNA or p54nrb/ NONO (Nishimoto, Nakagawa et al. 2013, Shelkovnikova, Robinson et al. 2014). FUS is also able to regulate NEAT1 levels and participate in paraspeckle formation (Shelkovnikova, Robinson et al. 2014). Cytoplasmic FUS inclusion accumulates other paraspeckle proteins such as p54nrb/NONO, PSP1, and PSF in cultured cells. Consistent with cell culture results, p54nrb/NONO positive inclusions are found in motor neurons of

ALS patient harboring FUS mutations, suggesting that a disruption of paraspeckle assembly may contribute to ALS pathogenesis.

Cajal Bodies Cajal bodies (CBs) were first described by the Spanish neurobiologist Santiago Ramon y Cajal in 1903 (Lafarga, Casafont et al. 2009). While coilin/p80 is the common CB component, the uridine-rich small nuclear RNA (U1, U2, U4, U5 and U6) and associated proteins are also found in CBs (Nizami, Deryusheva et al. 2010). The role of CBs has been proposed as the site for the assembly and modification of small nuclear ribonucleoprotein (snRNPs) and snoRNPs. The newly assembled snRNPs in cytoplasm are imported back to the nucleus and concentrated first in CBs. Later maturated snRNPs are translocated to nuclear speckles prior to the localization into the active genes for participating in pre-mRNA splicing. In addition, CBs may regulate telomerase RNP assembly and telomere length homeostasis (Mao, Zhang et al. 2011).

GEMs Gemini of coiled bodies (GEMs) concentrated with survival of motor neuron (SMN) is similar in size to CBs and often localize near CBs (Liu and Dreyfuss 1996). In primary neurons and in *Drosophila*, SMN is colocalized with coilin. Gems normally contain survival motor neuron (SMN) protein and serve functions related to snRNP assembly and RNA splicing (Liu and Dreyfuss 1996, Pellizzoni, Kataoka et al. 1998). The disruption of GEM formation is the pathological hallmark of spinal muscular atrophy (SMA), the childhood onset of motor neuron degenerative disease (Pellizzoni, Kataoka et al. 1998). The reduced expression levels of SMN can causes Gem depletion. The change in GEM numbers and the reduction of SMN expression are also observed in ALS cases,

suggesting the link between SMA and ALS. For instance, reduced GEM numbers is found in both HeLa cells with TDP-43 knockdown and spinal motor neurons in ALS patients harboring TDP-43 mutation (Ishihara, Ariizumi et al. 2013). Moreover, FUS mutant expression in cellular models and human fibroblasts mediated a reduction in Gem formation (Yamazaki, Chen et al. 2012). Gem loss is also associated with a decrease in the number of Cajal bodies and a concomitant increase in PML body number in SMA motor neurons (Tapia, Bengoechea et al. 2012), further supporting a role for nuclear bodies in motor neuron homeostasis and survival.

PML-NBs Promyelocytic leukemia bodies (PML-NBs) were first described in the early 1960s as the presence of dense spherical objects in the nucleus by electron microscopy (Lallemand-Breitenbach and de The 2010). Later, in 1991, the characterization of these nuclear bodies is initially observed and named nuclear dot protein 55 (NDP-55) (Ascoli and Maul 1991). PML-NBs form discrete nuclear foci 0.2-1.0 μm wide and present in most mammalian cells (Bernardi and Pandolfi 2007). The main component of PML-NB is PML protein. PML (also called RNF71 or TRIM19) is a member of the tripartite motif (TRIM) protein family characterized by structural elements including a RING (Really Interacting New Gene) finger, two B box zinc fingers, and a coiled-coil domain (RBCC motif). This RBCC motif contributes to self-dimerization to form PML-NBs and mediates the binding of PML to the SUMO E2 ligase UBC9 (de The, Le Bras et al. 2012). The proposed role of PML-NBs includes DNA damage response (Dellaire, Ching et al. 2006), apoptosis (Takahashi, Lallemand-Breitenbach et al. 2004,

Bernardi, Papa et al. 2008), cellular senescence (Vernier, Bourdeau et al. 2011), gene transcription (Block, Eskiw et al. 2006), and anti-viral response (Everett and Chelbi-Alix 2007). Recently, PML-NBs are reported to regulate nuclear protein quality control and oxidative stress response (Guo, Giasson et al. 2014, Sahin, de The et al. 2014, Sahin, Ferhi et al. 2014).

PML-NBs have been shown in the nervous system to influence neurodevelopment and synaptic plasticity under normal conditions (Regad, Bellodi et al. 2009, Butler, Martinez et al. 2013, Korb and Finkbeiner 2013). In several neurodegenerative conditions, PML is found in neuronal intranuclear inclusions in affected brain tissues (Woulfe 2008). Interestingly, intranuclear inclusions in some ALS patient tissues show immunoreactivity to PML that could be associated with ALS pathogenesis (Seilhean, Takahashi et al. 2004).

Mutant FUS expressions are reported to perturb the assembly of nuclear bodies including nuclear Gems (Yamazaki, Chen et al. 2012, Groen, Fumoto et al. 2013, Sun, Ling et al. 2015). The loss of nuclear Gems is the pathological hallmark in spinal muscular atrophy, a childhood-onset motor neuron disease (Pellizzoni, Kataoka et al. 1998). Interestingly, Gem loss may also be associated with a decrease in the number of Cajal bodies and accompanying increase in PML body number in SMA motor neurons (Tapia, Bengoechea et al. 2012). Collectively, these observations provide evidence that PML-NBs may play a role in motor neuron survival and homeostasis. However, the dynamic of PML-NBs has not been addressed in the condition of ALS.

In this thesis, I investigated the role of FUS mutants under stress conditions in cell culture and zebrafish models of ALS. Mutant FUS with a disrupted nuclear localization signal mislocalized to the cytoplasm and accumulated into stress granules in a proportion to FUS expressions in the cytoplasm under the condition of oxidative stress and heat shock. However, many FUS mutants are retained predominantly in the nucleus. This observation guided us to investigate nuclear perturbation of subnuclear bodies caused by FUS mutants, which had not previously been explored. PML-NBs play a role in nuclear protein quality control and nuclear stress responses. A human cell line (HEK293) expressing FUS mutants (R495X, R521G or P525L) and human fibroblasts from an ALS patient harboring FUS-R521G mutation showed impaired PML-NB dynamics under oxidative stress conditions, providing novel evidence that mutant FUS may contribute to ALS pathogenesis by gain-of-toxicity in the nucleus.

Chapter II:

Mutant FUS proteins that cause amyotrophic lateral sclerosis incorporate into stress granules

II.1 Preface

This work is published as:

Mutant FUS proteins that cause amyotrophic lateral sclerosis incorporate into stress granules

Daryl A. Bosco, Nathan Lemay, Hae Kyung Ko, Hongru Zhou, Chris Burke, Thomas J. Kwiatkowski Jr, Peter Sapp, Diane McKenna-Yasek, Robert H. Brown Jr, and Lawrence J. Hayward
(2010) Human Molecular Genetics 19(21): 4160-4175.

I performed all of the described zebrafish work including microinjection, immunostaining, confocal image acquisition.

All figures including supplemental figures were subsequently renumbered to incorporated to this chapter.

II.2 Abstract

Mutations in the RNA-binding protein FUS (fused in sarcoma) are linked to amyotrophic lateral sclerosis (ALS), but the mechanism by which these mutants cause motor neuron degeneration is not known. We report a novel ALS truncation mutant (R495X) that leads to a relatively severe ALS clinical phenotype compared with FUS missense mutations. Expression of R495X FUS, which abrogates a putative nuclear localization signal at the C-terminus of FUS, in HEK-293 cells and in the zebrafish spinal cord caused a striking cytoplasmic accumulation of the protein to a greater extent than that observed for recessive (H517Q) and dominant (R521G) missense mutants. Furthermore, in response to oxidative stress or heat shock conditions in cultures and in vivo, the ALS-linked FUS mutants, but not wild-type FUS, assembled into perinuclear stress granules in proportion to their cytoplasmic expression levels. These findings demonstrate a potential link between FUS mutations and cellular pathways involved in stress responses that may be relevant to altered motor neuron homeostasis in ALS.

II.3 Introduction

Amyotrophic lateral sclerosis (ALS) is a devastating neurodegenerative condition that kills motor neurons in the brain and spinal cord, causing progressive weakness and death within 3-5 years. Although 90% of cases occur sporadically, mechanistic insights relating specific gene defects to motor neuron death have been obtained by identifying familial ALS genes and observing the consequences of their expression in cellular and animal models (Dion, Daoud et al. 2009). The critical sequence of events leading to ALS is not known, but recurring themes in its pathogenesis include: (i) excitotoxicity, (ii) impaired intracellular transport, (iii) mitochondrial dysfunction and (iv) protein misfolding and aggregation. Since 2006, altered RNA-binding proteins or their mislocalization have been implicated in the pathogenesis of both familial ALS (fALS) and sporadic ALS (sALS) (Lemmens, Moore et al. 2010, van Blitterswijk and Landers 2010). The initial discovery of the RNA-binding protein TDP-43 (TAR DNA binding protein-43) as a major constituent of neuronal inclusions in sALS (Neumann, Sampathu et al. 2006, Wang, Wu et al. 2008) was followed by the identification of mutations in the TARDBP gene that encodes TDP-43 in a subset of both fALS and sALS cases (Kabashi, Valdmanis et al. 2008, Sreedharan, Blair et al. 2008). Since 2009, specific mutations in the gene that encodes the RNA-binding protein FUS were linked to fALS (Belzil, Valdmanis et al. 2009, Chio, Restagno et al. 2009, Kwiatkowski, Bosco et al. 2009, Ticozzi, Silani et al. 2009, Vance, Rogelj et al. 2009, Blair, Williams et al. 2010, Corrado, Del Bo et al. 2010, Damme, Goris et al. 2010) and also implicated in sALS (Belzil,

Valdmanis et al. 2009, Corrado, Del Bo et al. 2010, DeJesus-Hernandez, Kocerha et al. 2010, Lai, Abramzon et al. 2011). Both FUS and TDP-43 share related structural elements, suggesting that they function in roles linked to RNA processing or regulation (Lagier-Tourenne and Cleveland 2009, Lemmens, Moore et al. 2010). TDP-43 and FUS mutations each are associated with ~5% of fALS cases, which indicates that abnormalities in these two genes collectively approach the 10-20% prevalence of variants in Cu/Zn superoxide dismutase (SOD1) among individuals with fALS (Lemmens, Moore et al. 2010).

FUS (fused in sarcoma) was originally named TLS (translocated in liposarcoma) upon the discovery of a chromosomal translocation event in myxoid liposarcoma that produced a potent oncoprotein comprising amino acid residues 1-266 of FUS/TLS (encoded by exons 1-7) fused at its C-terminus to the transcription factor CHOP (Crozat, Aman et al. 1993, Rabbitts, Forster et al. 1993). The 526-residue full-length FUS/TLS (Crozat, Aman et al. 1993) was subsequently identified as the heterogeneous nuclear ribonucleoprotein (hnRNP) P2 (Calvio, Neubauer et al. 1995) and found to be expressed in both neuronal and non-neuronal tissues with a predominantly nuclear localization (Morohoshi, Arai et al. 1996, Andersson, Stahlberg et al. 2008). However, a redistribution of FUS into the cytoplasm has been observed in response to transcriptional inhibition (Zinszner, Albalat et al. 1994), and FUS also shuttles rapidly between the nucleus and cytoplasm for the transport of mRNA (Zinszner, Sok et al. 1997).

FUS is a member of the TET family of proteins (Law, Cann et al. 2006, Tan and Manley 2009), which, in addition to TLS/FUS, also includes EWS (Ewing's sarcoma) and TAF15 (TATA-binding protein-associated factor 15), which are thought to have originated from a common ancestral gene (Morohoshi, Ootsuka et al. 1998). These three proteins all share an amino terminus enriched in Ser, Tyr, Gln, and Gly residues, a conserved RNA-recognition domain, a zinc finger motif, and RGG-rich regions that may be important for RNA binding. The domain structure of FUS (Figure 2-1A) includes an N-terminal domain with transcriptional activating properties and a C-terminal domain capable of binding DNA, RNA, and splicing factors (Law, Cann et al. 2006), consistent with putative functions of FUS in DNA damage-repair, transcription, and splicing (Kuroda, Sok et al. 2000, Meissner, Lopato et al. 2003, Wang, Arai et al. 2008). The highly conserved C-terminus also harbors most of the reported fALS-linked FUS mutations (Belzil, Valdmanis et al. 2009, Chio, Restagno et al. 2009, Kwiatkowski, Bosco et al. 2009, Ticozzi, Silani et al. 2009, Vance, Rogelj et al. 2009, Blair, Williams et al. 2010, Corrado, Del Bo et al. 2010, Damme, Goris et al. 2010), which cluster within residues 514-525 (Figure 2-1A). One identified consequence of FUS mutations is an aberrant accumulation of FUS in the cytoplasm of motor neurons and glia in human post-mortem tissues (Kwiatkowski, Bosco et al. 2009, Vance, Rogelj et al. 2009), which has been recapitulated following acute expression of FUS mutants in mammalian cells (Kwiatkowski, Bosco et al. 2009, Vance, Rogelj et al. 2009, DeJesus-Hernandez, Kocerha et al. 2010). FUS immunoreactivity has been detected in the cytoplasmic and nuclear

aggregates that are a pathological hallmark in subtypes of frontotemporal lobar degeneration (Neumann, Rademakers et al. 2009, Neumann, Roeber et al. 2009), including conditions with overlapping motor neuron disease pathology (Munoz, Neumann et al. 2009). Nuclear aggregates characteristic of polyglutamine diseases also contain FUS (Neumann, Roeber et al. 2009, Doi, Koyano et al. 2010). Taken together, these initial clues suggest that altered FUS properties or its cytoplasmic mislocalization may play a causative role in neurodegeneration, but the cellular mechanism(s) most relevant to FUS aggregation and fALS pathogenesis have not been elucidated.

TDP-43 was recently shown to accumulate in cytoplasmic stress granules following oxidative stress (Colombrita, Zennaro et al. 2009). Stress granules are one type of intracellular aggregate that contains non-translating polyadenylated mRNAs, translation initiation factors, small ribosome subunits, and RNA-binding proteins (Buchan and Parker 2009). The dynamic formation of stress granules in response to insults such as oxidative stress, heat shock, or ischemia is thought to protect cells by allowing them to shift energy expenditure from translation towards repair and recovery (Anderson and Kedersha 2008). That TDP-43 associates with stress granules raises the possibility that motor neuron vulnerability in ALS could be related in part to impaired adaptation to certain cellular stresses.

Here, we investigated the effect of ALS-causing mutations in the C-terminus of FUS on the subcellular mislocalization of the protein, and also investigated whether specific stresses relevant to ALS may trigger the formation of cytoplamsic FUS inclusions. Upon

expressing FUS variants in both stable cell lines and zebrafish embryos, we observed a striking cytoplasmic accumulation of FUS for a novel C-terminal truncation mutation, R495X, that exhibits a relatively severe fALS clinical phenotype. Furthermore, we found that mutant FUS, but not the wild type protein, assembles into stress granules in response to translational arrest induced by either oxidative stress or heat shock.

II.4 Results

II.4.1 Cytoplasmic accumulation of FUS variants

The coding sequence of FUS (Figure 2-1A) contains a putative nuclear localization signal (NLS) spanning residues Pro508-Tyr526 at the C-terminus (Lee, Cansizoglu et al. 2006, Zakaryan and Gehring 2006), which differs from other known 'classical' NLS sequences (Sorokin, Kim et al. 2007). This region of FUS overlaps with the clustering of 11 fALS-linked missense mutations (Belzil, Valdmanis et al. 2009, Chio, Restagno et al. 2009, Kwiatkowski, Bosco et al. 2009, Ticozzi, Silani et al. 2009, Vance, Rogelj et al. 2009, Blair, Williams et al. 2010, Corrado, Del Bo et al. 2010, Damme, Goris et al. 2010), some of which lead to increased cytoplasmic localization of FUS in human central nervous system tissue or upon overexpression in mammalian cell cultures (Kwiatkowski, Bosco et al. 2009, Vance, Rogelj et al. 2009, DeJesus-Hernandez, Kocerha et al. 2010).

Here, we identified a family (FALS521) with early-onset ALS caused by a novel mutation (R495X) that segregated with ALS. The R495X mutation causes the truncation of the final 32 amino acids from the C-terminus of FUS (Figure 2-1A). Disease onset varied widely within FALS521, although in this pedigree the onset occurred earlier in later generations (16 and 18 years in generation V). The mean age of onset for affected individuals in this pedigree was 35 ± 16 years, with an average survival of 16.4 ± 10 months from disease onset. This disease course was relatively more severe than that described for the index F577 (autosomal recessive H517Q mutation) and F55 (autosomal dominant R521G mutation) pedigrees, which are associated, respectively, with onset ages

of 45 ± 4 and 40 ± 13 years, and disease durations of 168 and 27 ± 17 months (Kwiatkowski, Bosco et al. 2009). The R495X truncation mutant shares a common feature with the recently reported de novo FUS splice-acceptor site mutation (G466VfsX14), namely, removal of the C-terminal NLS. The G466VfsX14 mutation skips the inclusion of exon 14, produces a frameshift of exon 15 and thereby adds an aberrant tail of 13 amino acids at the C-terminus in place of the normal residues encoded by exons 14 and 15 in WT FUS. This mutation is also associated with an early onset age (20 years) and a short disease course (death within 2 years) for the single individual reported to date (DeJesus-Hernandez, Kocerha et al. 2010).

To establish whether an altered C-terminus perturbs FUS localization when expressed at near-endogenous levels, we engineered stable HEK-293 cell lines that express doxycycline-inducible GFP-tagged FUS constructs, including wild type (WT) FUS, mutants associated with autosomal recessive (H517Q) and dominant (R521G) fALS, and two truncation constructs (R495X and G515X). FUS R495X represents the aforementioned early-onset fALS mutant, while G515X is an experimental mutant that was engineered to remove only the C-terminal 12 amino acids encoded by exon 15, which includes the main cluster of ALS mutants (Figure 2-1A) .

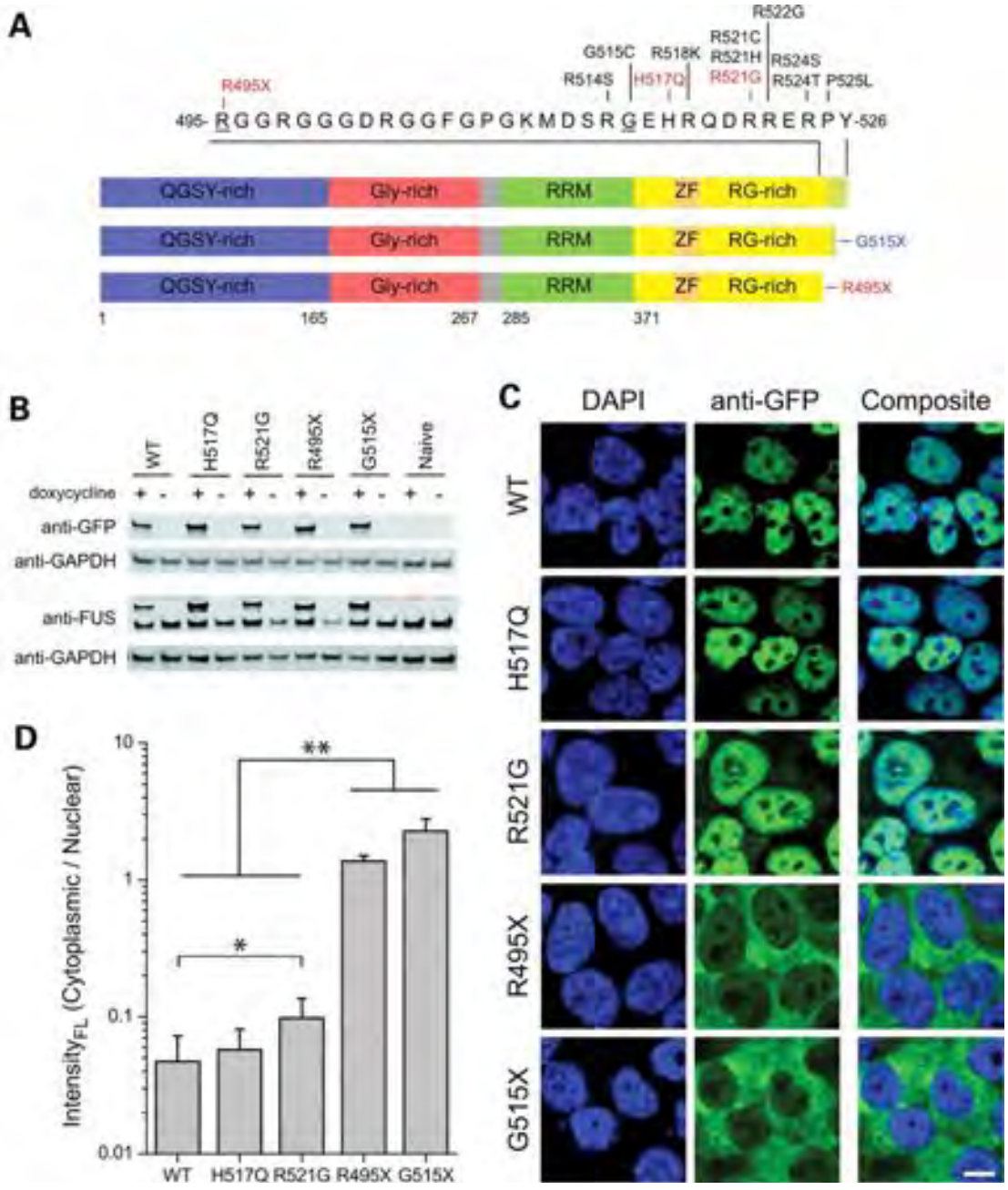

Figure 2-1 Domain structure of FUS and expression of normal and mutant FUS in HEK-293 cell lines.

Figure 2-1 Domain structure of FUS and expression of normal and mutant FUS in HEK-293 cell lines.

(A) The functional domains of FUS (www.uniprot.org) include a Gln-Gly-Ser-Tyr (QGSY)-rich region (blue), a Gly-rich domain (red), an RNA recognition motif (RRM; green), an Arg-Gly (RG)-rich region (yellow), which contains a RanBP2-type zinc finger domain (ZF; orange) and a putative NLS (light green). Labeled are fALS-linked mutants within exons 14 and 15, with those investigated here (R495X, H517Q and R521G) highlighted in red. Truncated FUS constructs of this study included an ALS-linked mutant (R495X) and an experimental mutant (G515X, blue), which removed the sequence encoded by exon 15. These residues are underlined in the primary sequence. **(B)** GFP-FUS stable lines and naïve HEK-293 cells were cultured with (+) or without (−) doxycycline for 40 h, and lysates containing 3 μg total protein/lane were analyzed by western blot using anti-GFP, anti-FUS and anti-GAPDH (loading control) antibodies. **(C)** Confocal microscopy of HEK-293 cell lines following induction with doxycycline for 40 h and staining with the nuclear dye DAPI (blue) and an anti-GFP antibody. A strong cytoplasmic GFP-FUS signal was observed for the R495X and G515X mutants with a truncated NLS, whereas GFP-FUS(WT, R521G and H517Q) exhibited a predominately nuclear localization. Scale bar, 10 μm. **(D)** Quantitative analysis of GFP fluorescence from live cells (see Materials and Methods) showed that the ratio of cytoplasmic:nuclear GFP fluorescence intensity was significantly higher for GFP-FUS(R521) compared with GFP-FUS(WT), and for the truncation mutants GFP-FUS(R495X and G515X) compared with the other GFP-FUS proteins (WT, R521G and H517Q). Asterisks indicate statistically significant differences between cell lines (n = 11–28 cells analyzed per line) as determined by the Kruskal–Wallis ANOVA followed by a Dunn's multiple comparison test (*$P < 0.05$, **$P < 0.01$).

Western blot analysis using an antibody to GFP confirmed that all GFP-FUS proteins were expressed in these cells lines at similar levels to each other upon induction with doxycycline for 40 h, although GFP-FUS proteins were not detected in the absence of doxycycline (Figure 2-1B). An anti-FUS antibody (see Materials and Methods) also showed that induced GFP-FUS proteins were expressed at near-endogenous levels (within 1–2-fold), and that the expression of these exogenous proteins did not greatly alter endogenous FUS expression levels (Figure 2-1B). Although this anti-FUS antibody recognized all GFP-FUS constructs, we observed in earlier experiments that an anti-FUS antibody targeted to the N-terminus (residues 1–50) unexpectedly did not efficiently detect the two C-terminal truncation mutants. Although the explanation for this differential antibody reactivity among the FUS constructs is unclear, it suggests that an absence of the normal C-terminus can influence the N-terminal epitope recognized by certain anti-FUS antibodies.

Confocal microscopy of these HEK-293 cells immunostained for GFP revealed an intense nuclear expression for WT, H517Q and R521G GFP-FUS, with additional weak cytoplasmic expression of the R521G mutant (Figure 2-1C). In contrast, the R495X and G515X truncation mutants exhibited a dramatic shift in the expression from the nucleus to the cytoplasm. The abnormal partitioning of GFP-FUS mutants remained stable during the period of 24–72 h after induction, and GFP-FUS expression at these levels through a continuous exposure to doxycycline was not associated with any overt change in cellular morphology, proliferation or viability for up to 6 days, the latter being measured by

trypan blue staining [$P > 0.05$ for the comparison of GFP-FUS (WT, R521G and R495X) and host HEK-293 cells by ANOVA; data not shown]. Furthermore, live-cell imaging indicated a similar pattern of GFP-FUS fluorescence and also revealed numerous highly mobile cytoplasmic granules upon the expression of the G515X and R495X truncation mutants. Quantitative measurements of GFP fluorescence intensity in live cells showed that the cytoplasmic:nuclear expression ratio per unit volume was significantly increased by 2-fold for GFP-R521G, by 29-fold for GFP-R495X and by 48-fold for GFP-G515X in comparison with that for GFP-WT FUS (Figure 2-1D). We hypothesized that a higher expression level following acute transfection may be an important determinant of the subcellular localization and aggregation propensity for FUS mutants. Indeed, transient transfection of GFP-FUS constructs into host HEK-293 cells yielded ~5-fold higher expression for all five GFP-FUS proteins compared to doxycycline-induced levels in the stable HEK-293 cell lines. In contrast to the faint, diffuse cytoplasmic expression pattern of GFP-FUS(R521G) in the inducible HEK-293 cells (Figure 2-1C), a 40 h transient transfection of this same construct into HEK-293 cells resulted in prominent cytoplasmic aggregates (Figure 2-2). Furthermore, the size of cytoplasmic inclusions containing GFP-FUS (R495X or G515X) was larger in the acutely transfected cells compared to the stable lines. However, transient transfection of GFP-FUS (WT or H517Q) constructs maintained a predominately nuclear localization (Figure 2-2), despite their elevated expression levels. These results are consistent with the previous reports of aggregate formation upon expression of Arg521 FUS mutants by acute transfection in both neuronal and non-

neuronal cell lines (Kwiatkowski, Bosco et al. 2009, Vance, Rogelj et al. 2009). These results show that i) the C-terminus of FUS plays a functional role in its nuclear localization and ii) an increase in the absolute level of FUS cytoplasmic expression likely contributes to its aggregation.

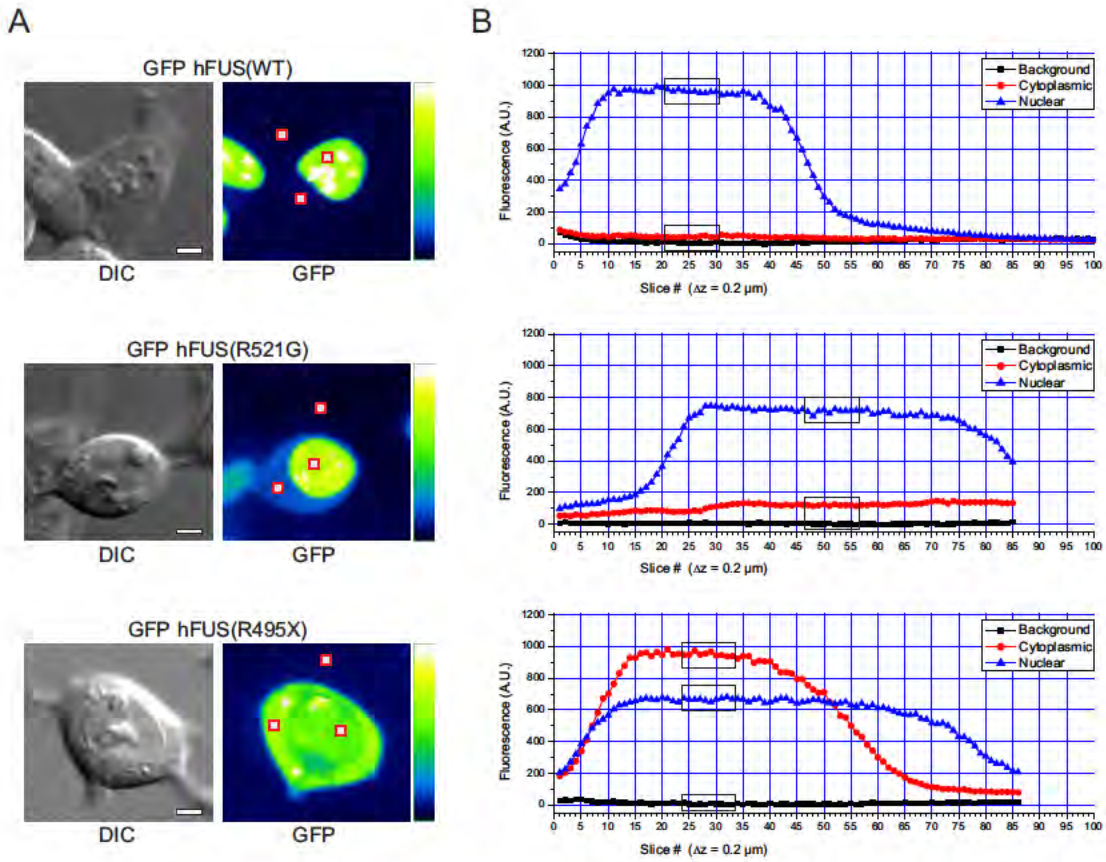

Figure 2-2 The expression level of GFP-FUS proteins are dependent upon the mode of transfection.

(A) GFP-FUS constructs were transiently transfected into empty HEK-293 cells for 40 h as desribed previously {Kwiatkowski, 2009 #1}, and HEK-293 cells stably expressing GFP-FUS proteins were induced with doxycycline for 40 h, after which cell lysates were prepared (Methods). Immunoblotting of these lysates (3 µg total protein/ lane) with anti-GFP and anti-GAPDH (loading standard) antibodies followed by a densitometry analysis revealed that transiently transfected cells express GFP-FUS at ~5-fold higher levels compared to the stable lines. **(B)** Fluorescence microscopy of the transiently transfected GFP-FUS HEK-293 cells described in (A) revealed prominent GFP-FUS cytoplasmic aggregates (green) for GFP-FUS(R521G, R495X, and G515X), whereas GFP-FUS(WT and H517Q) exhibited a relatively diffuse expression pattern in the nucleus (DAPI; blue). Scale bar, 10 µm.

We hypothesized that a higher expression level following acute transfection may be an important determinant of the subcellular localization and aggregation propensity for FUS mutants. Indeed, transient transfection of GFP-FUS constructs into host HEK-293 cells yielded ~5-fold higher expression for all five GFP-FUS proteins compared with doxycycline-induced levels in the stable HEK-293 cell lines (Figure 2-3). In contrast to the faint, diffuse cytoplasmic expression pattern of GFP-FUS(R521G) in the inducible HEK-293 cells (Figure 2-1C), a 40 h transient transfection of this same construct into HEK-293 cells resulted in prominent cytoplasmic aggregates (Figure 2-3). Furthermore, the size of cytoplasmic aggregates containing GFP-FUS(R495X or G515X) was larger in the acutely transfected cells compared with the stable lines. However, transient transfection of GFP-FUS(WT or H517Q) constructs maintained a predominately nuclear localization (Figure 2-3), despite their elevated expression levels. These results are consistent with the previous reports of aggregate formation upon expression of Arg521 FUS mutants by acute transfection in both neuronal and non-neuronal cell lines (Kwiatkowski, Bosco et al. 2009, Vance, Rogelj et al. 2009). Thus, our results here show that (i) the C-terminus of FUS plays a functional role in its nuclear localization, and (ii) an increase in the absolute level of FUS cytoplasmic expression likely contributes to its aggregation.

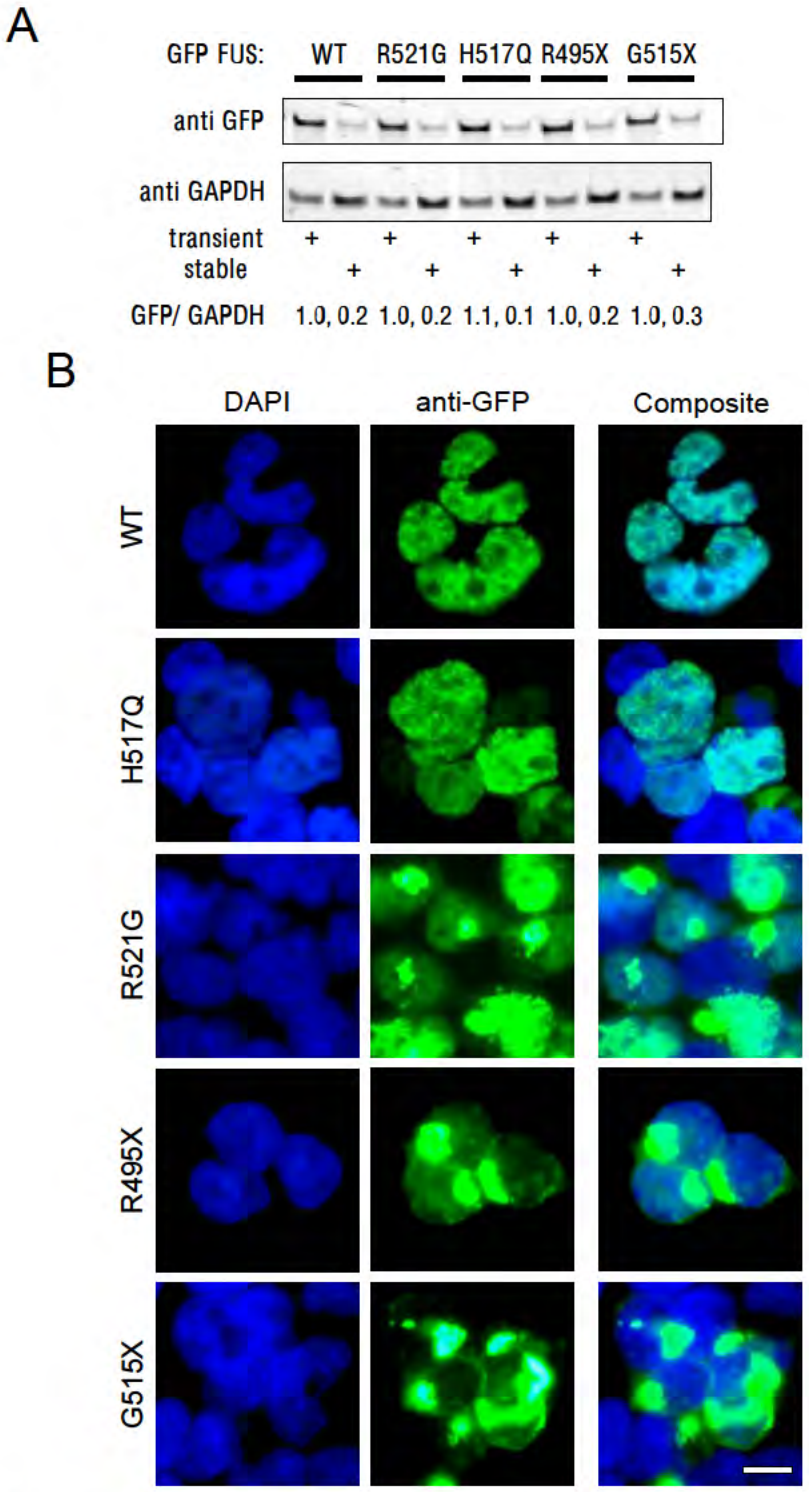

Figure 2-3 Transient transfection of GFP-FUS constructs into HEK-293 cells yields increased expression levels compared to indued cell lines.

Figure 2-3 Transient transfection of GFP-FUS constructs into HEK-293 cells yields increased expression levels compared to indued cell lines.

(A) GFP-FUS constructs were acutely transfected into naive HEK-293 cells for 40 h, and stable HEK-293 cells were induced to express the GFP-FUS proteins with doxycycline for 40 h, after which cell lysates were prepared (Methods). Immnoblotting of these lysates (3 μg total protein/ lane) with anti-GFP and anti-GAPDH (loading standard) antibodies followed by a densitometry analysis revealed that transiently transfected cells express GFP-FUS at ~5 fold higher levels compared to the stable lines. **(B)** Fluorescence microscopy of the transiently transfected GFP-FUS HEK-293 cells described in **(A)** revealed prominent GFP-FUS cytoplasmic aggregates (green) for GFP-FUS(R521G, R495X, and G515X), whereas GFP-FUS(WT and H517Q) exhibited a relatively diffuse expression pattern in the nucleus (DAPI; blue). Scale bar, 10 μm.

II.4.2 Cytoplasmic FUS mutants incorporate reversibly into stress granules in vitro

Given that the ALS-linked mutants affect the subcellular localization and aggregation propensity of FUS, we hypothesized that mutant FUS proteins may also exhibit an altered response to conditions of cellular stress compared to WT FUS. Markers of increased oxidative stress are a consistent finding in brain and spinal cord tissues from individuals with ALS (Ferrante, Browne et al. 1997, Barber, Mead et al. 2006). To investigate the response of FUS to oxidative stress, we exposed HEK-293 cells expressing GFP-FUS variants to 0.5 mM sodium arsenite for 1 h, which increases intracellular ROS (Lii, Lin et al. 2011) and is known to induce the formation of stress granules (Thomas, Martinez Tosar et al. 2009). Immunofluorescence with the anti-TIAR stress granule marker revealed that >95% of cells for each of the HEK-293 lines produced stress granules upon exposure to arsenite (Figure 2-4). This was consistent with observations under this condition in other cell types (Kedersha and Anderson 2007) and showed that the acute formation of stress granules was not compromised by the expression of fALS-linked FUS mutants. Moreover, the cytoplasmic versus nuclear partitioning of GFP-FUS proteins observed in untreated HEK-293 cells was not altered by arsenite exposure (compare Figures 2-1 and 2-4).

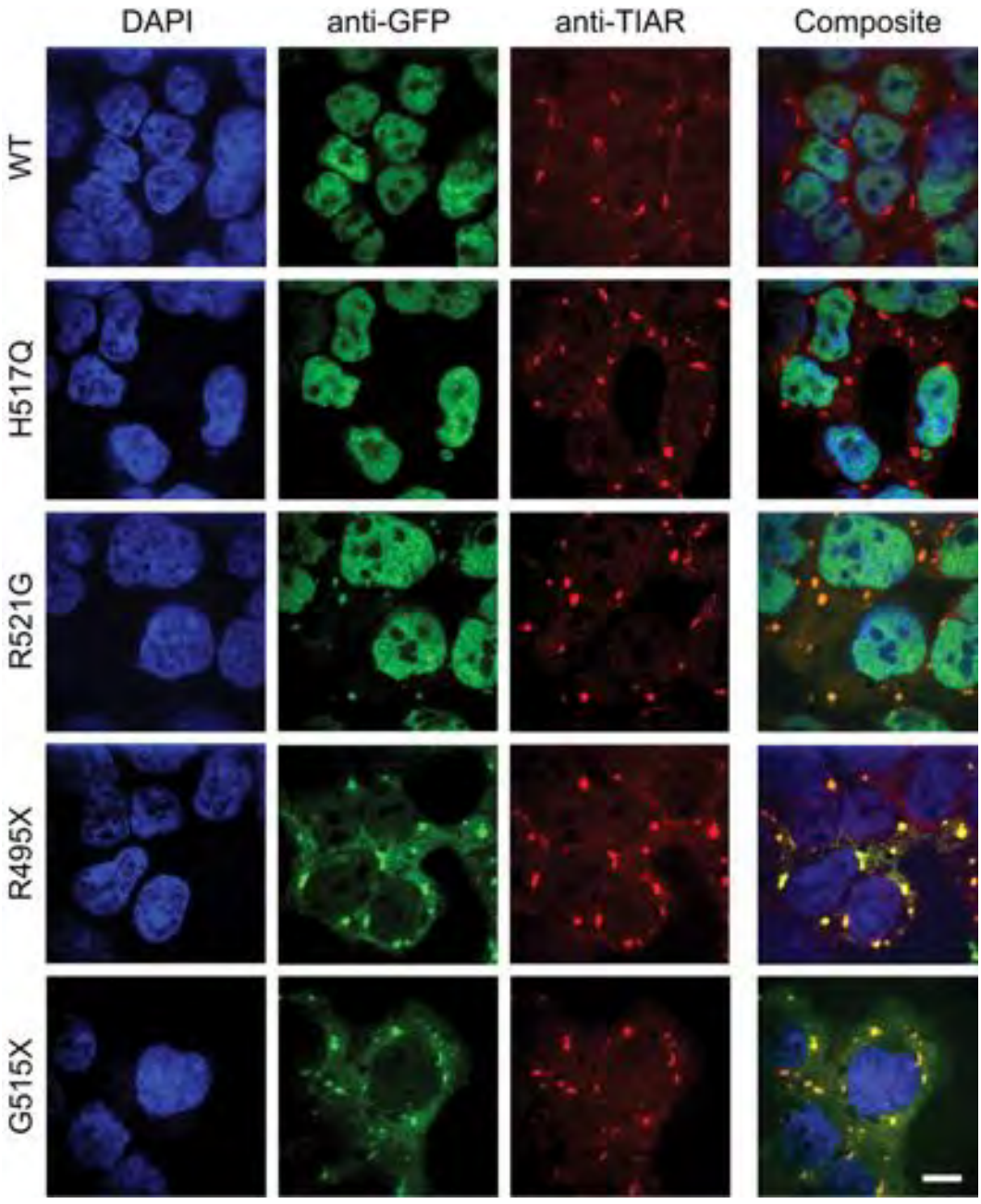

Figure 2-4 Incorporation of mutant FUS into stress granules in HEK-293 cells.

Each GFP-FUS HEK-293 stable cell line was induced with doxycycline for 40 h, treated with 0.5 mM sodium arsenite for 1 h, and then probed with anti-GFP (green) and anti-TIAR (red) antibodies, and the nuclear dye DAPI (blue). Cytoplasmic aggregates containing GFP-FUS were detected with anti-GFP for the R521G, R495X and G5151X lines, but not for the WT and H517Q lines. Composite images indicate that the accumulated GFP-FUS(R521G, R495X and G515X) co-localized with the TIAR stress granule marker. Scale bar, 10 μm.

A striking effect of arsenite treatment was that GFP-FUS mutants (R521G, R495X and G515X) were incorporated into the stress granules, as visualized by the co-localization of GFP with the TIAR (Figure 2-4) and G3BP (Figure 2-5A) stress granule markers. The majority (~70-80%) of TIAR-positive stress granules co-localized with the R495X and G515X mutants, while ~30% of stress granules co-localized with R521G. In contrast, <10% of stress granules co-localized with H517Q and WT FUS proteins under these conditions. We observed similar patterns of mutany FUS incorporation into stress granules when cells were treated with 10 mM thapsigargin for 2 h (Figure 2-5B), which also induces stress granules (Loschi, Leishman et al. 2009). Thapsigargin is a selective inhibitor of the endoplasmic reticulum (ER) Ca^{2+}-ATPase that induces ER stress, possibly related to depletion of intracellular Ca^{2+} stores (Yoshida, Monji et al. 2006). There were no overt signs of toxicity associated with the incorporation of mutant FUS into stress granules. Moreover, the viability as measured by the MTT cell proliferation assay following arsenite treatment for up to 4 h did not differ ($P > 0.05$ by ANOVA) among naïve cells or those expressing GFP-FUS(WT, R521G and R495X) (Figure 2-5C). These FUS cell lines also exhibited a similar capability to recover from sodium arsenite exposure ($P > 0.05$; Figure 2-5D).

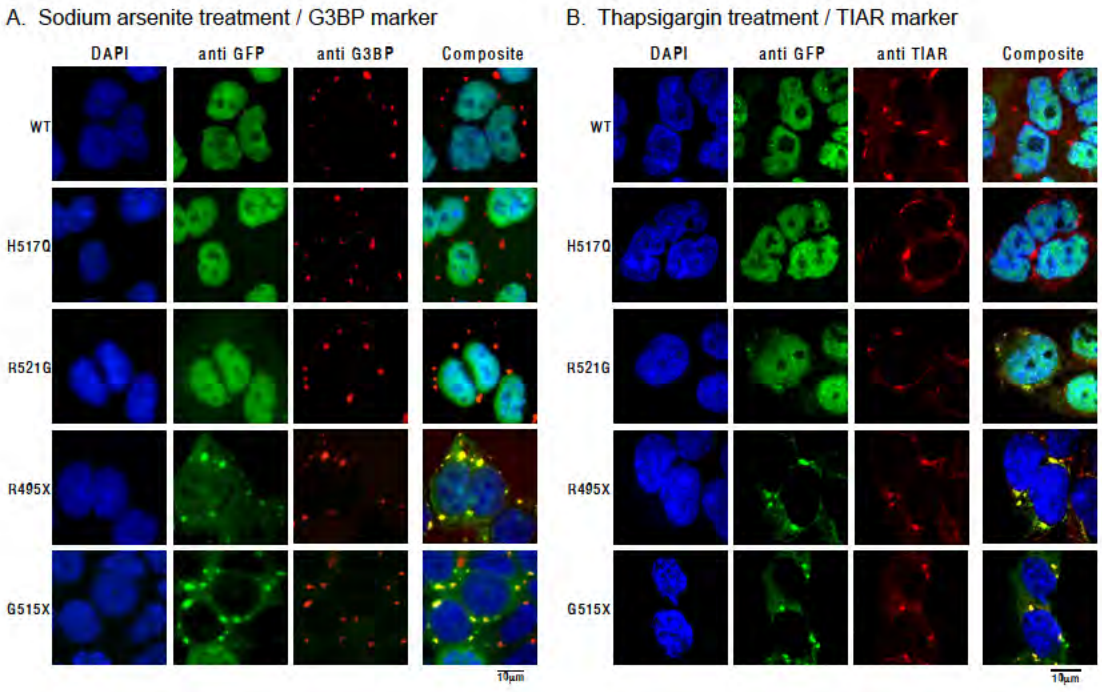

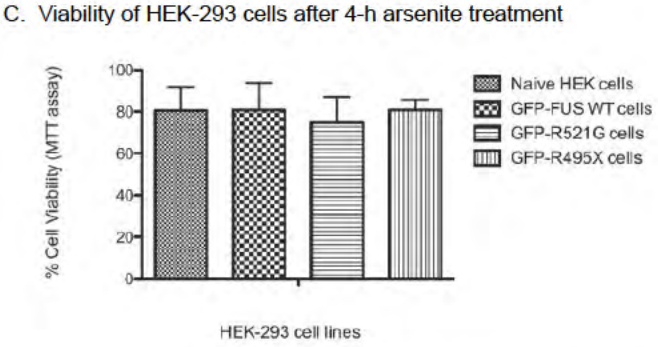

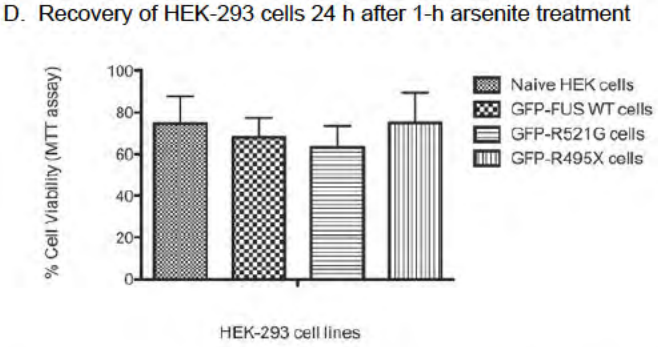

Figure 2-5 Stress granule formation was induced in HEK-293 cells upon both sodium arsenite and thapsigargin treatment.

Figure 2-5 Stress granule formation was induced in HEK-293 cells upon both sodium arsenite and thapsigargin treatment.

(A) Immunofluorescence of stable GFP-FUS HEK-293 cells treated with sodium arsenite was performed as described in Fig. 2, except that the G3BP (red) stress granule marker was employed here. Confocal microscopy revealed similar results as in Fig. 2, in that GFP-FUS(R521G, R495X, and G515X) co-localize to stress granules that are formed upon sodium arsenite treatment, whereas GFP-FUS(WT and H517Q) exhibited a predominately nuclear (DAPI, blue) expression pattern. **(B)** GFP-FUS(R521G, R495X, and G515X) also co-localized to TIAR-positive (red) stress granules as in (A) upon treatment with 10 μM thapsigargin for 2 h, whereas GFP-FUS(WT and H517Q) did not. **(C)** Transiently transfected (40 h) untagged-GFP did not co-localize to TIAR-positive (red) stress granules upon treatment with the sodium arsenite (described in Fig. 2), but rather exhibited a relatively diffuse nuclear and cytoplasmic expression pattern under these conditions. Scale bar, 10 μm.

The GFP tag itself does not mediate the recruitment of GFP-FUS(R521G, R495X and G515X) into stress granules because free GFP maintained a diffuse nuclear and cytoplasmic expression pattern upon oxidative insult with arsenite (Figure 2-6). In addition, transient transfection of untagged FUS constructs followed by sodium arsenite treatment produced the same results as those described above for the GFP-FUS stable lines; FUS(R521G and R495X) proteins incorporated into stress granules, whereas transfected FUS WT and endogenous FUS proteins were not detected in stress granules (Figure 2-6).

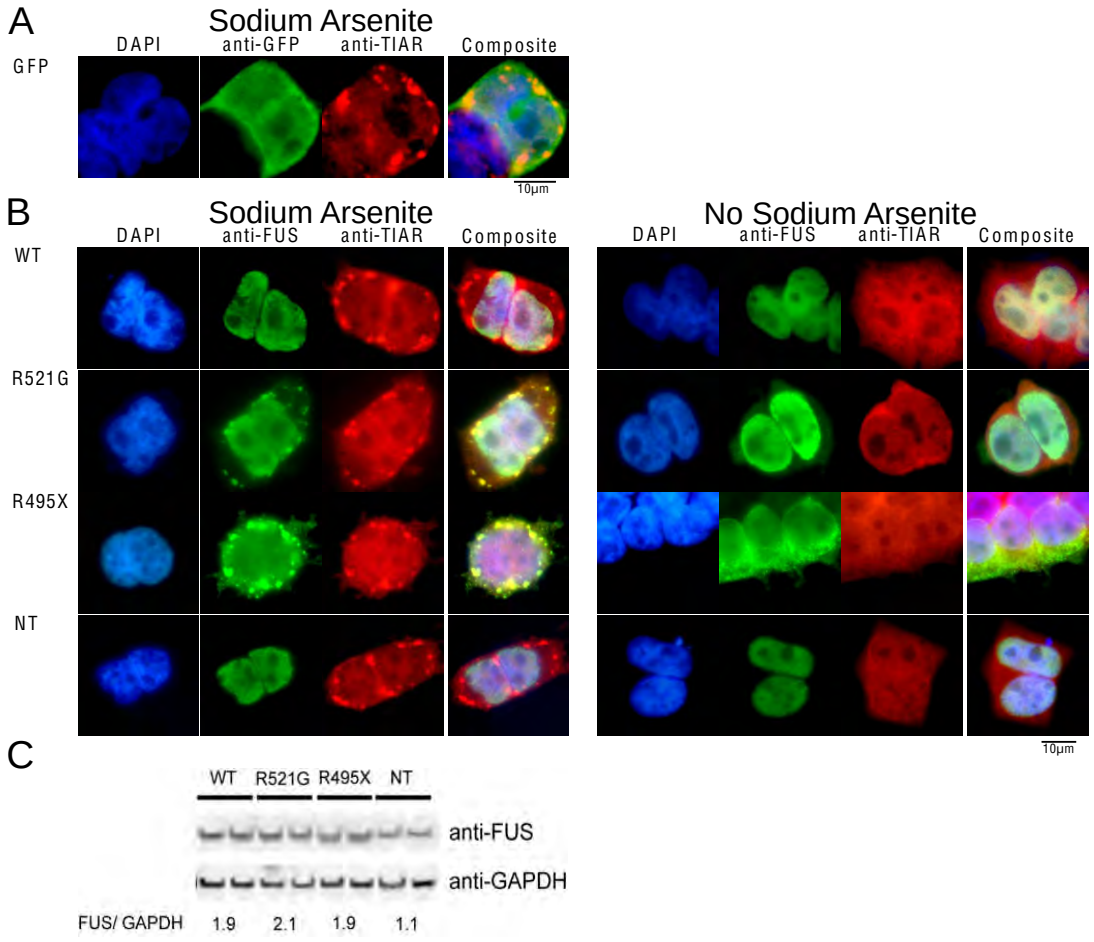

Figure 2-6 Incorporation of FUS into stress granules is not mediated by the GFP tag.

(A) Transiently transfected (40 h) untagged-GFP did not co-localized to TIAR-positive (red) stress granules upon treatment with sodium arsenate (described in Figure 2-4) within HEK-293 cells, but rather exhibited a relatively diffuse nuclear and cytoplasmic expression pattern under these conditions. **(B)** Untagged FUS (R521G and R495X) proteins, but not WT, were incorporated into stress granules upon transient transfection (16 h here, compared to 40 h in Figure 2-3) of the respective construct into HEK-293 cells followed by arsenate treatment. Endogenous FUS did not incorporate into stress granules, as illustrated by the image of non-transfected (NT) HEK-293 cells after arsenate treatment. FUS expression was detected by immunofluoresencec (Methods) with the anti-FUS antibody (Behtyl Labs, #A300-293A; 1:400). Scale bar, 10 µm (A and B). **(C)** Western analysis (Method) of cell lysates prepared from the experiment described in **(B)**. Duplicate experiments are shown for each cell line, and the ratio of FUS/GAPDH reflects the average of the densitometry measurement for these experiments.

To explore the dynamics of GFP-FUS (R521G, R495X, and G515X) recruitment into stress granules, we first exposed HEK-293 lines to arsenite and performed live cell confocal imaging at 37°C (Figure 2-7). We observed that only a minority of cells expressing the R495X or G515X mutants contained GFP-FUS aggregates prior to the addition of arsenite (Figure 2-7, t=0 min). Within 4-7 min of exposure to arsenite, cells expressing the G515X mutant began to accumulate larger perinuclear aggregates (Figure 2-7). Similarly, cells expressing the R495X mutant formed prominent aggregates by 7-10 min (Figure 2-7). Cells expressing GFP-FUS(R521G), which exhibited a much lower cytoplasmic expression level, eventually formed perinuclear foci with a significant delay and weaker intensity compared to the other mutants (Figure 2-7). In agreement with our analysis of fixed HEK-293 cells (Figure 2-4), live cells expressing GFP-FUS(WT) (Figure 2-7) or GFP-FUS(H517Q) (not shown) maintained the nuclear localization of GFP without forming detectable cytoplasmic aggregates. These results suggested that the abundance of FUS variants in the cytoplasm contributes both to the extent and to the speed of their recruitment into stress granules following an oxidative insult.

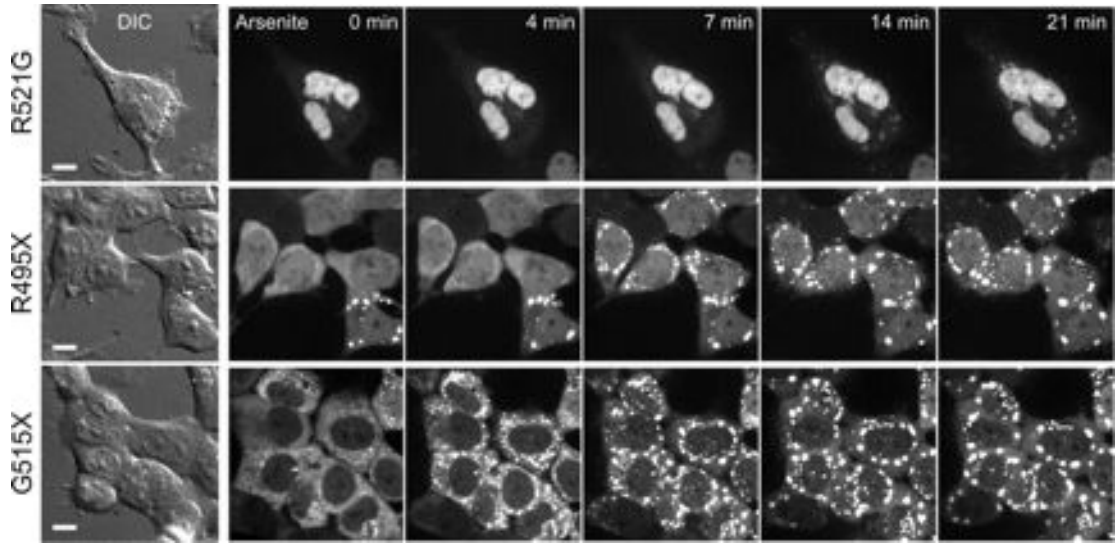

Figure 2-7 Recruitment of GFP-FUS into perinuclear stress granules was more rapid and extensive for truncation mutants.

GFP-FUS(R521G, R495X or G515X) was induced for 4 days in HEK-293 cells, and a time series of GFP intensities was acquired in live cells at 37°C over 30 min following the addition of 0.5 mM sodium arsenite. Differential interference contrast (DIC) images (left) indicate cell positions, and confocal fluorescence images (right) show maximum-intensity z-projections obtained from serial 0.2 μm slices using a 60× objective. GFP fluorescence revealed a rapid (within 4–7 min) formation of FUS(R495X and G5151X) aggregates, whereas FUS(R521G) formed smaller, less intense aggregates with a slower time course. Scale bar, 10 μm.

To determine whether the accumulation of FUS variants into stress granules was reversible, we measured the response of GFP-FUS-expressing cell lines to heat shock, another stress granule inducer (Buchan and Parker 2009). Live cell confocal imaging was performed on HEK-293 cells at 37°C to observe the distribution of GFP-FUS at baseline, and the microscope stage and objective were then heated to 42.5°C within an enclosed chamber. We observed the assembly of intense perinuclear GFP-FUS aggregates within 7-10 min for the R495X and G515X mutants, while smaller and less intense aggregates of the H517Q and R521G mutants required ~15 min to form and continued to evolve over 30 min (Figure 2-8). Upon return of the microscope stage to 37°C, we observed that aggregates containing GFP-FUS disassembled within minutes (Figure 2-8), consistent with the reversible nature of these structures (Buchan and Parker 2009). Overall, these results showed that the fALS-linked FUS mutants (R495X > R521G, H517Q) and the engineered truncation (G515X), but not WT FUS, were dynamically and reversibly incorporated into stress granules in response to conditions that impair cellular translation initiation.

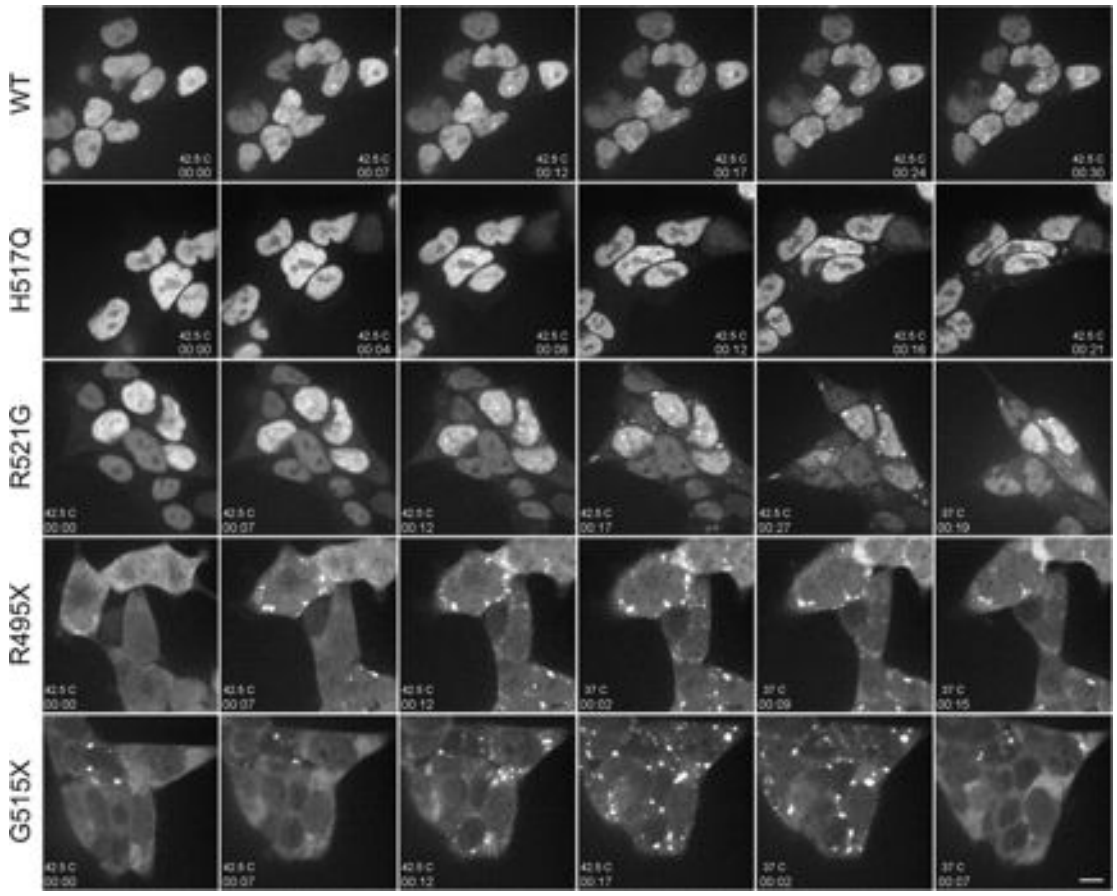

Figure 2-8 Formation of cytoplasmic GFP-FUS aggregates was reversible after heat shock.

GFP-FUS(WT, H517Q, R521G, R495X or G515X) was induced for 3 days in HEK-293 cells, and a time series of GFP intensities (acquired as in Fig. 3) was detected in live cells over the indicated time course (hh:mm) upon shifting from 37–42.5°C. Cytoplasmic FUS inclusions assembled most rapidly (by 7–12 min) in cells expressing GFP-FUS(R495X and G5151X) and to a lesser extent in cells expressing GFP-FUS(R521G and H517Q). Aggregate formation was reversible within minutes of a temperature shift back to 37°C, as shown for GFP-FUS(R521G, R495X and G5151X). Scale bar, 10 μm.

II.4.3 FUS variants do not localize to processing bodies under conditions of oxidative Stress

Whereas stress granules form transiently in response to stress, processing bodies (P-bodies) are distinct cytoplasmic silencing foci that are present constitutively and can be augmented by stress (Moore 2005). Since stress granules are physically and functionally associated with P-bodies, which play a role in mRNA degradation, we probed for the co-localization of GFP-FUS with GE-1/hedls, a constituent of P-bodies but not stress granules (Kedersha and Anderson 2007). We observed P-bodies under baseline conditions in HEK-293 cells expressing GFP-FUS (WT and mutants) but saw no evidence of co-localization with GFP (data not shown). Furthermore, no co-localization of P-bodies and GFP-FUS was observed upon treatment of cells with 1 mM sodium arsenite for 2 h, despite the close contact of P-bodies with stress granules containing GFP-FUS (Figure 2-9). Thus, although GFP-FUS variants are recruited into stress granules under conditions of acute stress, these variants i) do not incorporate acutely into associated P-bodies, and ii) do not prevent the normal docking of P-bodies to stress granules.

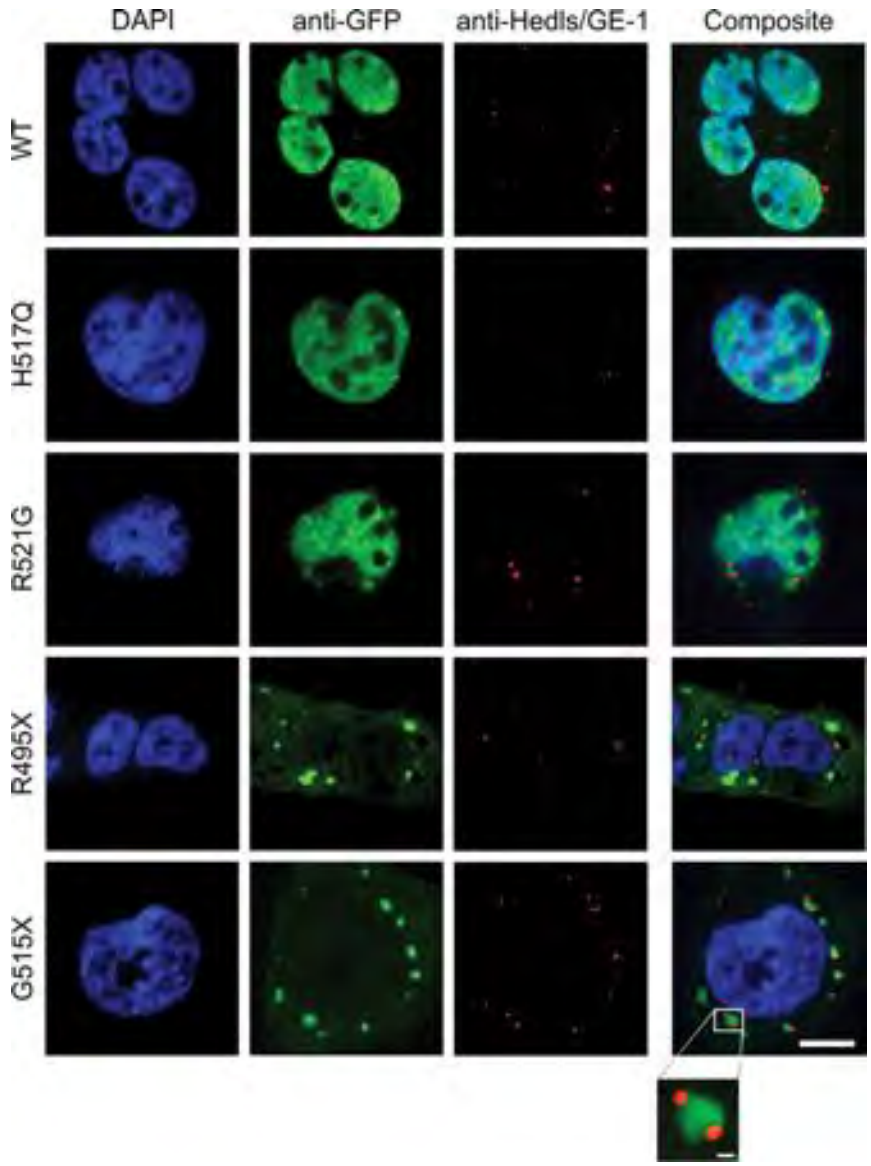

Figure 2-9 Cytoplasmic GFP-FUS in stress granules did not co-localize with adjacent P-bodies.

HEK-293 cell lines stably expressing GFP-FUS proteins were treated as described in Figure 2, except that 1 mM sodium arsenite was administered for 2 h and cells were probed with anti-Hedls/GE-1, a marker of P-bodies (red). Scale bar, 10 μm. None of the GFP-FUS proteins co-localized with the P-body marker. However, P-bodies localized in close proximity to stress granules containing the GFP-FUS(R521G, R495X and G515X) variants, and in some cases P-bodies appeared docked to these stress granules (see inset for G515X; scale bar, 1 μm).

II.4.4 GFP-FUS variants localize to the cytoplasm and accumulate into stress granules in zebrafish embryos

To determine whether the mislocalization of human FUS mutants to the cytoplasm in HEK-293 cells also occurs in spinal neurons or other cell types relevant to ALS, we injected zebrafish embryos at the 1-2 cell stage with mRNAs encoding GFP-FUS(WT, H517Q, R521G, R495X, or G515X). Under these conditions, the GFP-FUS gene product can be expressed in a mosaic pattern throughout the embryo for several days. At 25 h post-fertilization (hpf), we observed the distribution of expressed GFP-FUS proteins in the spinal cord and somatic musculature near the region of the yolk sac extension (Figure 2-10 and Figure 2-11). Similar to the expression in HEK-293 cells, human FUS WT and the H517Q and R521G mutants each exhibited a predominantly nuclear pattern in the spinal cord, whereas the R495X and G515X truncation mutants accumulated in the cytoplasm.

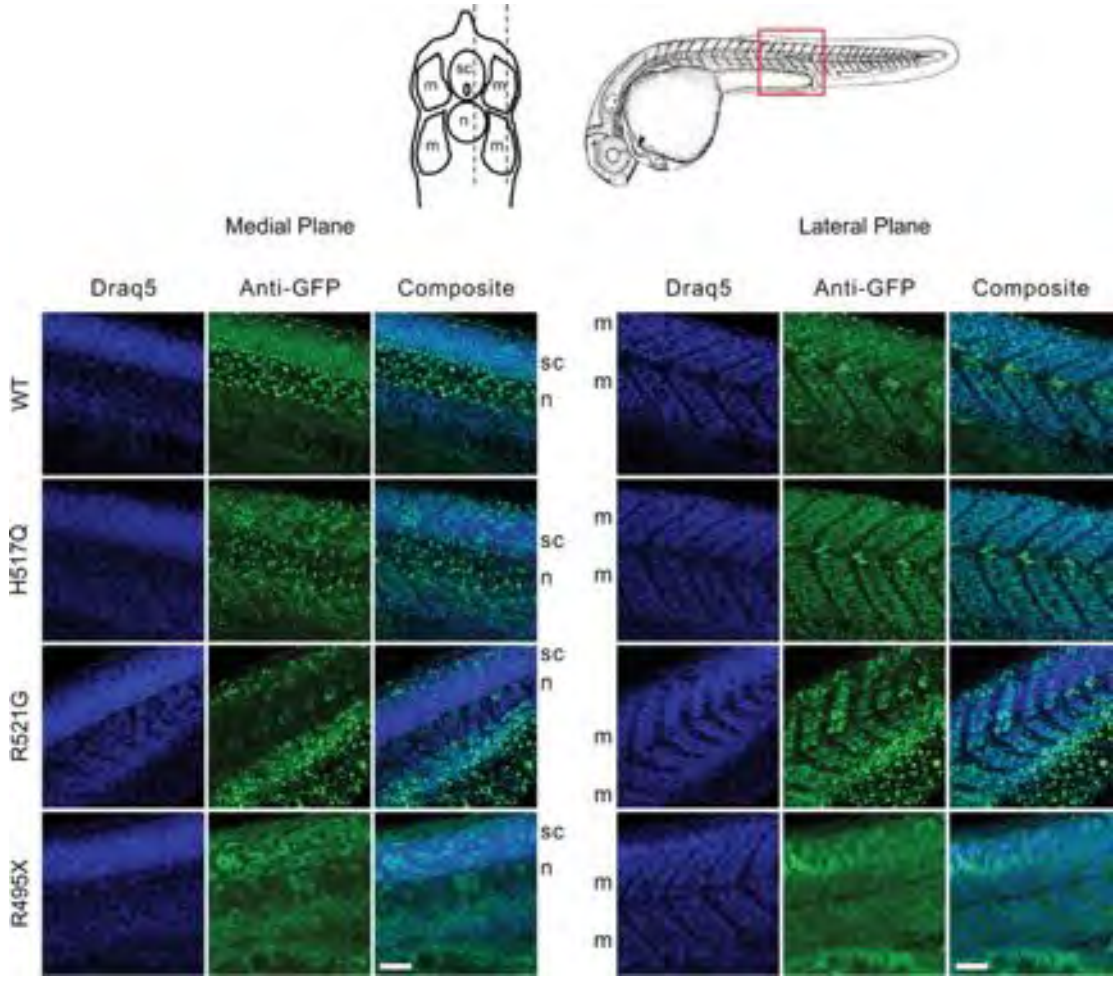

Figure 2-10 Expression of GFP-FUS variants in spinal cord and body wall muscle of zebrafish embryos.

Zebrafish eggs were injected at the 1–2 cell stage with mRNAs encoding GFP-FUS variants. Embryos were fixed at 25 hpf, and the intact body wall region was immunostained with anti-GFP (green) and a nuclear marker (Draq5, blue). Confocal image stacks (40× objective, Δz = 1.0 μm) were acquired in a longitudinal orientation (red box) from the lateral body muscle (m) extending medially through the spinal cord (sc) and notochord (n). Shown are representative medial and lateral slices. For embryos expressing GFP-FUS(WT, H517Q and R521G), the GFP signal was predominantly nuclear, whereas for embryos expressing the R495X truncation mutant, the GFP localized mostly to the cytoplasm. Scale bar, 50 μm.

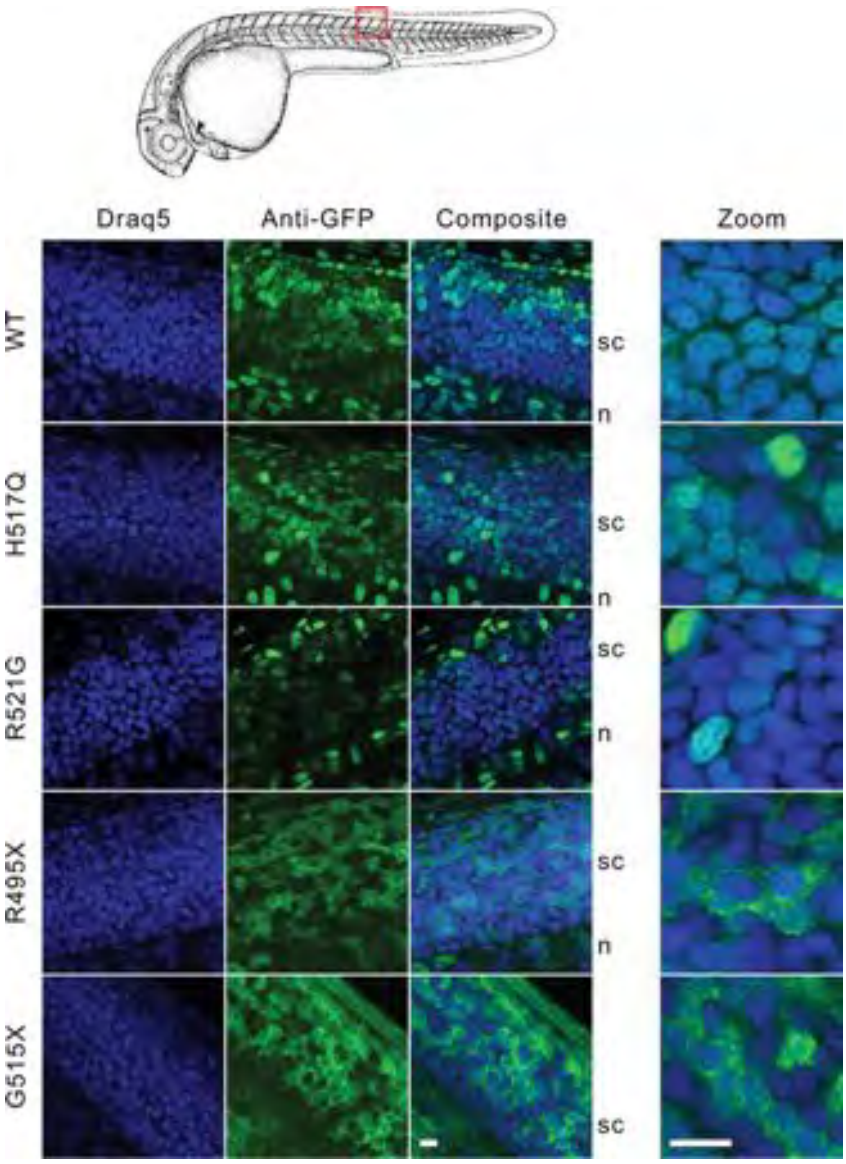

Figure 2-11 Expression of GFP-FUS variants in spinal cord of zebrafish embryos.

Zebrafish eggs were injected with mRNAs encoding GFP-FUS variants, and embryos were processed for confocal microscopy (100×) as described in Figure 6. Shown are representative 0.9 μm slices (left panels) and 0.4 μm slices acquired using a 3.44× optical zoom (right panel). The higher magnification clearly showed the nuclear expression of GFP-FUS(WT, H517Q and R521G) variants and cytoplasmic accumulation of the R495X or G515X truncation mutants in the spinal cord. Scale bars, 10 μm.

To investigate the behavior of FUS-mutants in response to a physiological stress in vivo, we next applied a heat shock to zebra fish embryos expressing FUS variants. After heat shock to 42.5°C for 45 min, we observed TIAR-containing foci indicative of stress granule formation (Figure 2-12). Moreover, the R521G, R495X, and G515X mutants formed perinuclear aggregates that co-localized with anti-TIAR immunofluorescence (Figure 2-12), demonstrating their incorporation into stress granules in vivo. Surprisingly, the recessive H517Q mutant exhibited a granular cytoplasmic expression pattern in some regions upon heat shock to 42.5°C, representing the only insult employed in the present study that could shift the expression of this mutant from the nucleus to the cytoplasm (Figure 2-12). Under this condition, cells expressing GFP-FUS(WT) occasionally showed cytoplasmic expression, but to a lesser extent than H517Q (Figure 2-12). Overall, our experiments suggest that multiple factors influence the subcellular localization of GFP-FUS in vivo, including the presence of mutant residues near the C-terminus and the nature and extent of imposed stresses.

In additional experiments, we injected zebrafish eggs from a transgenic line expressing GFP in motor neurons (Flanagan-Steet, Fox et al. 2005) with mRNAs encoding untagged FUS mRNA variants (human WT, H517Q and R521G). The gross morphology of embryos injected with the mutant constructs was similar to controls for up to at least 3 days of development (data not shown). We occasionally observed shorter ventrally projecting GFP-positive motor axons in the region of the yolk sac extension for those injected with R521G versus WT or H517Q mRNAs (data not shown), but this was

not a consistent finding, and we were unable to document any convincing defects in motor axon outgrowth or arborization pattern compared with controls.

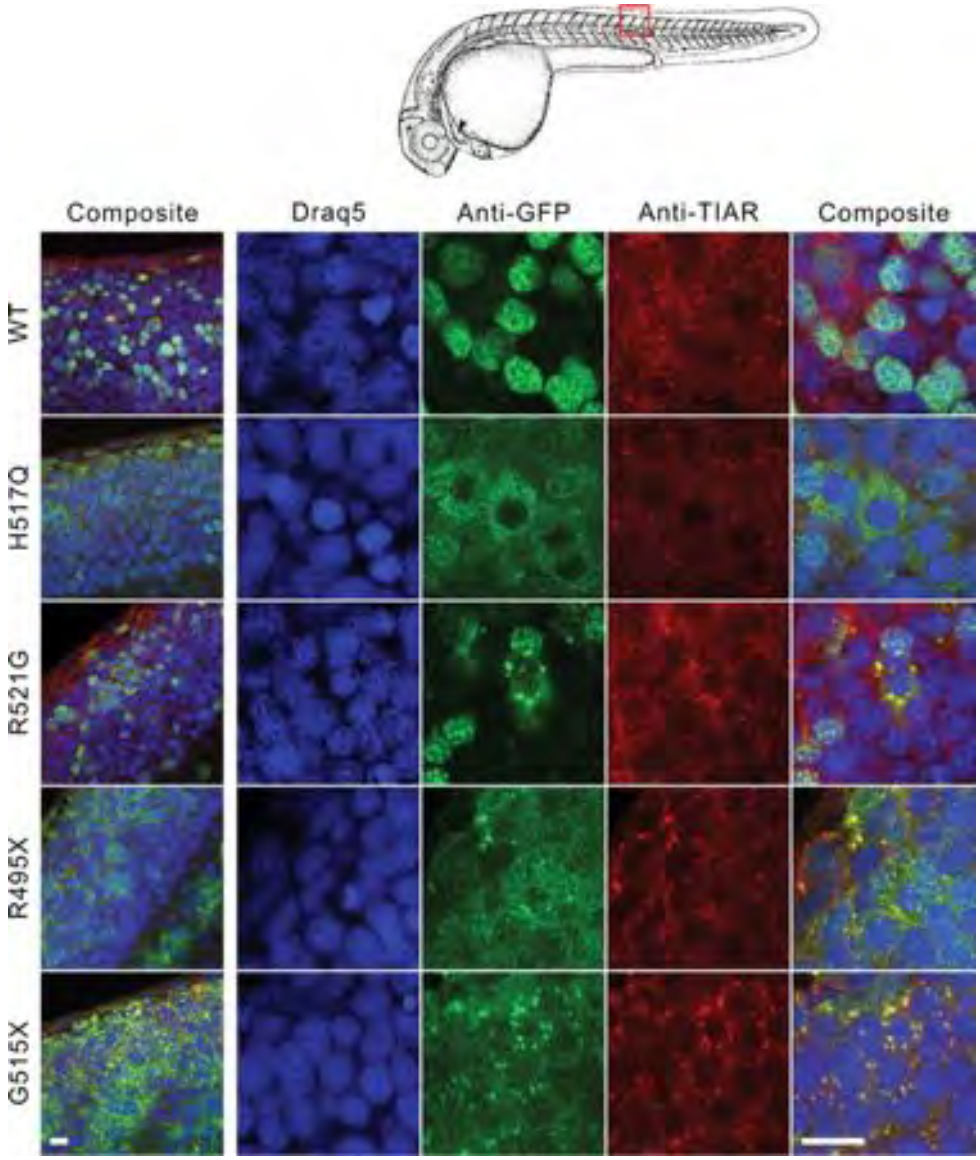

Figure 2-12 Heat shock increased the cytoplasmic localization of the H517Q mutant and triggered accumulation of R521G, R495X and G515X into stress granules in vivo.

Confocal slices of zebrafish spinal cord from 25 hpf embryos incubated at 42.5°C for 45 min followed by immediate fixation and double immunostaining with anti-GFP (green) and anti-TIAR (red). For a group of spinal cord cells from embryos expressing the H517Q mutant, the GFP redistributed to the cytoplasm in a granular pattern without incorporating prominently into stress granules, whereas this occurred only rarely for cells expressing GFP-WT FUS. For embryos expressing the R521G, R495X and G515X mutants, the GFP assembled into aggregates that co-localized with anti-TIAR staining. Nuclei were stained with Draq5. Left panel obtained at 100×, right panels obtained using 3.44× optical zoom. Scale bars, 10 μm.

II.5 Discussion

This study has identified a critical role of the C-terminus of FUS in nuclear localization and its perturbation by a subset of FUS mutants that cause fALS. Furthermore, our results revealed a mutant-specific response to cellular stress that leads to the incorporation of cytoplasmic fALS-linked FUS protein into stress granules.

Although the C-terminus of FUS differs from classical nuclear localization signals that are recognized by karyopherin α (importin α) (Sorokin, Kim et al. 2007), an analysis of the evolutionarily related EWS protein (Zakaryan and Gehring 2006) suggested that the C-terminus of FUS may nonetheless function to mediate nuclear localization. Moreover, the C-terminal sequence of FUS is consistent with a 'PY-NLS' type of nuclear targeting signal that binds to the human karyopherin β2/transportin (Kapβ2) receptor (Lee, Cansizoglu et al. 2006, Lange, Mills et al. 2008). Our results showed that truncation of this putative FUS NLS in the R495X and G515X mutants (Figure 2-1A) caused a dramatic increase in cytoplasmic accumulation of FUS compared to the missense (H517Q and R521G) mutants, which have only a single amino acid substitution within the NLS (Figure 2-1C and 1D). Thus, these studies provide compelling evidence that the C-terminus of FUS is required for normal nuclear–cytoplasmic partitioning of the protein and that fALS-linked mutations disrupt this equilibrium.

Although cytoplasmic FUS accumulation was observed previously for some overexpressed fALS-linked missense mutants (Kwiatkowski, Bosco et al. 2009, Vance, Rogelj et al. 2009, DeJesus-Hernandez, Kocerha et al. 2010), the downstream

consequence(s) of this mislocalization on cellular pathways, including those involved with stress responses, remains largely unknown. Here, we showed that GFP-FUS mutants retained in the cytoplasm assemble into stress granules in response to acute insults, including oxidative stress (Figure 2-4, Figure 2-5A and Figure 2-7), ER stress (Figure 2-5B) and heat shock (Figure 2-8 and figure 2-12). Although inhibition of transcription causes a redistribution of WT FUS from the nucleus to the cytoplasm (Zinszner, Albalat et al. 1994), we found here that inhibition of translation induced by other cellular stresses does not prominently alter the subcellular localization of WT-FUS. However, an enhanced cytoplasmic accumulation of the autosomal recessive mutant (H517Q) was detected upon heat shock in vivo (Figure 2-12), which may have implications for ALS (discussed below).

Why does cytoplasmically localized mutant FUS assemble into stress granules? One possibility is that FUS associates directly with specific mRNAs or other proteins that mediate the integration of FUS into stress granules. FUS has been shown to bind mRNAs encoding actin-related proteins, such as actin-stabilizing protein Nd1-L, which may be important for the transport of this mRNA to dendrites for local translation and maintenance of spine morphology (Fujii, Okabe et al. 2005, Fujii and Takumi 2005); however, comprehensive data regarding mRNAs bound by FUS are lacking. The fALS-linked R521G mutant retains the ability to complex with GGUG-containing RNAs (Lerga, Hallier et al. 2001, Kwiatkowski, Bosco et al. 2009), indicating that FUS mutations do not abrogate RNA binding. Moreover, our data demonstrate that the C-

terminal NLS does not directly mediate interactions with other RNPs or RNAs required for targeting of FUS to stress granules, as evidenced by the significant incorporation of the truncation mutants (R495X and G515X) into these structures.

The association of FUS and other RNA-binding proteins with stress granules appears to be specific, as cytoplasmic free GFP does not localize to stress granules (Figure 2-6) (Andersson, Stahlberg et al. 2008). Although some RNA-binding proteins such as Nova1 do not incorporate into stress granules (Colombrita, Zennaro et al. 2009), others such as TDP-43 show this property under conditions of translational arrest induced by oxidative stress (Colombrita, Zennaro et al. 2009) or upon expression of a pathogenic, fragmented form of this protein (Nishimoto, Ito et al. 2010). One study reported the co-localization of transfected GFP-FUS (WT) into stress granules in HT-1080 cells (Andersson, Stahlberg et al. 2008); however, the association of GFP-FUS (WT) with stress granules was not observed in acutely transfected HEK-293 cells (Gal, Zhang et al. 2011). In addition, we did not observe stress granules in the absence of an applied stress for our stable HEK-293 cell line expressing the GFP-FUS (R521G) mutant or in HEK-293 cells acutely transfected (16 h) with FUS(R521G) (Figure 2-6), although stress granules have been detected for this mutant under acute transfection conditions in other laboratories (Gal, Zhang et al. 2011). These apparent discrepancies may result from a difference in cell lines, transfection procedures, or exogenous FUS expression levels. Consistent with this hypothesis was our observation of increased cytoplasmic aggregation for FUS mutants when expressed at higher levels in transiently transfected (40 h) cells compared with

stable cell lines (Figure 2-3). These data indicate that the aggregation propensity of FUS, as well as its cellular localization and binding interactions, may be sensitive to the expression level of FUS, the translational state of individual cells and factors related to cell type; this sensitivity to altered cellular homeostasis may be expected based on the regulatory functions of proteins within the hnRNP family (Dreyfuss, Matunis et al. 1993). Although mutant FUS incorporates into stress granules, it does not significantly associate with P-bodies (Figure 2-9). A specific association with stress granules over P-bodies has also been reported for the ALS-associated TDP-43 protein (Colombrita, Zennaro et al. 2009).

The observation that both FUS and TDP-43 can associate with stress granules raises the possibility that ALS-related mutants might perturb the normal response to stress in maladaptive ways. Although we cannot exclude the possibility that under some conditions FUS WT may also associate with stress granules, the fALS-linked mutations significantly shift the subcellular equilibrium of FUS towards the cytoplasm and enhance its association with stress granules. In fact, the R495X mutation that truncates the NLS results in the highest levels of cytoplasmic FUS compared with the other fALS-linked mutants studied here (Figure 2-1). Furthermore, cytoplasmic expression of R495X correlated with its incorporation into stress granules. That this mutation is also associated with a severe, early-onset clinical phenotype, which is similar to the de novo FUS G466VfsX14 mutation (DeJesus-Hernandez, Kocerha et al. 2010), raises the possibility that the vulnerability of motor neurons to mutant FUS is proportional to FUS expression

in the cytoplasm. In contrast to FUS R495X, the autosomal recessive FUS H517Q mutant exhibits weak cytoplasmic expression under homeostatic cellular conditions (Figure 2-4 and Figure 2-10). That this mutant protein could more readily translocate to the cytoplasm upon induction of heat shock in vivo (Figure 2-12) suggests an enhanced susceptibility to thermal stress compared with FUS WT. Although it is not clear whether motor neuron vulnerability stems from a loss of normal FUS nuclear function or an altered cytoplasmic function, or both, the notion that cytoplasmic expression levels of RNA-binding proteins may correlate with ALS pathogenesis has also been supported for TDP-43 based on cell culture and animal model studies with mutant forms of that protein (Wegorzewska, Bell et al. 2009, Barmada, Skibinski et al. 2010).

We observed that mutant FUS recruitment to stress granules is reversible following an acute insult (Figure 2-8). In addition, we found no evidence of acute toxicity associated with the incorporation of mutant FUS into stress granules, as measured by the MTT cell proliferation assay (Figure 2-5). In light of these observations, how might this mutant-specific property, i.e. incorporation of mutant FUS into stress granules, play a role in ALS pathogenesis? It is plausible that more chronic changes in cellular homeostasis as a consequence of mutant FUS expression could produce a maladaptive outcome. For example, the inappropriate sequestration of mutant FUS and its biological binding partners into stress granules may impair the cellular response to chronic oxidative stress, protein misfolding, heat shock or other insults that cause translational arrest. Further, chronic stress may culminate in the conversion of stress granules into larger pathological

aggregates, a possibility that is supported by the detection of mRNA-associated proteins within the inclusions of adult onset motor neuron disease (Fujita, Ito et al. 2008). A similar mechanism has been proposed for the accumulation of aggresomes into end-stage Lewy bodies, the pathological hallmark of Parkinson's disease and other synucleinopathies (Olanow, Perl et al. 2004). However, the detection of mRNA and its associated proteins in ALS aggregates is not a consistent finding in all reports (Colombrita, Zennaro et al. 2009). Thus, it remains to be determined whether FUS-associated stress granules are linked to the formation of end-stage ALS aggregates, and whether FUS-containing aggregates detected in post-mortem CNS tissues of affected individuals are neurotoxic themselves or simply markers of altered cellular homeostasis.

Although we did not observe acute toxicity as a consequence of mutant FUS expression at near-endogenous levels in either the HEK-293 cells or the zebrafish embryos, further studies using model systems that more closely recapitulate the relevant neuronal environment, such as primary motor neurons and/or transgenic models, may reveal mutant-specific phenotypes related to FUS toxicity. We note that, to date, there has been no evidence published that directly links mutant FUS expression or its localization to cellular dysfunction. Nevertheless, our findings suggest that candidate pathways related to the regulation of stress defenses in motor neurons may be appropriate for further investigation of the pathogenic role of FUS in ALS. Dysregulation of specific stress responses may also contribute to the preferential motor neuron vulnerability

observed in other forms of ALS caused by mutant SOD1, mutant TDP-43 and, perhaps, in sALS.

II.6 Materials and Methods

Human subjects

The clinical information and biological samples (blood and/or autopsy tissues) were collected from fALS cases and control individuals after informed consent was obtained. All protocols were approved by the Institutional Review Board at the institutions involved.

Identification of the FUS-R495X mutation in human fALS

DNA was available from two of the eight affected individuals in family F521. The coding region of exon 14 of the FUS gene was amplified by polymerase chain reaction from the DNA of a fALS patient using flanking primers with 19 and 21 base pair tails added to the 5′-end to standardize sample sequencing. Samples were sequenced by the method described previously (Kwiatkowski, Bosco et al. 2009), and the FUS c.1566C>T mutation that truncates FUS translation at Arg495 was confirmed using bidirectional Sanger methods. Sequencing data were aligned and analyzed for heterozygous polymorphisms using Consed (Gordon, Abajian et al. 1998): FUS_ex14F: tagtaaaacgacggccagtAGGCTCGGGGAACATAGG; FUS_ex14R: taggaaacagctatgaccatgAGCCCTCAAAATGAAACCAC.

Stable inducible HEK-293 cell lines

Isogenic cell lines expressing GFP-FUS variants under doxycyline-inducible control were established using the Flp-In T-REx system (Invitrogen). The Flp-In T-REx 293 line (Invitrogen, R780-07) contained a single stably integrated FRT site that allowed targeted integration of each GFP-FUS expression cassette into the same transcriptionally active genomic locus. Flp-In T-REx 293 cells were co-transfected with the expression vector (pcDNA5/FRT/TO-TOPO containing GFP-FUS) and the Flp recombinase vector (pOG44) using the Effectene transfection reagent (Qiagen). Selection for stable integration was performed beginning 48 h after transfection using medium that contained 150 μg/ml Hygromycin B (Invitrogen, 10687-010). This yielded isogenic cell populations that could induce GFP-FUS at approximately one to two times that of endogenous FUS (Fig. 1B) upon incubation with 1 μg/ml doxycycline for 40 h.

Cell culture and drug treatments

HEK-293 cells with stably integrated GFP-FUS constructs (described above) were maintained in Dulbecco's modified Eagle's medium (DMEM) supplemented with 10% TET-tested fetal bovine serum (Atlanta Biologicals, s10350H), 2 mM L-glutamine (Gibco, 25030), 15 μg/ml blasticidin (Invitrogen, R210-01), 150 μg/ml hygromycin B (Invitrogen, 10687-010) and 1% penicillin and streptomycin solution (Gibco, 15140). For drug treatments, the following stocks were prepared and stored at freezing temperatures: 50 mg/ml doxycycline (Sigma, D9891) in water (−80°C), 100 mM sodium arsenite (Sigma, 71287) in water (−20°C) and 1 mM thapsigargin (Sigma, T9033) in DMSO

(−20°C). Prior to treatment with drugs, cells were plated at 1×10^5 cells/ml into 24-well dishes containing 12 mm coverslips (Fisher, NC9708845) that were pre-treated with poly-L-lysine (Sigma, P8920) according to the manufacturer's instructions. Cells were allowed to adhere to the coverslips overnight, and FUS expression was induced upon addition of 1 μg/ml doxycycline (Sigma, D9891) for 40 h. Cells were then exposed to either 0.5 or 1 mM sodium arsenite for 1–2 h (as noted) or 10 μM thapsigargin for 2 h.

Immunofluorescence of HEK-293 cells

Cells were fixed with 4% paraformaldehyde for 15 min and permeabilized with 1% Triton X-100 for 10 min, or with cold 100% methanol for 10 min on ice. Cells were then blocked with 2% goat serum (Jackson ImmunoResearch Labs, 005-000-121), 0.1% Triton X-100, 50 mM NH_4Cl and 10 mg/ml bovine serum albumin (BSA) in Dulbecco's phosphate-buffered saline (PBS) for 1 h at 37°C. Antibodies were diluted in 0.15% goat serum, 0.1% Triton X-100 and PBS. Primary antibody incubation conditions were as follows: 1:250 mouse anti-TIAR (BD Transduction Labs, 610352) for 30 min at 37°C; 1:500 mouse anti-G3BP (BD Transduction Labs, 611126) for 30 min at 37°C; and 1:250 mouse anti-GE-1/hedls/p70 S6 kinase (Santa Cruz Biotechnology, sc-8418) for 12 h at 4°C. Secondary anti-mouse IgG antibody conjugated to Dylight 549 (Jackson ImmunoResearch Labs, 715-505-151) was used at 1:1500–1:3500. The GFP signal was enhanced by 1:1000 Alexa Fluor 488-conjugated rabbit anti-GFP (Invitrogen, A21311). Coverslips were mounted with Vectashield hard-set mounting medium containing DAPI

(Vector Laboratories, H-1500). Confocal microscopy was performed using a Solamere Technology Group CSU10B spinning disk confocal system equipped with a Yokogawa CSU10 spinning disk confocal scan head, a laser assembly consisting of an argon ion laser (50 mW at 488 and 514 nm and 13 mW at 457 nm), and three solid-state lasers (25 mW at 561 nm, 30 mW at 636 nm and 45 mW at 405 nm). Image stacks were acquired using a 100× oil objective, a Roper Coolsnap HQ2 camera and MetaMorph V7.6.3 software, using a slice thickness, Δz, of 2 μm. Images were analyzed using NIH ImageJ software (http://rsb.info.nih.gov/ij), optimized for contrast using linear scaling only, and compiled using CorelDraw software.

Live-cell imaging and fluorescence quantitation

Cells were cultured on 35 mm glass-bottom dishes coated with poly-D-lysine (P35GC-1.5-14-C; MatTek, Ashland, MA, USA) and washed with PBS containing 0.9 mM $CaCl_2$ and 0.5 mM $MgCl_2$ (Ca/Mg/PBS) immediately before imaging. Confocal microscopy was performed on a Solamere Technology Group (Salt Lake City, UT, USA) CSU10B spinning disk confocal system attached to a Nikon TE2000-E2 motorized inverted fluorescence microscope equipped with a Nikon Perfect Focus System (Nikon Instruments, Melville, NY, USA). This system included a custom laser assembly with an AOTF for rapid wavelength change via fiber optics coupled to a Yokogawa CSU10 spinning disk confocal scan head with high efficiency dichroic mirrors and laser-blocking filters. For GFP confocal imaging, cells were illuminated with an argon ion laser

operating in standby mode (20 mW at 488 nm at the laser) using a Nikon VC Plan Apo 60× oil objective (NA: 1.4), and the fluorescence emission passed through a 525/50 nm GFP bandpass filter before entering a Rolera MGi EMCCD 14-bit camera (Qimaging, Surrey, BC, Canada). MetaMorph V7.6.3 (Molecular Devices) software was used for equipment control and image acquisition. Images were analyzed using NIH ImageJ software and plug-ins from the McMaster University Biophotonics Facility (http://www.macbiophotonics.ca/imagej/).

For quantitative GFP imaging of live cells (Figure 2-1D and Figure 2-2), a stack of 60–100 thin slices (Δz = 0.2 μm, t = 1500 ms, EM gain = 3800 for each slice) was acquired at room temperature. The dark-current image (acquired for t = 1500 ms with the laser off) was subtracted from each raw image, and variations in illumination and detection efficiencies at each pixel were corrected by dividing the dark-adjusted intensities by a normalized flat-field image of a uniformly green fluorescent slide (Chroma Technology, Rockingham, VT, USA) acquired using the same 525/50 nm bandpass filter. For the quantitation of cytoplasmic versus nuclear signal per unit volume for each cell, the average intensity of 10 × 10 pixel (1.83 μm × 1.83 μm) regions of cytoplasm (c), nucleus (n) and background (b) were obtained for each of 6–10 representative and contiguous 0.2 μm slices. The cytoplasmic/nuclear ratio for each representative slice was calculated as $(c-b)/(n-b)$, and the ratios obtained from the contiguous slices were averaged for each cell.

For live-cell movies, cells were washed in Ca/Mg/PBS as above and then maintained in either Ca/Mg/PBS or DMEM without vitamins to minimize oxidative photobleaching of GFP (Bogdanov, Bogdanova et al. 2009) at 37°C in a humidified chamber exposed to 5% CO_2. For some experiments, heat shock to 42.5°C and cooling back to 37°C was performed using stage and objective heaters (20/20 Technology, Inc., Wilmington, NC, USA). Focus was maintained between time points with the Perfect Focus System, which was turned off during z-series acquisition. Maximum intensity z-projections of the fluorescent signal from stacks assembled from slices (each 0.2 μm thick) at each time point were constructed using ImageJ. Images were optimized for contrast using linear scaling only, and movies of sequential time points were assembled using ImageJ.

GFP-FUS expression in zebrafish embryos

The maintenance of zebrafish and associated experimental procedures were conducted according to an approved Institutional Animal Care and Use Committee (IACUC) protocol. Tricaine stock solution (pH 7.0) was made using 0.4 g ethyl 3-aminobenzoate methanesulfonate salt (Sigma, A5040) plus 2.1 ml 1 M Tris (pH 9.0) in 100 ml of water and stored at −20°C. mRNAs encoding GFP-FUS constructs (WT or mutant) were synthesized using mMessage mMachine SP6 or T7 Ultra kits (Ambion) and stored in 1 mM Na citrate (pH 6.4). mRNAs were diluted with nuclease-free water to 500 ng/μl, and 2–3 nl of the diluted solution was injected into the yolk sac at the 1–2 cell stage of zebrafish eggs from strain crawfish. Embryos were maintained in egg water (60

mg of instant ocean sea salt in 1 l of water containing 0.05% methylene blue) in an incubator at 28.5°C. GFP-FUS fusion proteins were detected at 24–30 hpf either by live embryo GFP imaging or by immunofluorescence. For immunostaining, embryos were dechorionized and fixed for 2 h at room temperature in PBS containing 4% paraformaldehyde, permeabilized with ice-cold acetone for 9 min at −20°C and then washed for 5 min with PBS containing 0.1% Tween-20 (PBS-T) four times at room temperature. Embryos were equilibrated in blocking solution (1% DMSO, 1% BSA, 2% goat serum and 0.05% Triton X-100 in PBS) for 1 h at room temperature and then incubated with mouse anti-TIAR antibody (above, 1:1000 in blocking solution) overnight at 4°C. A rabbit anti-mouse secondary antibody conjugated to Alexa Fluor 568 (Invitrogen A11061, 1:2000) and rabbit anti-GFP antibody conjugated to Alexa Fluor 488 (above, 1:400) were applied for 1 h in blocking buffer at room temperature. Embryos were then rinsed four times in PBS-T for 15 min, and nuclei were stained with Draq5 (DR50200, Biostatus) for 10 min. After wash in PBS-T for 15 min, the whole-body wall region excluding head and yolk sac was isolated and mounted in Prolong Gold Anti-Fade reagent (Invitrogen P36934). Image stacks were acquired in longitudinal orientation from the skin epithelial layer through the somatic muscles to the spinal cord and notochord using a Leica SP1 laser-scanning confocal microscope with a 40× oil objective (NA: 1.25), 100× oil objective (NA: 1.40), 3.44× zoom capability and Leica LCS acquisition software (Version 2.61). For 100× image stacks, each slice was 0.9 μm thick, whereas for 344× image stacks, each slice was 0.4 μm thick. For heat shock experiments,

dechorionized embryos at 25 hpf were incubated at 42.5°C for 45 min in egg water+4% Tricaine stock solution and then immediately fixed in pre-heated PBS containing 4% paraformaldehyde for 10 min at 42.5°C followed by 2 h at room temperature. At least five embryos for each condition were examined, and all experiments were performed at least three times.

Western blots

HEK-293 cells stably or transiently transfected with GFP-FUS constructs were allowed to express FUS for 40 h. Cells were then lysed in 50 mM Tris–HCl (pH 7.5) supplemented with 0.5 M NaCl, 1% NP-40, 1% deoxycholic acid, 0.1% SDS, 2 mM EDTA and complete protease inhibitor (Roche) for 30 min on a rocker at 4°C. A bicinchoninic acid (BCA) assay (ThermoScientific, 23227) was used to quantify the total protein concentration in each lysate, and the indicated amount of total protein in NuPAGE LDS sample buffer (Invitrogen, NP0007) was separated by SDS–PAGE using NuPAGE 4–12% Bis-Tris 1.0 mM precast gels and electrotransferred to PVDF membranes (Millipore, IPFL00010) using the XCell SureLock Mini-Cell system according to the manufacturer's instructions (Invitrogen). Blots were blocked and antibodies diluted with Odyssey Blocking Buffer (LiCor, 927–40000) according to the manufacturer's instructions. Primary antibody incubation conditions were as follows: 1:10 000 dilution of rabbit anti-FUS (Bethyl Laboratories, A300-293A, epitope maps to the region of FUS comprised residues 400–450; we note that the A300-302A antibody,

which maps to FUS residues 1–50, is less reactive for the FUS truncation mutants described herein) and 1:1000 rabbit anti-GAPDH (Sigma, G9545) or a 1:5000 dilution of mouse Living Colors (anti-GFP; Clontech, 632380) and 1:1000 rabbit anti-GAPDH (Sigma, G9545) for 1 h at 25°C. Secondary antibody conditions were as follows: 1:10 000 anti-rabbit IRDye 800 (LiCor, 926-32211) and 1:10 000 anti-rabbit IRDye 680 (LiCor, 926-32220) when probed with anti-FUS/anti-GAPDH or 1:10 000 anti-mouse IRDye 800 (LiCor, 926-32210), and 1:10 000 anti-rabbit IRDye 680 (LiCor, 926-32220) when probed with Living Colors/anti-GAPDH for 1 h at 25°C. Bands were visualized with an Odyssey Infrared Imager (LiCor, Model 9120), and densitometry performed with the Odyssey Software (LiCor, V3.0).

Chapter III

Expression of ALS-linked FUS/TLS mutants inhibits PML nuclear body turnover

III.1 Preface

The following work is the final manuscript in preparation:

Hae Kyung Ko, Sudarsanareddy Lokireddy, Hongru Zhou, Alfred L. Goldberg, and Lawrence J. Hayward

I performed all experiments present here except the experiments for proteasome composition and activity. I performed the cell culture experiments, immunostaining, confocal image acquisition and quantitation, and Western blotting and EdU assays.

III.2 Abstract

Amyotrophic lateral sclerosis (ALS) is a progressive neurodegenerative disease characterized by preferential motor neuron death in the brain and spinal cord. Mutations in FUS/TLS (FUsed in Sarcoma/ Translocated in LipoSarcoma) cause ~4% of familial ALS cases, and the most consistently identified mutations cluster within a nuclear localization signal (NLS) sequence at the FUS C-terminus. While some FUS mutants that perturb the NLS mislocalize to the cytoplasm, others remain predominantly nuclear and may impair motor neuron homeostasis by a gain of toxicity within the nucleus.

We observed that HEK293 cells expressing human FUS mutants (R495X, R521G, or P525L) exhibited enlarged promyelocytic leukemia nuclear bodies (PML-NBs) compared to control cells expressing endogenous FUS or a human WT FUS cDNA. Furthermore, following oxidative insult with arsenic trioxide (ATO) for 24 h, the turnover of PML-NBs was greatly impaired for mutant cells, concomitant with accumulation of the transcriptional repressor Daxx in enlarged PML-NBs. Although the expression of proteasome subunits was not altered, the peptidase activities of 26S proteasomes purified from mutant cells were significantly reduced. Cells expressing FUS mutants also contained larger PML-NBs than controls upon proteasome inhibition with 1 μM MG132. The polyubiquitin-binding protein p62/SQSTM1 colocalized with a fraction of large PML-NBs in FUS mutant cells. Furthermore, we observed that primary fibroblasts from an ALS patient harboring the FUS mutant R521G exhibited enlarged PML-NBs under

baseline conditions and a striking impairment of PML-NB turnover following ATO exposure.

These findings indicate that mutant FUS expression in human cellular models of ALS (i) impairs the turnover of PML-NBs, a vulnerability that can be unmasked further upon ATO exposure, and (ii) leads to an inhibition of proteasome function. Our results reveal a robust yet previously unrecognized nuclear pathology specific to mutant FUS expression at endogenous levels that may contribute to ALS pathogenesis.

III.3 Introduction

Amyotrophic lateral sclerosis (ALS) is a progressive neurodegenerative disease characterized by preferential motor neuron death in the brain and spinal cord (Rowland and Shneider 2001). Affected individuals succumb to complications of weakness that include respiratory failure, typically within 3-5 years after disease onset. While ~10% of ALS cases show familial inheritance (fALS) that may be linked to specific gene mutations, 90% of cases occur sporadically in the context of genetic, epigenetic, or other environmental susceptibilities. The number of genes linked to ALS has increased dramatically over the past decade, and these include nucleic acid binding proteins such as TDP-43 and FUS/TLS, potentially implicating disruption of RNA metabolism in ALS pathogenesis (Sreedharan, Blair et al. 2008, Kwiatkowski, Bosco et al. 2009, Vance, Rogelj et al. 2009).

FUS/TLS (Fused in Sarcoma/ Translocated to liposarcoma) also known as heterogeneous nuclear ribonucleoprotein P2 (hnRNP P2) (Calvio, Neubauer et al. 1995), is a nucleic acid binding protein localized predominantly to the nucleus. FUS comprises several domains including a Q/G/S/Y-rich domain, RGG-rich regions, an RNA recognition motif (RRM), a zinc finger motif and a PY-type nuclear localization signal (PY-NLS) recognized by the nuclear import receptor, Transportin 1 (Dormann, Rodde et al. 2010). More than 50 mutations in the FUS gene are linked to ~4% of fALS (Deng, Gao et al. 2014), and many of these may perturb the PY-NLS to cause cytoplasmic FUS accumulation (Ito, Seki et al. 2011, Kino, Washizu et al. 2011). Cytoplasmic mutant FUS

can be recruited into stress granules upon exposure to thermal, oxidative, or ER stress (Bosco, Lemay et al. 2010, Dormann, Rodde et al. 2010, Ito, Seki et al. 2011, Bentmann, Neumann et al. 2012, Baron, Kaushansky et al. 2013, Daigle, Lanson et al. 2013, Vance, Scotter et al. 2013). Proposed roles of FUS include regulation of RNA splicing (Orozco, Tahirovic et al. 2012), transcription (Tan, Riley et al. 2012), DNA damage repair (Wang, Pan et al. 2013, Rulten, Rotheray et al. 2014), and microRNA processing (Morlando, Dini Modigliani et al. 2012).

Mammalian cell nuclei contain a variety of self-assembled membrane-less nuclear bodies including nucleoli, nuclear speckles and paraspeckles, Cajal bodies, nuclear Gems, histone locus bodies and promyelocytic leukemia nuclear bodies (PML-NBs) (Mao, Zhang et al. 2011). While our understanding of the organization and functions of these nuclear bodies remains incomplete, dysregulation of these bodies has been linked to conditions including neurodegenerative disease and cancer (Zimber, Nguyen et al. 2004, Woulfe 2008, de The, Le Bras et al. 2012). For example, FUS mutant expression in cellular models and human fibroblasts has been reported to be associated with decreased Gem formation (Yamazaki, Chen et al. 2012). Gems normally contain survival motor neuron (SMN) protein and serve functions related to snRNP assembly and RNA splicing (Liu and Dreyfuss 1996, Pellizzoni, Kataoka et al. 1998). Furthermore, acute overexpression of FUS mutants cause axonal defects in cultured cortical neurons associated with mislocalization of SMN into cytoplasmic complexes containing FUS, thereby decreasing axonal SMN (Groen, Fumoto et al. 2013). The RGG motifs of FUS

can interact with the Tudor domain of SMN, and ALS mutants can increase this interaction, potentially dysregulating SMN functions (Sun, Ling et al. 2015). Deficiency of SMN is a hallmark of spinal muscular atrophy (SMA), a childhood-onset motor neuron disease. Gem loss is also associated with a decrease in the number of Cajal bodies and concomitant increase in PML body number in SMA motor neurons (Tapia, Bengoechea et al. 2012), further supporting a role for nuclear bodies in motor neuron homeostasis and survival.

PML protein forms the structural scaffold of PML-NBs, which have been implicated in diverse cellular processes, including in DNA damage response (Dellaire, Ching et al. 2006), apoptosis (Takahashi, Lallemand-Breitenbach et al. 2004, Bernardi, Papa et al. 2008), cellular senescence (Vernier, Bourdeau et al. 2011), gene transcription (Block, Eskiw et al. 2006), and anti-viral response (Everett and Chelbi-Alix 2007). PML is a member of the tripartite motif (TRIM) protein family characterized by structural elements including a RING finger, two B box zinc fingers, and a coiled-coil domains (RBCC motif). This RBCC motif contributes to self-dimerization to form PML-NBs and mediates the binding of PML to the SUMO E2 ligase UBC9 (de The, Le Bras et al. 2012). The PML gene can specify several isoforms by alternative splicing in its carboxyl terminus, and so far seven isoforms have been characterized (Condemine, Takahashi et al. 2006, Bernardi and Pandolfi 2007). A (15;17) chromosomal translocation involving the genes encoding PML and the retinoic acid receptor alpha (RARα) produces a PML-RARα fusion protein that disrupts PML-NB function and triggers the pathogenesis of

acute promyelocytic leukemia (APL). Exposure to low concentrations of arsenic trioxide (As2O3, ATO) was found empirically to promote PML-RARα degradation and thereby improve PML-NB function, contributing to the cure of up to 70% of APL patients (Lallemand-Breitenbach, Zhu et al. 2012). In addition to leukemia, ATO-induced PML degradation is also observed in cultured cell lines (Lallemand-Breitenbach, Jeanne et al. 2008, Geoffroy, Jaffray et al. 2010). Acute exposure in vitro to ATO (1 μM) potentiates PML crosslinking and sumoylation to strongly induce the formation of PML-NBs within 1 h (Jeanne, Lallemand-Breitenbach et al. 2010). Upon prolonged exposure to ATO for >12 h, sumolyated PML and other sumoylated proteins recruited to PML-NBs normally are ubiquitinated by a key SUMO-dependent E3 ubiquitin ligase RNF4, which may target them for degradation via the ubiquitin-proteasome system (Lallemand-Breitenbach, Zhu et al. 2001, Geoffroy, Jaffray et al. 2010, Sahin, Ferhi et al. 2014).

PML-NBs have been shown in the nervous system to influence neurodevelopment and synaptic plasticity (Regad, Bellodi et al. 2009, Butler, Martinez et al. 2013, Korb and Finkbeiner 2013). PML regulates neural progenitor cells in the developing CNS, and PML knockdown decreases cerebral cortex thickness observed at postnatal day 0 (Regad, Bellodi et al. 2009). PML-deficient adult mice also exhibit impaired learning and memory performance (Butler, Martinez et al. 2013). Moreover, neuronal intranuclear inclusions recognized by anti-ubiquitin antibody localize into PML-NBs in affected brain tissues for several neurodegenerative conditions (Woulfe 2008). Expression of polyglutamine expanded mutant ataxin-7 produces intranuclear inclusions of ataxin-7 that

disrupt PML-NBs (Janer, Werner et al. 2010), and induction of PML-NBs with interferon β increases the clearance of mutant ataxin-7 in a transgenic mouse model (Chort, Alves et al. 2013). Interestingly, intranuclear inclusions in some ALS patient tissues show immunoreactivity to PML that could be associated with ALS pathogenesis (Seilhean, Takahashi et al. 2004). While these observations collectively suggest that dysregulation of PML-NB functions may be relevant to neurodegenerative diseases, the potential role of PML-NBs in ALS has not been specifically addressed.

Accumulation of proteins linked to several neurodegenerative diseases may result from impaired activity of the cellular machinery for degradation of misfolded proteins (Goldbaum, Oppermann et al. 2003, Goldberg 2003, Broe, Shepherd et al. 2005, Amador-Ortiz, Lin et al. 2007, Bennett, Shaler et al. 2007, Goldberg 2007, Kristiansen, Deriziotis et al. 2007, Blokhuis, Groen et al. 2013, Jucker and Walker 2013). High concentrations of mutated or misfolded proteins in cells can lead to their aggregation into oligomeric complexes or larger inclusions, which may frequently be ubiquitinated and have been proposed to be toxic to cells (Goldberg 2003, Liu, Wei et al. 2009). The major proteolytic system that blocks the buildup of misfolded proteins prior to aggregation, especially within the nucleus, is the ubiquitin proteasome system (UPS) (Goldberg 2003, Finley 2009). Proteasomes are large ATP-dependent proteolytic complexes that are the primary sites for protein degradation in eukaryotic cells (Goldberg 2003, Finley 2009). The 26S proteasome degrades ubiquitinated proteins selectively through a multistep process that includes conjugate binding to its 19S regulatory complex, substrate deubiquitination,

unfolding and translocation into 20S core particles (Goldberg 2003, Finley 2009). Proteins then are hydrolyzed by three endopeptidase activities located within the 20S core particle (Goldberg 2003, Finley 2009). Impaired proteasome function has been associated with accumulation of misfolded proteins in several different cell models of neurodegenerative diseases (Goldbaum, Oppermann et al. 2003, Bennett, Shaler et al. 2007, Kristiansen, Deriziotis et al. 2007). Furthermore, nuclear proteasomes, including both the 20S proteasome complex and 11S/PA28 regulatory factors, can localize to the vicinity of PML-NBs, suggesting that PML-NBs may serve an important role in nuclear protein quality control (Lallemand-Breitenbach, Zhu et al. 2001, Guo, Giasson et al. 2014).

In this study, we examined how FUS ALS mutants influence the dynamics of PML-NBs in a human ALS cell model and in human ALS primary fibroblasts. We observed that FUS mutants expressed at near-endogenous levels affected the size of PML-NBs under baseline conditions and perturbed their normal turnover during exposure to prolonged oxidative stress. In addition, FUS mutants also inhibited proteasome activity with no apparent reduction in the amount of proteasomes.

III.4 Results

III.4.1 Expression of FUS mutants expanded PML nuclear bodies

To gain insights relevant to pathogenic mechanism caused by FUS mutant expression, we established inducible HEK293 cells expressing GFP-FUS variants from a single genetic locus (Bosco, Lemay et al. 2010). Human FUS variants included wild type (WT) and the ALS-linked mutants R495X, R521G, and P525L (Figure 3-1A). Treatment with doxycycline (2 μg/ml) for 48 h induced GFP-FUS expression at levels comparable to endogenous FUS (Figure 3-1B). Upon detection of GFP-FUS by direct visualization of GFP fluorescence, we observed that the WT and R521G FUS fusion proteins were localized primarily to the nucleus, while the R495X and P525L mutants were prominent both in the nucleus and the cytoplasm (Figure 3-1C), as has been reported previously (Dormann, Rodde et al. 2010, Baron, Kaushansky et al. 2013). We also observed the focal accumulation of intense nuclear GFP-FUS puncta in cells expressing either WT or mutant FUS (Figure 3-1C); similar foci have been reported in association with paraspeckle markers, including PSF, PSP1or p54nrb/NONO (Nishimoto, Nakagawa et al. 2013, Shelkovnikova, Robinson et al. 2014) but not with SMN, coilin, or PML-NBs in cells expressing wild type FUS (Shelkovnikova, Robinson et al. 2014). While we also noted no evidence that GFP-FUS puncta colocalized with PML-NBs, we did observe a significant increase in the fluorescence signal of PML-NBs in FUS mutant cells compared to FUS WT or non-induced control cells (Figure 3-1C). We integrated the fluorescence intensity from confocal slices for voxels comprising individual PML-NBs

using Image J (see Methods) and plotted their cumulative frequency for mutant and control cells (Figure 3-1D). The population of PML-NBs in mutant cells showed significantly greater fluorescence compared to those in control cells (WT or non-induced), with an increase in the median values by 38% and an increase in the values at the 75th percentile by 54% (Figure 3-1D, $p < 0.001$ by Kruskal-Wallis test followed by Dunn's multiple comparison test, n= 77-174 cells per group). The largest PML-NBs, with intensities >20,000 in relative fluorescence units (RFU), were observed in >50% of cells expressing FUS mutants but were much less frequent in control cells (Figure 3-1E). The presence of enlarged PML-NBs upon FUS mutant expression was independent of whether FUS remained primarily nuclear (R521G) or mislocalized partially to the cytoplasm (R495X and P525L). However, the number of PML-NBs per cell did not change significantly (Figure 3-1F), which was consistent with a larger size rather than an increased number of PML-NBs. These results suggested an association between FUS mutant expression and expansion of the PML-NB compartment, which we decided to explore further.

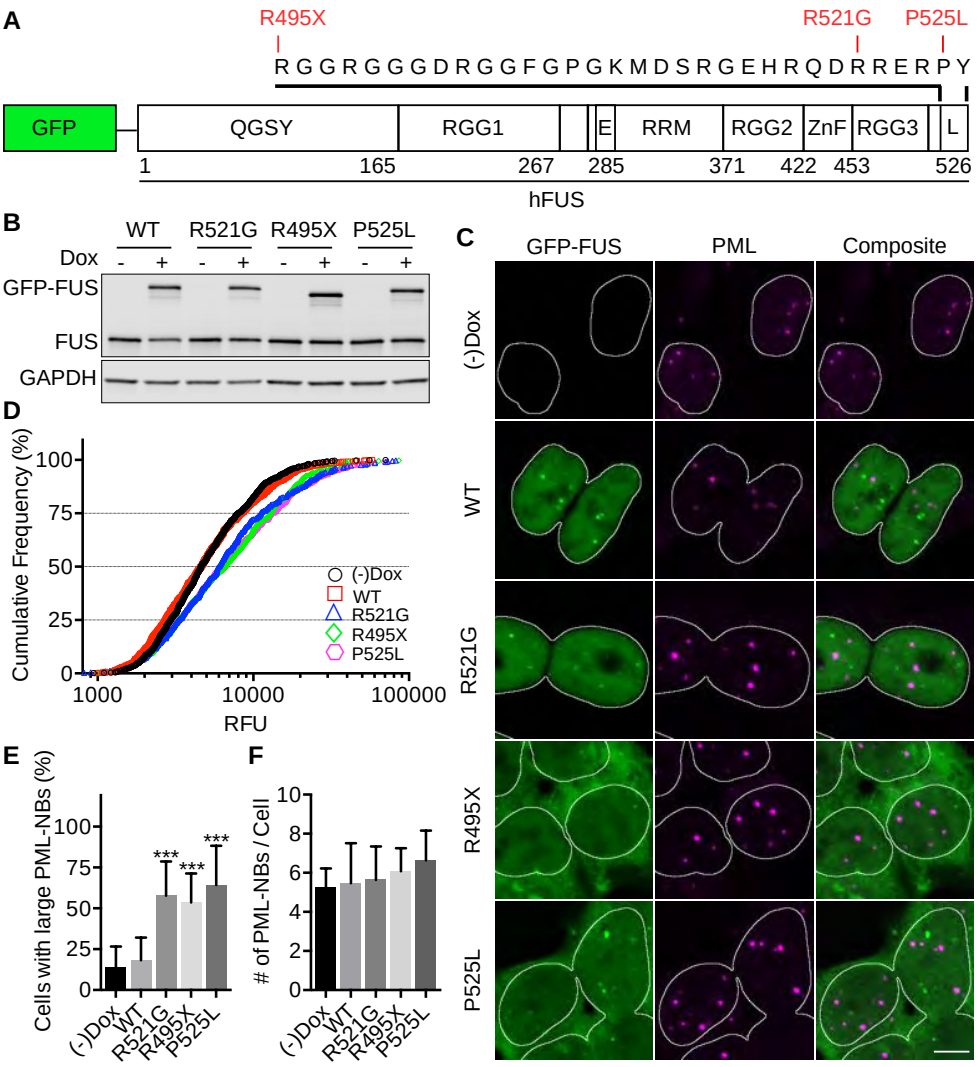

Figure 3-1 HEK293 cells expressing FUS mutants exhibited large PML-NBs.

(A) FUS contains several domains including a Gln-Gly-Ser-Tyr (QGSY)-rich region, three Arg-Gly-Gly (RGG)-rich regions, an RNA recognition motif (RRM), a zinc-finger motif (ZnF) and a PY-type of nuclear localization signal (L). Human FUS (hFUS) -WT and ALS-linked mutant constructs (R495X, R521G and P525L) were fused to GFP and stably inserted into a single locus for inducible expression in HEK293 cells. **(B)** Western blots of cellular lysates (5 µg of protein loaded per lane) using anti-FUS detected endogenous FUS and induction of GFP-FUS with doxycycline (Dox) treatment. **(C)** PML-NBs were identified in maximum-intensity confocal z-projections from HEK293 cells immunostained with anti-PML antibody. Nuclei were outlined based on DAPI staining, and GFP-FUS was detected by GFP fluorescence. Scale bar, 5µm. **(D)** Cumulative frequency plot of PML-NB intensities (in relative fluorescence units, RFU) showed that the fluorescence of PML-NBs from mutant cells was larger compared to that from control cells (77-174 cells were analyzed from seven independent experiments, $p < 0.001$). **(E)** Cells containing large PML-NBs (integrated intensity > 20,000 RFU) were more frequent for mutant compared to control cells (shown are mean ± S.D.; ***, $p < 0.001$ compared to controls). **(F)** The number of PML-NBs per cell did not differ between mutant and control cells (shown are mean ± S.D.).

III.4.2 FUS mutant expression inhibited the turnover of PML-NBs

PML-NBs are highly dynamic structures implicated in the regulation of stress responses, DNA repair pathways, cellular senescence, and apoptosis (Sahin, Ferhi et al. 2014). Under oxidative conditions in vivo, disulfide crosslinking of PML proteins organizes the physical scaffold for PML-NBs (Ishov, Sotnikov et al. 1999). We therefore examined how FUS mutants might affect the dynamic behavior of PML-NB formation and turnover upon exposure to mild oxidative stress.

Cells were treated with a low concentration of ATO (1 μM) for 1 h to stimulate PML-NB assembly after 48 h induction of GFP-FUS variants (Figure 3-2). As shown in Figure 3-2, we observed a robust increase in PML incorporation into PML-NBs within 1 h after ATO exposure for the WT and (-)Dox control cells. The extent of acute PML-NB formation in controls was similar to that observed for the mutant cells before treatment, while PML-NBs in the mutant cells only mildly increased further. This suggests that competency to respond acutely to the stress imposed by ATO seen in the control cells may be blunted in the mutant cells, possibly related to the increase in their constitutive PML-NB activation. Moreover, upon longer exposure to ATO (24 h), the PML signal within nuclear bodies decreased in FUS WT and (-)Dox control cells by 32% at the median and by 46% at the 75^{th} percentile compared to 1 h ATO-treated control cells ($p<0.001$), as expected following the induction of ATO-triggered turnover. The fluorescence of PML-NBs in mutant cells after ATO for 24 h increased further by 50% at the median and 103% at the 75^{th} percentile compared to 1 h ATO treated mutant cells

(Figure 3-2B, $p < 0.001$ by Kruskal-Wallis test followed by Dunn's multiple comparison test).

The fraction of control cells harboring one or more large PML-NBs increased from <20% at baseline to >80% after 1 h ATO exposure, returning to only ~30% after 24 h ATO (Figure 3-2C). In contrast, >50% of cells expressing ALS mutants exhibited large PML-NBs before ATO treatment, and this fraction increased further and was maintained following treatment (Figure 3-2C). For all cell lines, the number of PML-NBs per cell increased significantly after 1 h ATO compared to untreated cells, while the number of PML-NBs per cell returned to pre-treatment levels after 24 h ATO (Figure 3-2D). Soluble PML protein recruited to PML-NBs is thought to partition away from a diffuse nuclear fraction and associate with a highly insoluble nuclear matrix fraction (Lallemand-Breitenbach, Zhu et al. 2001). Consistent with this, the accumulation of PML protein in the RIPA buffer insoluble pellet (P) fraction for FUS mutant cells compared to FUS WT cells was increased by 2.1 ± 0.4 fold after ATO treatment for 24 h (Figure 3-2E).

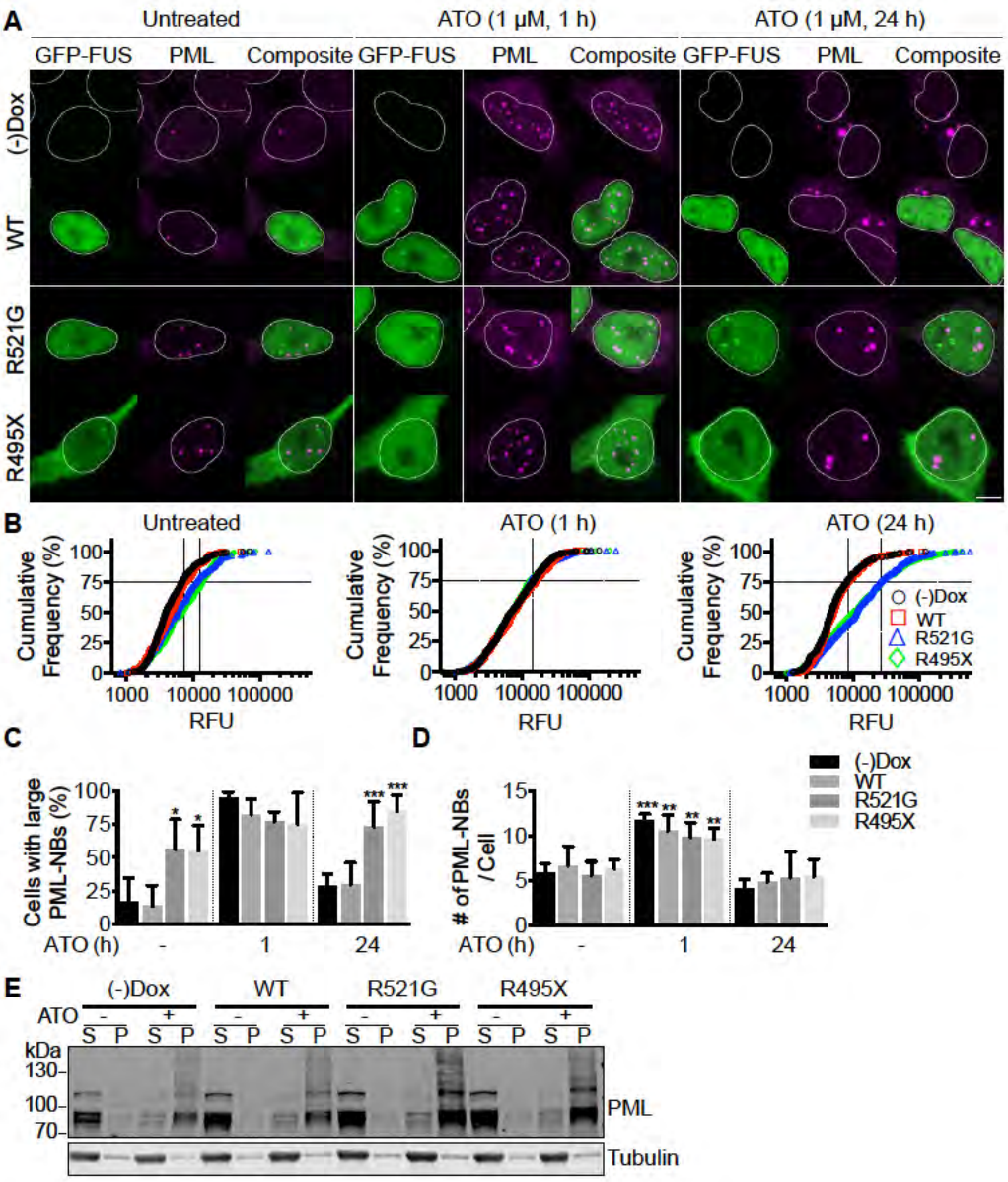

Figure 3-2 Expression of FUS mutants inhibited PML-NB turnover upon ATO treatment.

Figure 3-2 Expression of FUS mutants inhibited PML-NB turnover upon ATO treatment.

(A) HEK293 cells treated with ATO (1 μM) showed enlargement of PML-NBs after 1 h and divergent properties for mutant compared to control cells after exposure for 24 h. Shown are maximum-intensity z-stacks of GFP fluorescence and anti-PML antibody staining. Nuclei were outlined based on DAPI staining. Scale bar, 5μm. **(B)** Cumulative frequency plots show the intensities of individual PML-NBs on a log scale in untreated cells (left, n=43-64 cells) or those treated with ATO for 1 h (middle, n=44-69 cells) or 24 h (right, n=70-100 cells). Guide lines indicate 75th percentile RFU values. **(C)** The fraction of mutant cells containing large PML-NBs (>20,000 RFU) was increased in the absence of ATO (two way ANOVA with Sidak's multiple comparison test; *, $p < 0.05$ compared to controls). Acute treatment with ATO for 1 h increased the fraction of all cells expressing large PML-NBs, which was maintained for mutant cells after ATO treatment for 24 h (***, $p < 0.001$ compared to controls). Shown are mean ± S.D. **(D)** ATO treatment for 1 h increased the number of PML-NBs per cell (two way ANOVA followed by Tukey's multiple comparison test; **, $p < 0.01$;, ***, $p < 0.001$ compared to untreated). **(E)** Cell lysates were separated into RIPA soluble (S) or pellet (P) fractions following no treatment or 1 μM ATO for 24 h. Western blot showed increased PML accumulation in the RIPA-insoluble pellet of mutant cells after ATO.

A fraction of the PML protein in cells treated with ATO for 24 h redistributed into large cytoplasmic aggregates just outside the nuclear membrane both in control and mutant cells (Figure 3-2A and 3-3A). Such cytoplasmic assemblies of PML have been reported following mitosis in other cell lines, and these are stabilized in the presence of ATO, which inhibits the re-importation of PML during the cell cycle G1 phase (Lang, Grudic et al. 2012). To determine whether the rate of cell proliferation differed between our mutant and control cell lines in the absence or presence of ATO, we measured 5-ethynyl-2'-deoxyuridine (EdU) incorporation over 1 h (Figure 3-3B). Under baseline growth conditions, a decrease in the fraction of cells incorporating EdU was observed for FUS mutant cells compared to controls. After treatment with ATO for 24 h, both mutant and control cells showed a similar decrease in EdU incorporation. Overall, these results suggested that FUS mutant expression may slow the cellular proliferation rate at baseline and that prolonged ATO exposure decreases the proliferation of control cells to a rate comparable to that of the mutant cells. This implies that mechanisms distinct from altered proliferation may contribute to the observed increase in PML-NB expansion in mutant cells following ATO treatment.

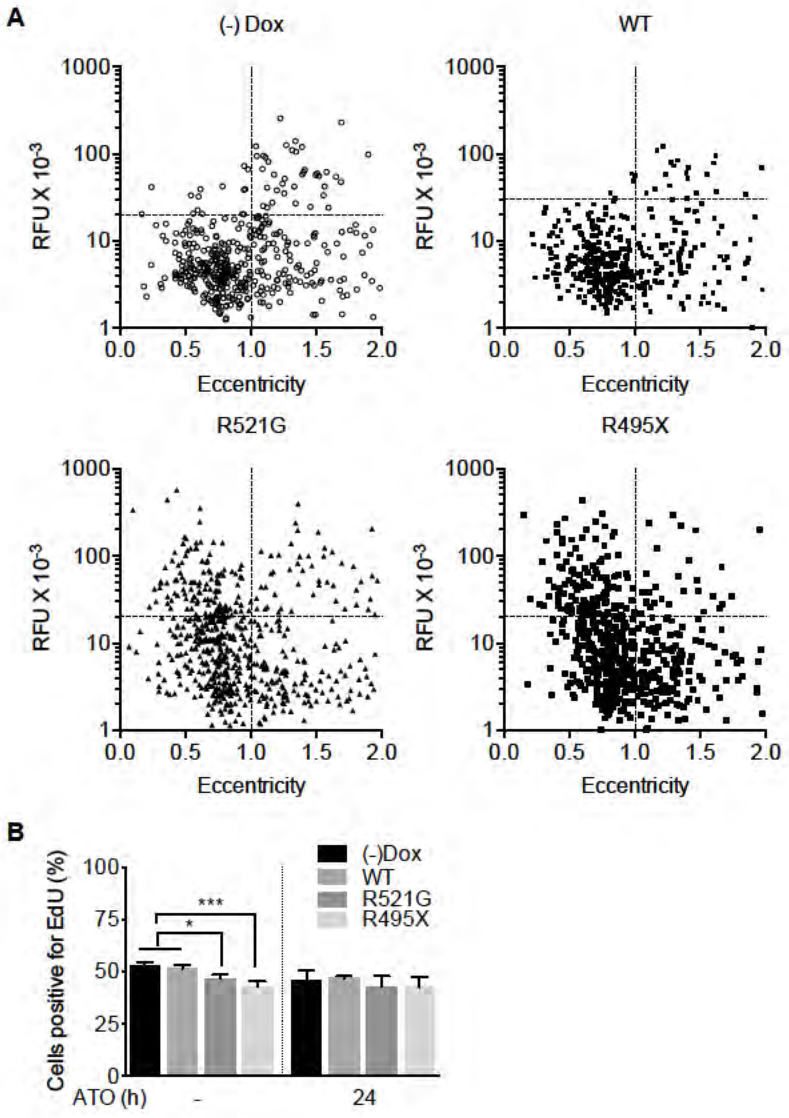

Figure 3-3 HEK293 cells expressing FUS mutants exhibited a population of large PML-NBs that were largely absent from control cells.

(A) The fluorescence intensities of individual PML foci following ATO treatment for 24 h are plotted on a log scale with respect to their position inside or outside the nucleus. Eccentricity was defined as the radial position of each PML focus along a vector in 3D space extending from the center of the nucleus (E=0) through the center of each PML focus and continuing to the nuclear membrane (E=1). Eccentricity values >1 indicate cytoplasmic localization of PML foci. **(B)** EdU incorporation was decreased in FUS mutant cells compared to controls. Shown are mean ± S.D., n= 551-987 cells from three independent experiments. *, $p < 0.05$; ***, $p < 0.001$.

III.4.3 Enlarged PML-NBs in FUS mutant cells recruited Daxx

PML-NBs dynamically sequester a variety of partner proteins, including transcription factors, post-translational modifiers, DNA repair proteins, and viral components that may influence cellular homeostasis (Hofmann and Will 2003, Sahin, Ferhi et al. 2014). Since the PML-NB scaffold forms, proteins capable of undergoing sumoylation are attracted to the site via SUMO-interaction motif (SIM) domains on PML and related components. For example, the death domain-associated protein Daxx is a transcriptional repressor known to localize into PML-NBs (Li, Leo et al. 2000), and Daxx-PML interactions can induce apoptosis (Zhong, Salomoni et al. 2000, Bernardi and Pandolfi 2003, Bernardi, Papa et al. 2008). Also, an increased number of Daxx-containing nuclear bodies was observed in spinal cord motor neuron sections from presymptomatic transgenic mice expressing ALS mutants of SOD1 (G93A or G85R), supporting a role for Daxx in a signaling pathway relevant to motor neuron death (Raoul, Buhler et al. 2006).

We next examined whether PML-NBs induced by ATO treatment accumulated Daxx. While Daxx was expressed throughout the nucleoplasm and to a lesser degree in the cytoplasm in cells at baseline, Daxx became more concentrated in PML-NBs within 2 h upon ATO treatment (Figure 3-4A). Following exposure to ATO for 6-12 h in control cells, Daxx resumed a diffuse nuclear distribution (not shown), which was maintained even after 24 h of ATO (Figure 3-4A). In contrast, large PML-NBs in cells expressing FUS mutants maintained strong colocalization with Daxx after 24 h ATO (Figure 3-4A).

We quantified Daxx colocalization as a function of PML-NB intensity and found that the PML-NBs with the strongest fluorescence were most likely to maintain colocalization with Daxx (Figure 3-4B). The median intensity of PML-NBs colocalized with Daxx was greater for cells expressing FUS-R521G (by 3.9-fold) or FUS-R495X (by 4.2-fold) compared to FUS-WT (Figure 3-4C). Next, we analyzed whether Daxx accumulation affected cell viability after treatment with 1-5 μM ATO using a luciferase reporter assay to indicate ATP production in metabolically active cells. ATO exposure for 24 h did not differentially impair the viability of HEK293 cells expressing FUS mutants (Figure 3-4D). This agrees with our previous study that indicated a lack of vulnerability to oxidative stress for these cells (Bosco, Lemay et al. 2010).

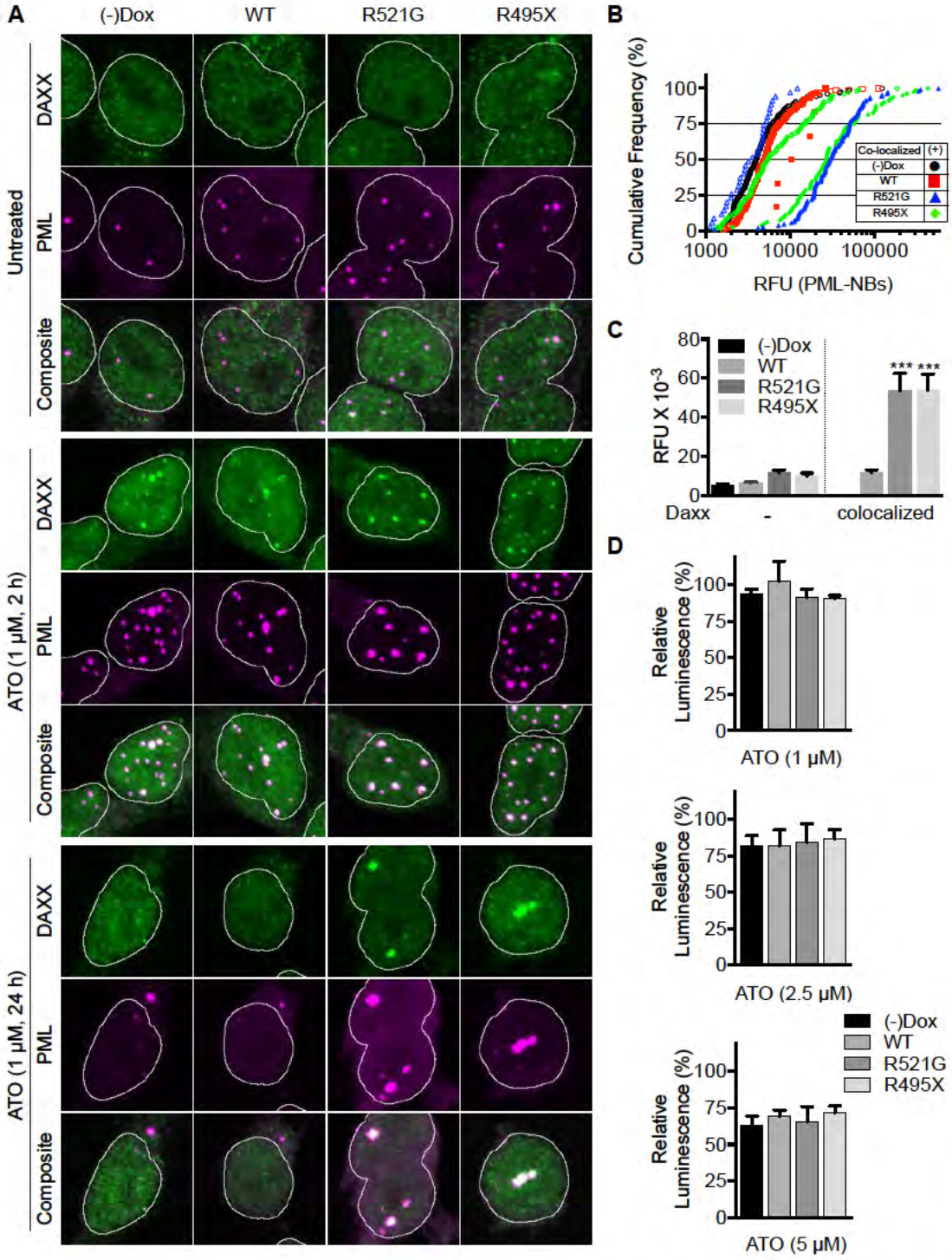

Figure 3-4 ATO induced localization of Daxx into large PML-NBs in FUS mutant cells.

Figure 3-4 ATO induced localization of Daxx into large PML-NBs in FUS mutant cells.

HEK293 cells were treated with 1 μM ATO for 24 h, and confocal z-stack images show localization of Daxx into large PML-NBs. Scale bar, 5μm. **(B)** Individual PML-NBs were sorted in 3D into those that colocalized with Daxx (solid symbols) and those that did not colocalize (open symbols). Shown are the PML-NB intensity distributions for each group. **(C)** The fluorescence intensity of PML-NBs that colocalized with Daxx (from n=29-61 cells) was greater for mutant compared to control cells. Shown are mean ± S.E.M. from three independent experiments. ***, $p < 0.001$. **(D)**Treatment with 1-5 μM ATO for 24 h did not differentially affect the viability of FUS mutant compared to control cells. Shown are mean ± S.D. from three independent experiments.

PML-NBs also facilitate the ubiquitination of sumoylated proteins by the SUMO-dependent E3 ubiquitin ligase RNF4, which targets proteins to nuclear proteasomes for degradation (Lallemand-Breitenbach, Zhu et al. 2001, Lallemand-Breitenbach, Jeanne et al. 2008, Maroui, Kheddache-Atmane et al. 2012). One plausible mechanism to account for the observed increase in PML-NB size at baseline and the defect in PML-NB turnover after ATO could involve impaired recruitment of proteasomal subunits or regulators to PML-NBs in mutant-expressing cells. For instance, it has been shown that PML mutants (K160R or triple K65/160/490R) shows impaired degradation/turnover related to decreased accumulation to PML-NBs of the 11S proteasome regulator (comprising PA28αβ mixed heptamers), the 20S proteasome, or ubiquitin (Lallemand-Breitenbach, Zhu et al. 2001, Lallemand-Breitenbach, Jeanne et al. 2008). Therefore, we tested whether FUS mutant expression affected 11S proteasome regulator recruitment to PML-NBs and observed strong colocalization between PML-NBs and the 11S regulator (detected with anti-PA28β antibody) in all of our cell lines (Figure 3-5). Even after ATO treatment for 24 h, the 11S regulator remained localized to large PML-NBs in cells expressing FUS mutants (Figure 3-5A). Cumulative frequency analysis confirmed that the 11S regulator colocalized persistently with the larger PML-NBs in cells after exposure to ATO for 24 h (Figure 3-5B). In addition, the median intensity of these PML-NBs colocalized with the 11S regulator was greater for cells expressing FUS-R521G (by 3.7-fold) or FUS-R495X (by 3.3-fold) compared to control cells (Figure 3-5C).

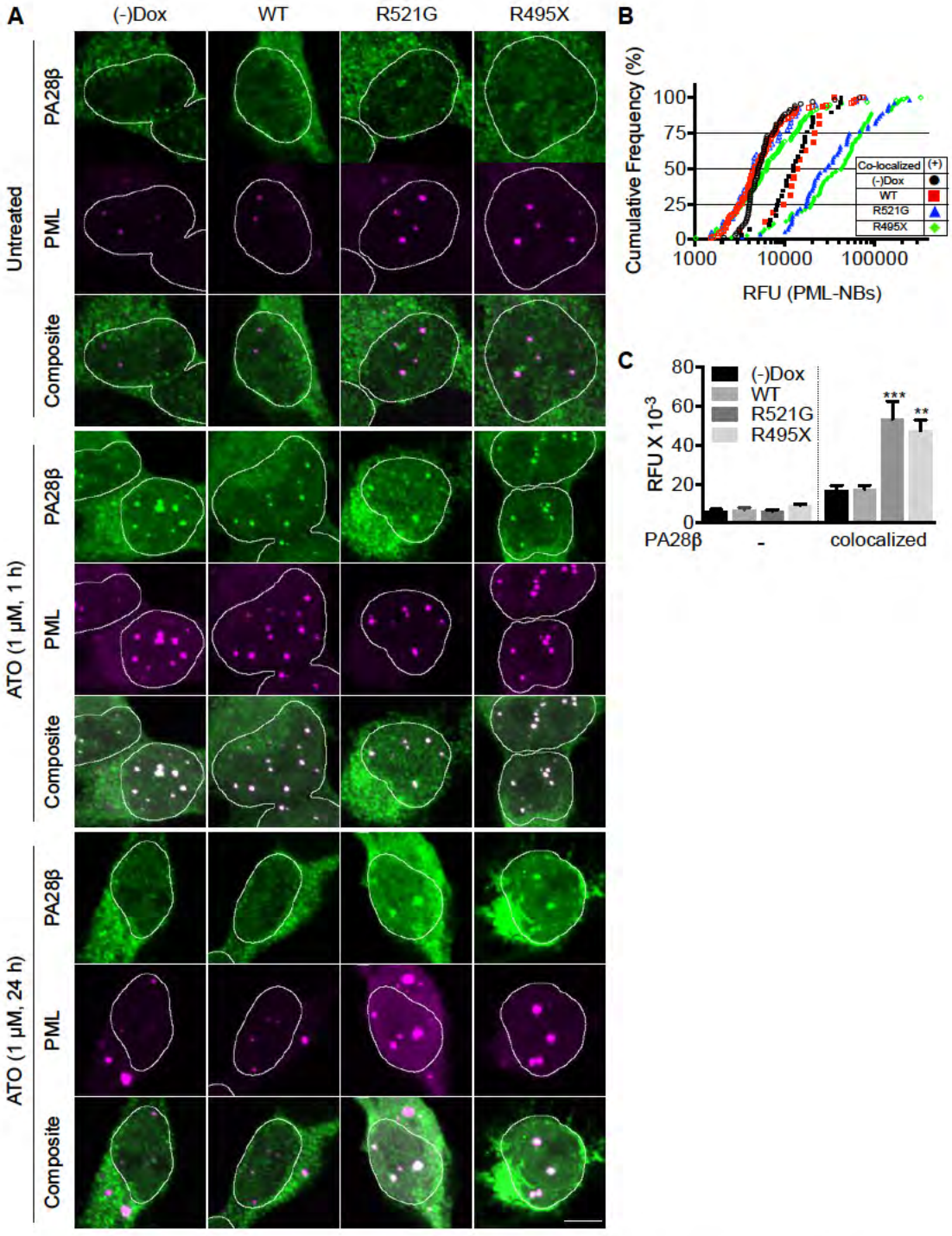

Figure 3-5 ATO triggered accumulation of 11S/PA28 into large PML-NBs in FUS mutant cells.

Figure 3-5 ATO triggered accumulation of 11S/PA28 into large PML-NBs in FUS mutant cells.

(A) HEK293 cells were treated with 1 μM ATO for 24 h, and confocal z-stack images show localization of 11S/PA28 regulator into large PML-NBs. Scale bar, 5μm. **(B)** Individual PML-NBs were sorted in 3D into those that colocalized with 11S/PA28 (solid symbols) and those that did not colocalize (open symbols). Shown are the PML-NB intensity distributions for each group. **(C)** The fluorescence intensity of PML-NBs that colocalized with 11S/PA28 (from n=27-39 cells) was greater for mutant compared to control cells. Shown are mean ± S.E.M. from three independent experiments. **, $p < 0.01$; ***, $p < 0.001$.

III.4.4 Mutant FUS expressions reduces 26S proteasome activities

We considered the possibility that mutant FUS expression might impair proteasome activities, which could contribute to the defect in PML-NB turnover following ATO treatment as shown above. We did not observe any obvious difference in 26S proteasome subunit component levels including PA200, Rnp2, Rpt5, Rpn13 and MCP in both total lysate and affinity-purified 26S proteasomes from FUS mutant cells compared to (-)Dox and FUS-WT cells (Figure 3-6B). However, affinity-purified 26S proteasomes from cells expressing FUS mutants did show decreases in all three peptidase activities compared to cells with comparable WT FUS expression, including chymotrypsin-like activity (by 21 ± 5%) assayed with suc-LLVY-amc, caspase-like activity (by 36 ± 18%) with suc-nLPnLD-amc, and trypsin-like activity (by 19 ± 6%) with suc-VLR-amc (Figure 3-6A). These findings would suggest that protein breakdown by the ubiquitin-proteasome pathway is impaired in the cells expressing FUS mutants. To test this prediction, we transfected cells with the cDNA encoding Ub-G76V-GFP, a ubiquitin fused degradation (UFD) substrate that is rapidly degraded by this pathway (Dantuma, Lindsten et al. 2000). As shown in Figure 3-6C, overexpression of FUS mutants caused the accumulation of UFD substrate above levels in control cells.

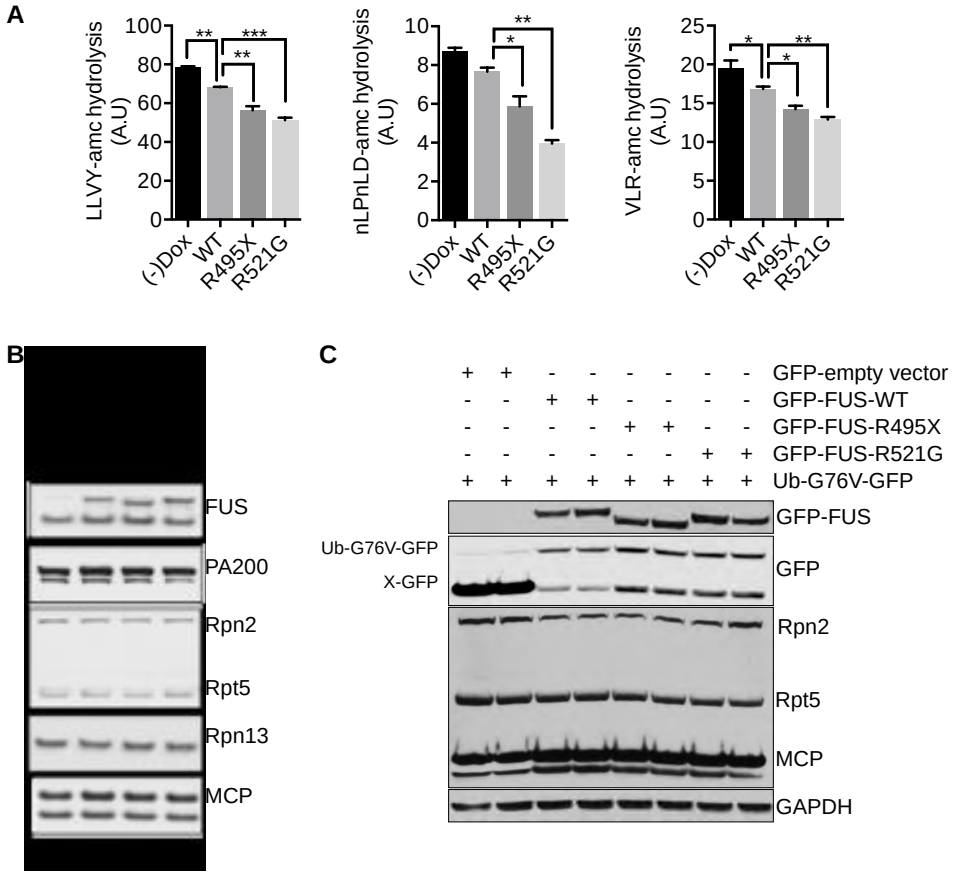

Figure 3-6 FUS variant overexpression reduced 26S proteasome activities

(A) 26S proteasomes were purified from HEK293 cells, and their peptidase activities including the chymotrypsin-like activity assayed with suc-LLVY-amc, caspase-like activity with suc-nLPnLD-amc, and trypsin-like with suc-VLR-amc were measured. Shown are means ± S.D. **(B)** No apparent difference was evident in the subunit composition of proteasomes purified by the UBL affinity method as shown by Western blot of total lysate analyzed against FUS, PA200/Blm10, Rnp2, Rpt5, Rpn13 and MCP. **(C)** Overexpression of FUS variants caused accumulation of a UPS pathway reporter substrate, Ub^{G76V}-GFP. HEK293 cells were transfected with Ub^{G76V}-GFP cDNA, and levels of GFP, FUS, Rpn2, Rpt5 and MCP were analyzed by immunoblotting. *, $p < 0.05$; **, $p < 0.01$; ***, $p < 0.001$.

One additional possible consequence of impaired proteasome activities is the accumulation of ubiquitinated proteins in cells. However, we found no evidence for increased ubiquitinated proteins in either the Triton X-100 soluble (A) or insoluble (B) fractions (Figure 3-7). Interestingly, we observed a significant increase in the accumulation of sumolyated proteins detected by anti-SUMO2/3 antibody in Triton X-100 insoluble fractions after expression of FUS mutants (Figure 3-7B).

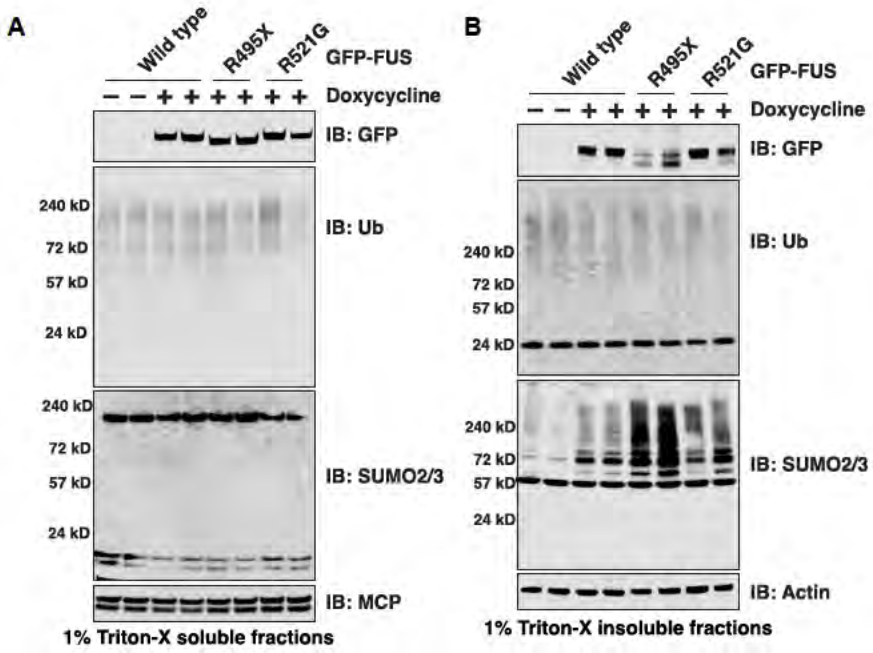

Figure 3-7 Expression of mutant FUS did not affect proteasome subunit expression or ubiquitinated protein accumulation.

Total levels of ubiquitinated and sumoylated proteins were detected in both Triton X-100 soluble **(A)** and insoluble fractions **(B)** after induction of FUS variants in HEK293 cells. Loading controls: MCP for the 1% Triton-X100 soluble fraction, actin for the 1% Triton-X100 insoluble fraction.

III.4.5 Inhibition of proteasome activity with MG-132 increased the size of PML-NBs in FUS mutant cells

Impaired PML-NB turnover could be consistent with possible dysfunction of nuclear protein homeostasis. We next asked whether inhibition of the proteasome with MG132 (1 μM) could also cause a similar enlargement of PML-NBs. HEK293 cells were exposed to MG132 for 24 h and stained with anti-PML antibody (Figure 3-8A). First, we examined if 1 μM of MG132 treatment induced the incorporation of FUS mutants into stress granules because others have shown that much stronger treatment with MG132 (10 μM) induces stress granule formation in HeLa cells (Mazroui, Di Marco et al. 2007). However, 1 μM MG132 for 24 h did not alter FUS localization (Figure 3-8A). Second, MG132 at 5-10 μM has been reported to increase the number of PML-NBs observed in cultured cells (Everett, Earnshaw et al. 1999, Kurki, Latonen et al. 2003). Notably, we also found that 1 μM MG132 treatment increased the number of PML-NBs per cell, but only for FUS-WT cells (Figure 3-8C). Interestingly, the integrated fluorescence intensities of PML foci in FUS mutant cells increased following MG132 treatment (Figure 3-8B) in a manner that resembled our observations in cells treated with ATO (Figure 3-2). MG132 treatment increased the average fluorescence intensity of PML-NB by >2-fold in FUS mutant cells compared to cells expressing WT FUS (Figure 3-8B). PML-NB fluorescence in mutant cells increased by 46% at the median and by 73% at the 75th percentile compared to control cells ($p < 0.001$ by Kruskal-Wallis test followed by Dunn's multiple comparison test). In contrast, 1 μM MG132 treatment did not change the

integrated intensity distribution of PML foci in FUS-WT cells. Our results are consistent with chronic proteasome inhibition in FUS mutant cells as a possible contributing factor in the enlargement of PML-NBs.

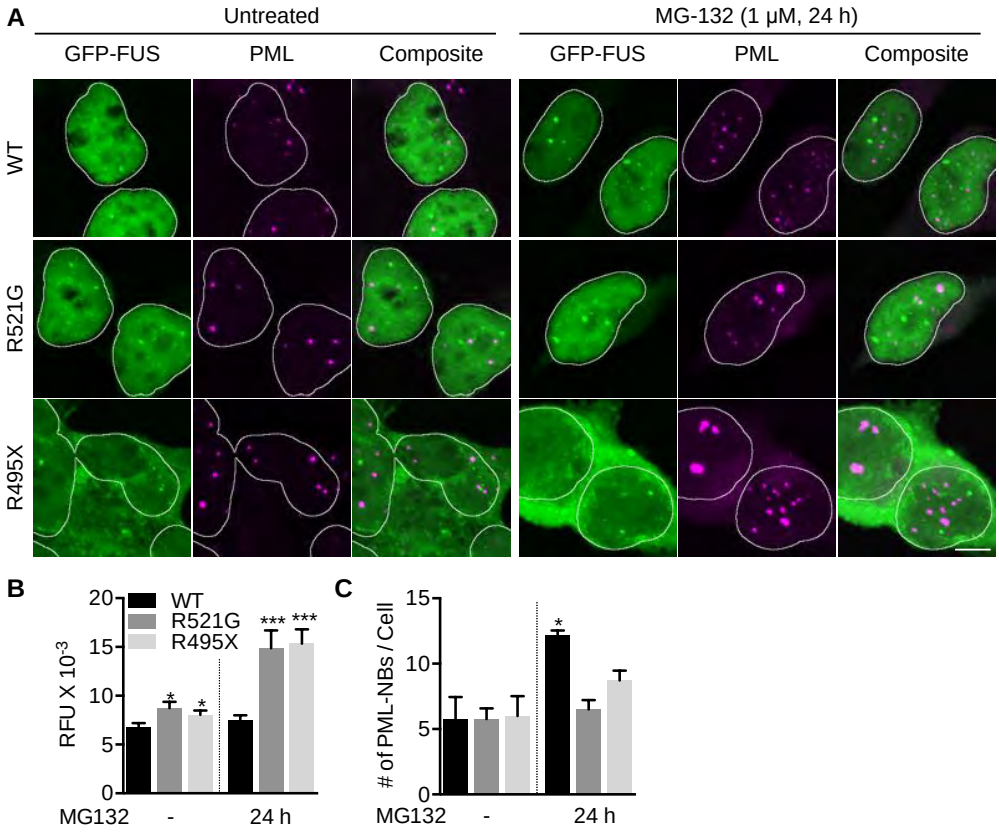

Figure 3-8 FUS variant overexpression reduced 26S proteasome activities and enlarged PML-NBs after MG-132 treatment.

(A) Confocal image z-stacks show HEK293 cells treated with 1 μM MG132 for 24 h and stained with anti-PML antibody. Scale bar, 5μm. **(B)** MG132 caused an increase in the average intensity of PML-NBs in FUS mutant cells. Shown are mean ± S.E.M. **(C)** The number of PML-NBs per cell increased after MG-132 treatment for FUS-WT cells. Shown are mean ± S.D. n= 53-69 cells from three independent experiments. *, $p < 0.05$; ***, $p < 0.001$.

III.4.6 FUS mutant cells increased abnormal nuclear p62 accumulation

Protein aggregation is a hallmark in several neurodegenerative diseases, including ALS (Ross and Poirier 2004, Blokhuis, Groen et al. 2013, Jucker and Walker 2013). Proteasome subunits, chaperones, ubiquitin and p62/SQSTM1 can be major components in these inclusions, which may form when the production of misfolded proteins exceeds their rate of clearance. While we did not detect increased polyubiquitinated protein accumulation in Triton X-100 insoluble fractions (Figure 3-7B), we examined whether HEK293 cells expressing mutant FUS might show an increase in p62/SQSTM1 foci. We induced FUS variants with Dox for 48 h in HEK293 cells and stained with anti-p62 antibody (Figure 3-9A). In addition to cytoplasmic p62, we observed both diffuse and focal immunoreactivity to p62 within the nucleus. Increased nuclear foci containing p62 were present in FUS mutant cells compared to controls (Figure 3-9B). Next, we analyzed the expression levels of p62 by Western blotting of nuclear and cytoplasmic fractions as a function of RIPA solubility (Figure 3-9D and Figure 3-9E). These results showed that the more prominent p62 foci in the nucleus of FUS mutant cells were not related to any increase in total expression of p62. Previously, p62 nuclear foci in HeLa cells were reported to co-localize with PML-NBs (Pankiv, Lamark et al. 2010). In that system, siRNA-mediated knockdown of p62 inhibited the accumulation of polyubuquitinated proteins into PML-NBs upon treatment with the CRM1 inhibitor leptomycin B, which suggested that p62 may be a critical factor to recruit polyubiquitinated proteins into PML-NBs (Pankiv, Lamark et al. 2010). We asked whether PML-NBs in HEK293 cells

expressing FUS variants colocalized with p62 and found this to be true, especially for large PML-NBs in FUS mutant cells (Figure 3-9C).

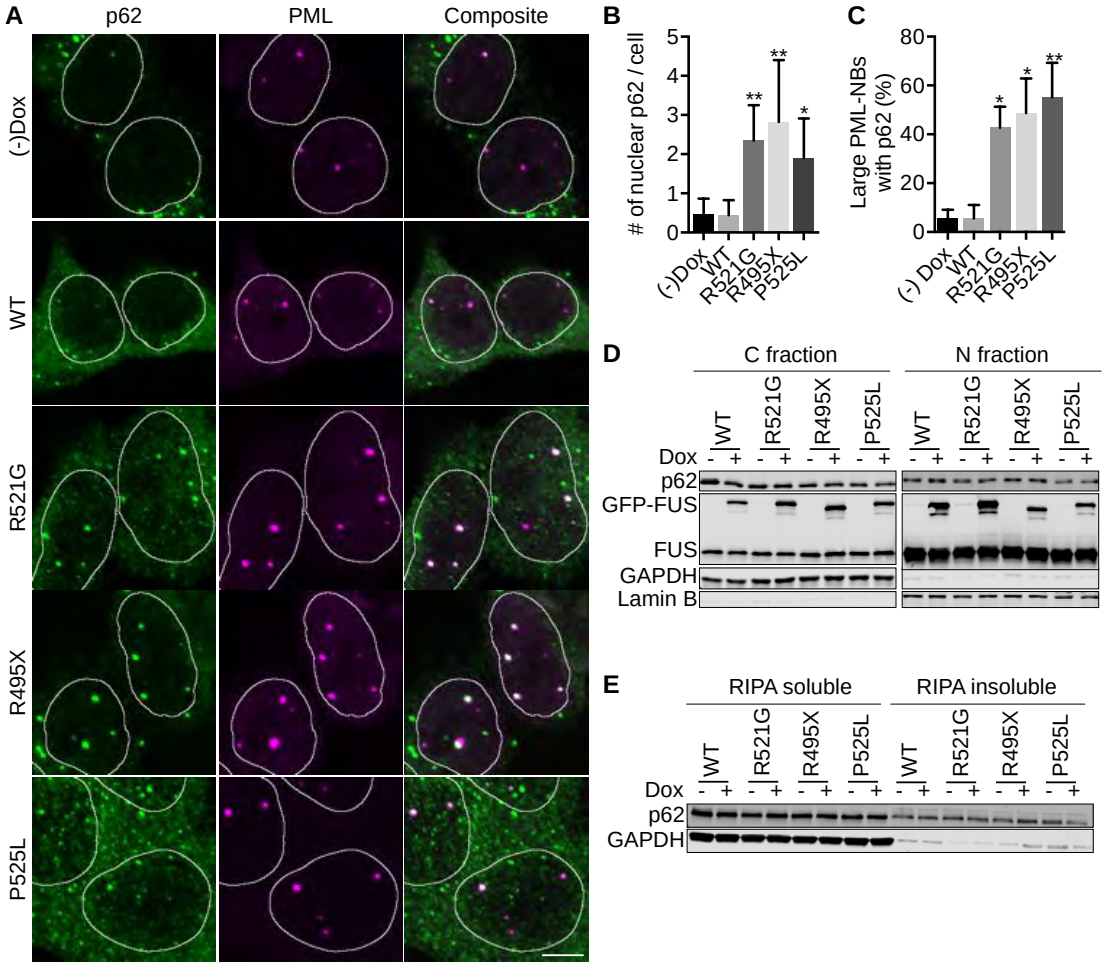

Figure 3-9 Expression of FUS mutants increased the accumulation of nuclear p62/ SQSTM1 foci near large PML-NBs.

(A) Confocal image z-stacks showed partial overlap of PML and p62 immunofluorescence staining. Scale bar, 5µm. **(B)** FUS mutant cells showed an increase in nuclear p62 foci per cell compared to controls (n= 34-87 cells from >3 independent experiments). **(C)** More than 40% of large PML-NBs (integrated intensity > 20,000 RFU) colocalized with p62 in FUS mutant cells. **(D)** Western blotting of subcellular protein fractions showed no obvious change in nuclear or cytoplasmic p62 expression levels for mutant cells. **(E)** p62 levels did not change in RIPA-soluble or RIPA-insoluble fractions. Shown in **(B)** and **(C)** are mean ± S.D.; *, $p < 0.05$, **, $p < 0.01$.

III.4.7 ALS patient fibroblasts exhibited impaired PML-NB degradation upon ATO exposure

We next analyzed PML-NB properties in human fibroblasts harboring the FUS-R521G mutation. While control cells expressed FUS almost exclusively in the nucleus, FUS-R521G fibroblasts exhibited only subtle cytoplasmic mislocalization of FUS (Figure 3-10A). The integrated fluorescence intensity of PML-NBs in fibroblasts was analyzed using the same method as for HEK293 cells. The intensity of PML-NBs in FUS mutant fibroblasts under basal conditions increased by 62% at the median and by 67% at the 75th percentile compared to control cells (Figure 3-10B). Consistent with the results observed in HEK293 cells, PML-NB turnover was strikingly impaired in FUS-R521G fibroblasts compared to controls (Figure 3-10A and Figure 3-10B). While the intensity of PML-NBs decreased in control cells, PML-NB fluorescence in fibroblast-R521G cells increased by 4.8-fold at the median and by 7.7-fold at the 75th percentile compared to control cells (Figure 6B, $p< 0.001$ by Kruskal-Wallis test followed by Dunn's multiple comparison test). While ~50% of cells expressing the R521G mutant exhibited large PML-NBs at baseline, only ~2.5% of control cells expressed large PML-NBs (Figure 3-10C). This fraction in FUS mutant cells increased further following ATO treatment, but only ~10% of control cells harbored large PML-NBs after ATO for 24 h (Figure 3-10C). The number of PML-NBs per cell in FUS-R521G fibroblasts was only modestly increased compared to control cells under baseline conditions (Figure 3-10D). ATO treatment for 24 h

decreased the average number of PML-NBs significantly in both control and FUS mutant cells (Figure 3-10D).

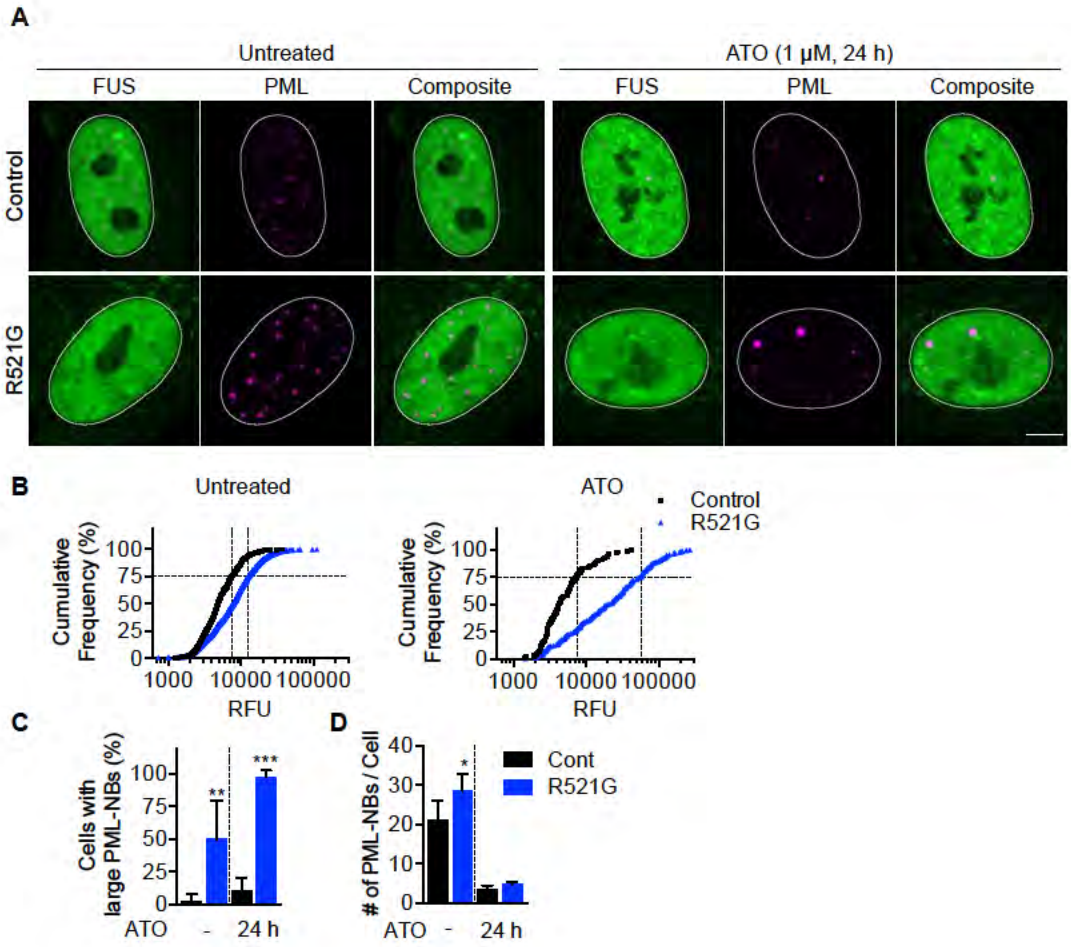

Figure 3-10 Human fibroblasts harboring the FUS-R521G mutant showed enlarged PML-NBs and impaired PML-NB turnover.

(A) Confocal z-stack maximum projections immunostained for FUS and PML showed larger PML-NBs in mutant compared to control fibroblasts. Scale bar, 5μm. **(B)** The population of individual PML-NBs in mutant fibroblasts showed greater fluorescence intensity both in the untreated condition and following 24 h exposure to ATO ($n > 34$ cells, $p < 0.001$ for both conditions from three independent experiments). Guide lines indicate 75th percentile RFU values. **(C)** A majority of FUS mutant fibroblasts contained large PML-NBs with integrated intensity > 25,000 RFU. **(D)** The number of PML-NBs per fibroblast nucleus increased only modestly in cells expressing FUS-R521G. Shown in **(C)** and **(D)** are mean ± S.D.; *, $p < 0.05$; **, $p < 0.01$; ***, $p < 0.001$.

3.5 Discussion

In this study, we examined the dynamics of PML-NBs in a cellular ALS model expressing GFP-FUS variants and in primary human fibroblasts expressing endogenous mutant FUS. Our main observations upon FUS mutant expression include an enlargement of PML-NBs in the absence of imposed stress, failure to disassemble or degrade PML-NBs following sustained ATO exposure, recruitment of Daxx and the 11S proteasome regulator to enlarged PML-NBs, decreased activity of isolated proteasomes without changes in 26S proteasome component levels, an increase in nuclear foci containing p62/SQSTM1 that colocalized with large PML-NBs and impaired ATO-induced PML-NB degradation in ALS patient fibroblasts harboring the FUS-R521G mutant.

PML-NB dynamics following oxidative stress is thought to require several steps, including PML sumolyation, RNF4 localization, ubiquitination of sumolyated PML-NB components, and recruitment and activity of proteasomes (Sahin, Ferhi et al. 2014). Impairment of one or more of these processes would be expected to perturb PML-NB turnover following prolonged exposure to ATO. For instance, the knockdown of RNF4 expression or insufficient sumolyation of PML mutants (K160R or triple K65/160/490R) blocked ATO-induced PML-NB degradation (Lallemand-Breitenbach, Zhu et al. 2001, Lallemand-Breitenbach, Jeanne et al. 2008). The expression of FUS mutants in HEK293 cells may perturb one of these critical events related to PML-NB degradation. We observed that acute treatment of HEK293 cells with ATO for 1 h induced enlargement of PML-NBs and the accumulation of both Daxx and the 11S proteasome regulator in all

cell lines; however, only in the cells expressing FUS mutants was PML-NB turnover blocked.

To investigate mechanisms contributing to the impairment of PML-NB turnover, we measured the activities of isolated 26S proteasomes, which we found to be significantly decreased in FUS mutant cells compared to controls. Consistent with this result, global inhibition of proteasome activity with MG132 treatment was previously reported to inhibit ATO induced PML-NB degradation (Mattsson, Pokrovskaja et al. 2001, Tatham, Geoffroy et al. 2008, Sahin, Ferhi et al. 2014). Impaired proteasome activity has also been implicated as a pathogenic factor in ALS (Kabashi and Durham 2006). In a case of sporadic ALS and in a transgenic mouse model expressing SOD1-G93A, spinal cord tissues showed decreased proteasome activity measured with fluorogenic substrates, concomitant with a decrease in the level of 20S β5 catalytic subunits (Kabashi, Agar et al. 2008, Kabashi, Agar et al. 2012). In addition, a mouse model with altered proteasome function exhibited motor neuron degeneration, further suggesting that decreased proteasome activity may contribute to ALS pathogenesis. Impaired proteasome activity may also explain our observation that nuclear p62/SQSTM1foci were increased abnormally in FUS mutant cells. Large PML-NBs co-localized with p62, which may help to sequester ubiquitinated protein into PML-NBs. Given that PML-NBs can localize with nuclear proteasomes, PML-NBs may play an important role in the degradation of ubiquitinated nuclear proteins under stressful conditions (Pankiv, Lamark et al. 2010). It is also possible that dysfunction of proteasomes impairs PML-NB function in FUS

mutant cells even in the absence of ATO treatment, which is further supported by our observation of PML-NB enlargement in FUS mutant cells following proteasomal inhibition by MG132.

Our observation of abnormal Daxx accumulation associated with impairment of PML-NB turnover may also be relevant to ALS pathophysiology. Daxx is known to accumulate acutely in PML-NBs and has previously been identified as a Fas-interacting protein participating in Fas-mediated cell death (Yang, Khosravi-Far et al. 1997). Daxx accumulation into PML-NBs was reported to promote pro-apoptotic gene expression in HT1080 cells exposed to anti-Fas antibody (10 ng/ml-1 μg/ml) (Torii, Egan et al. 1999). Furthermore, increased Daxx accumulation within PML-NBs in the spinal cord of ALS-SOD1 transgenic mice was associated with motor neuron death (Raoul, Buhler et al. 2006). This event occurred weeks before disease onset, suggesting that Daxx accumulation with Fas ligand up-regulation may contribute to motor neuron death in ALS-SOD1 mouse models (Raoul, Buhler et al. 2006). Although we observed abnormal Daxx accumulation into PML-NBs with ATO treatment, cell death in our FUS mutant cell lines was not induced (Figure 3-4). As Daxx is sumoylated when it is localized into PML-NBs, it is likely that FUS mutant cells accumulate sumolyated proteins. Consistent with this, we observed that HEK293 cells expressing FUS-R495X increased the accumulation of SUMO2/3-modified proteins in Triton X-100 insoluble fractions (Figure 3-7). Evidence for abnormal SUMO accumulation is emerging as one component of ALS pathogenesis (Dangoumau, Veyrat-Durebex et al. 2013). For example, ALS mice

expressing mutant SOD1 down-regulate astroglial glutamate transporter EAAT2 expression and activity, and the C-terminal fragment of EAAT2 conjugated with SUMO-1 (CTE-SUMO1) localizes to PML-NBs in the mutant SOD1 spinal cord (Gibb, Boston-Howes et al. 2007, Foran, Bogush et al. 2011).

Fibroblasts obtained from ALS patient skin biopsies provide a useful tool for understanding the phenotypic effects of ALS mutant gene expression at endogenous levels. For example, fibroblasts from three sALS patients and individuals harboring either TDP-43-M337V mutant or UBQLN2-T487I recapitulated specific pathological features of ALS, including aggregate formation upon exposure to oxidative stress or proteasome inhibition (Yang, Zhang et al. 2015). We observed here that fibroblasts expressing the FUS-R521G mutant exhibited enlargement of PML-NBs under normal growth conditions and showed strikingly altered PML-NB turnover under stress conditions, both of which were consistent with our results using HEK293 cells. Going forward, it is exciting to consider the possibility that a readily observable PML-NB phenotype in accessible cells such as fibroblasts from ALS patients may be informative as a biomarker for susceptibility to FUS-mediated or even more general causes of ALS.

HEK293 cells expressing ALS-linked FUS mutants showed impaired stress-responsive PML-NB turnover and decreased proteasome activity. Furthermore, fibroblasts from an ALS patient harboring mutant FUS-R521G exhibited similarly enlarged PML-NBs and impaired PML-NB turnover. Overall, our results suggest that a

previously unappreciated gain of nuclear toxicity by mutant FUS could contribute to the pathogenesis of ALS by perturbing nuclear homeostasis.

3.7 Materials and Methods

Cell culture

Doxycycline-inducible FlpIn HEK293 (human embryonic kidney 293) cells expressing GFP-hFUS-WT, R521G or R495X were previously generated and cultured in DMEM media (Gibco) with 10% FBS (Sigma), 2mM L- glutamine (Gibco), 1% penicillin-streptomycin solution (Gibco), blasticidin and hygromycin B (Bosco, Lemay et al. 2010). The GFP-hFUS-P525L construct was a gift from Catherine L. Ward and Daryl A. Bosco (Univ. of Massachusetts Medical School) and was transfected with Flp recombinase vector (pOG44) into FlpIn T-Rex 293 cells to generate this additional cell line. Human fibroblasts from an individual with ALS harboring the FUS-R521G mutation and control fibroblasts were obtained from Dr. Robert H. Baloh (Washington University in St. Louis) and cultured in DMEM media (Gibco) with 10% FBS (Sigma), 1% penicillin-streptomycin solution (Gibco) and 1% MEM non-essential amino acid solution (Gibco). For ATO experiments, ATO (Sigma) was dissolved in 1 M NaOH to make a 0.25 M stock solution, and a 1 mM working solution was freshly prepared in Tris-buffered saline at pH 7.4 (Lallemand-Breitenbach, Zhu et al. 2001). ATO (1 μM) was added for 1 - 24 h to HEK293 cultures induced for 48 h to express FUS variants or to human fibroblasts.

Western blots

HEK293 cells were treated with 2 μg/ml doxycycline (Dox) to induce GFP-FUS expression for 48 h, and cells were lysed in RIPA buffer (50 mM Tris-HCl pH 7.4, 150 mM NaCl, 1% NP-40, 0.5% sodium deoxycholate, 0.1% SDS and 5 mM EDTA) with complete protease inhibitor for 40 min on ice. Protein concentrations were measured using a BCA assay (ThermoScientific, 23227). 10-20 μg of protein was separated by 10% Tris-HCl precast gels, transferred to nitrocellulose membranes and blocked in Odyssey blocking buffer for 1 h at room temperature. Anti-FUS (Santa Cruz Biotech, sc-47711, 1:1000), p62 (BD Biosciences, 610832, 1:1000), GAPDH (Sigma, G9525, 1:10,000) or PML (Bethyl Laboratories, Montgomery, TX, A301-168A, 1:1000) antibodies were diluted in Odyssey blocking buffer with 0.1% Triton X-100 and incubated for overnight at 4 °C. IRDye 800 or 680 (LiCor) secondary antibody in Odyssey blocking buffer was incubated for 1 h at room temperature. Signals were detected using an Odyssey Infrared Imager (Licor), and the intensities were analyzed with the Licor Image Studio Lite Ver 3.1.

Immunofluorescence

HEK293 cells were grown on glass coverslips coated with 10% poly L-lysine in 24-well plates, and GFP-FUS expression was induced with Dox for 48 h. Cells were fixed in 4% paraformaldehyde in phosphate buffered saline (PBS) for 15 min at room temperature (RT) and permeabilized in 0.2% Triton X-100 in PBS for 5 min. Cells were incubated with blocking solution containing 2% goat serum (Invitrogen), 0.1% Triton X-100 and

1% bovine serum albumin (BSA) in PBS for 1h at RT and primary antibodies in PBS with 0.15% goat serum and 0.1% Triton X-100 were applied for overnight at 4 °C. The rabbit anti-p62 (Santa Cruz Biotech, sc-255575), mouse monoclonal anti-PML (Santa Cruz Biotech, sc-966), rabbit anti-Daxx (Santa Cruz Biotech, sc-sc-7152) or rabbit anti-11S/PA28β proteasome regulator (Enzo, BML-PW8240) antibodies were diluted as 1:200, 1:200, 1:500 and 1:500, respectively. Secondary antibodies, Alexa fluor 568 conjugated goat-anti-rabbit (Invitrogen, A11011) or Alexa fluor 633 conjugated goat anti-mouse (Invitrogen, A21050) were incubated in PBS with 0.15% goat serum and 0.1 % Triton X-100 for 1 h at RT. Coverslips were mounted with Prolong Gold mounting medium containing DAPI (Invitrogen, P36941), and images were acquired using a Leica TCS SP5 II laser scanning confocal microscope with 60X oil objective and 5X zoom. All images were acquired by sequential scanning with 0.42 μm thick slices and analyzed with Leica LAS AF Lite software or Fiji Image J (Schindelin, Arganda-Carreras et al. 2012).

Human fibroblast cells were plated on glass coverslips coated with 10% poly L-lysine in 24-well plates. Following ATO treatment for 24 h, cells are fixed in 4% PFA for 15 min at RT and stained cells with anti-FUS (Bethyl Laboratories, Montgomery, TX, A301-168A, 1:500) and anti-PML (Santa Cruz Biotech, sc-966, 1:200) antibodies. All procedures are the same as for HEK293 cells.

Quantification of confocal images

We wrote a macro program for Image J Fiji that incorporates the 3D ROI Manager of Thomas Boudier (Ollion 2013) to define individual PML-NBs as 3D objects and to quantitate the integrated intensity of voxels within each PML-NB. DAPI images were used to segment the nuclear regions in 3D. Distinct PML-NBs were segmented in 3D using radial Gaussian local thresholding from background-subtracted and filtered images, and the raw intensities within each 3D object were then integrated to obtain the total signal attributed to each PML-NB. The integrated intensities were then plotted either as a cumulative distribution or as a function of distance from the nuclear center. The integrated intensities of Daxx, 11S/PA28, and p62 foci were also analyzed with the same method using different thresholding parameters.

Cell proliferation assay

HEK293 cells were plated on poly-L lysine coated glass coverslips at a density of 1000 cells per well and the next day treated with 2 μg/ml doxycycline to induce GFP-FUS expression. After 48 h of induction, ATO (1 μM) was added for 24 h and cells were treated with 10 μM of EdU (Click-iT EdU Alexa Fluor 594 Imaging Kit, Invitrogen, C10339) for 1 h to incorporate labeled EdU into newly synthesized DNA. The procedure for EdU staining was performed according to manufacturer's instructions and immunofluorescence images were obtained using a Nikon fluorescence microscope equipped with a 100x oil (1.3 N.A) objective. The number of DAPI positive and EdU incorporated cells was counted manually using Cell Counter software in Image J.

Cell viability assay

HEK293 cells were plated on 96-well plates at a density of 800 cells per well. After 48 h of doxycycline induction (2 μg/ml), cells were treated with different concentrations of ATO (0, 1, 2.5, or 5 μM) for 24 h. Cell viability was measured using the CellTiter-Glo Luminescent Cell Viability Assay (Promega, G7571) according to the manufacturer's instructions. The luminescent signal generated by recombinant luciferase reports upon the amount of ATP present in metabolically active cells.

Affinity purification of 26S proteasomes by UBL-method

Purification of intact 26S proteasomes using the ubiquitin-like domain (UBL) was described previously (Besche, Haas et al. 2009, Besche and Goldberg 2012). Briefly, cells were harvested by scraping in cold PBS and centrifuged at 1000x*g*, 4°C for 5 min. The cell pellet was resuspended in buffer containing 25 mM HEPES, 5 mM $MgCl_2$, 1 mM DTT, 1 mM ATP, 150 mM NaCl and Phosphatase inhibitor cocktail (#88667, Thermo Scientific, USA) and lysed by sonication (5 bursts of 10 sec each with 50 sec rest on ice). The crude lysate was centrifuged at 3,000×*g*, 4°C, for 5 min. The supernatant was centrifuged for 1 h at 100,000×*g*, 4°C. The resulting clarified lysates (100,000×*g*) were incubated for 2 h at 4°C with 2 mg purified GST-Ubl protein (Besche, Haas et al. 2009, Besche and Goldberg 2012) and a corresponding amount of glutathione-sepharose. After 2 h of incubation, the slurry containing 26S proteasomes bound to GST-Sepharose was poured into an empty disposable column and washed with buffer. Proteasomes were

eluted by incubating the resin with excess purified His-UIM (2 mg/ml) at 4°C for 15 min (Besche, Haas et al. 2009, Besche and Goldberg 2012). His-UIM was removed from the eluate by incubating with Ni^{2+}-NTA-agarose for 20 min at 4°C. Concentration of 26S proteasomes was calculated based on total protein content and assuming a molecular weight of 2.5 MDa.

Measuring peptidase activity of affinity purified 26S proteasomes

Proteasome peptidase activities have been measured using a protocol described elsewhere (Besche, Haas et al. 2009, Besche and Goldberg 2012). Briefly, the activity of proteasomes after affinity purification of 26S (~1 nM) or in extract (1-2 µg) was measured with 20 µM of fluorogenic substrates (suc-LLVY-amc, suc-nLPnLD-amc and suc-VLR-amc) in a buffer containing 50 mM Tris-HCl (pH 7.5), 10 mM $MgCl_2$, 1 mM ATP, and 1 mM DTT. Fluorogenic hydrolysis was monitored at λ_{ex}=380 nm and λ_{em}=460 nm at 37°C for 60 min. Rate of hydrolysis was calculated based on the slope of fluorescence increase over time between 30-60 min (linear phase of the reaction).

Cellular fractionation

Cell fractionation was performed by lysing in 1% Triton-X buffer containing 50 mM Tris-Cl (pH 7.4), 150 mM NaCl, 1% [v/v] Triton X-100, 1 mM EDTA, 1 mM dithiothreitol (DTT), 1 mM Na3VO4, 0.1 mM NaF, and a cocktail of protease inhibitors by mixing for 20 min at 4 °C. Total lysate was centrifuged at 12,500*xg* for 30 min. The

supernatant were used as Triton-X-soluble fraction. The pellet was resuspended in a buffer containing 50 mM Tris-HCl (pH 7.4) plus 2% SDS, sonicated briefly (10 sec, Twice), and used as Triton-X-insoluble fractions.

Statistics

Data are presented as mean ± S.D. with significance indicated by *, $p < 0.05$; **, $p < 0.01$; ***, $p < 0.001$, unless otherwise indicated. Significance was accepted for $p < 0.05$. Cumulative frequency was analyzed by the Kruskal-Wallis test followed by Dunn's multiple comparison test. Other comparison data were analyzed by one-way ANOVA followed by Tukey's multiple comparison test or two-way ANOVA followed by Sidak's multiple comparison test.

Chapter IV

Discussion and Conclusion

ALS is a progressive neurodegenerative disease characterized by loss of motor neurons in the brain and spinal cord. About 10% of ALS cases are caused by specific gene mutations and the number of genes linked to ALS has increased dramatically over the past decade (Renton, Chio et al. 2014). Mutations in FUS were identified in 2009, and many of these may perturb the nuclear localization signal sequence to cause cytoplasmic FUS accumulation (Kwiatkowski, Bosco et al. 2009, Vance, Rogelj et al. 2009). Although FUS has been proposed to regulate several events, including RNA splicing, transcription and DNA damage response (Deng, Gao et al. 2014), the mechanism by which FUS mutants cause motor neuron loss is not established. Several molecular mechanisms have been proposed, including oxidative stress, mitochondria dysfunction, protein aggregation, axonal transport defects and neuroinflammation (Ferraiuolo, Kirby et al. 2011). It is plausible that impaired cellular stress responses may serve as the initial step in disease pathogenesis. For example, oxidative stress is able to induce protein oxidation, which leads to the formation of protein aggregates (Mirzaei and Regnier 2008). Furthermore, these aggregates may sequester essential proteins including RNA binding proteins to cause axon defects (Groen, Fumoto et al. 2013). Therefore, we aimed to investigate the properties of FUS mutants in the absence and presence of stress conditions.

In chapter II, we found that oxidative stress, ER stress, and heat shock induced incorporation of FUS mutants into stress granules in proportion to their degree of cytoplasmic mislocalization in both cell culture and zebrafish models of ALS. Our study

suggests that the incorporation of FUS mutants into stress granules may perturb cellular stress responses.

Although cytoplasmic FUS inclusions are the pathological features in postmortem tissues from ALS patients, FUS mutants in the nucleus may also contribute to motor neuron degeneration by perturbing one or more nuclear functions. Mammalian cell nuclei contain several nuclear bodies including nucleoli, nuclear speckles and paraspeckles, Cajal bodies and nuclear Gems, and PML-NBs (Mao, Zhang et al. 2011). Dysfunction of these assemblies has been linked to several diseases (Woulfe 2007, Woulfe 2008). PML-NBs are reported to regulate nuclear protein quality control and oxidative stress response, which are essential for nuclear homeostasis (Guo, Giasson et al. 2014, Sahin, Ferhi et al. 2014). Therefore, we aimed to examine how FUS mutant expression alters the dynamics of PML-NBs in the absence and presence of oxidative stress.

In chapter III, we first observed that mutant FUS expression was associated with enlarged PML-NBs under baseline culture conditions in HEK293 cells. Later, HEK293 cells expressing FUS variants were exposed to arsenic trioxide (ATO), which is known to produce reactive oxygen species. We found that PML-NBs responded differently to the insult of oxidative stress in FUS mutant cells. Control cells progressed through normal PML-NB enlargement followed by turnover, whereas in FUS mutant cells, ATO-triggered PML-NB degradation was inhibited such that enlarged PML-NBs accumulated, concomitant with accumulation of the transcriptional repressor Daxx (Figure 4).

Next, we tried to find a possible mechanism involved in impaired PML-NB turnover. For normal turnover mechanism, SUMO-modified PML-NBs are ubiquitinylated by RNF4 and undergo degradation through the nuclear proteasome machinery (Sahin, Ferhi et al. 2014). One plausible mechanism to account for the observed increase in PML-NB size at baseline and the defect in PML-NB turnover after ATO could involve impaired recruitment of proteasomal subunits or regulators to PML-NBs in FUS mutant cells. We found that the 11S proteasome regulator in all cell lines was recruited into PML-NBs within 1 hour of ATO exposure. The 11S proteasome regulator resumed a diffuse nuclear distribution in control cells within 24 hour ATO exposure. In contrast, FUS mutant cells continued accumulation of the 11S proteasome regulator into enlarged PML-NBs with ATO treatment. Persistent accumulation of the proteasome regulator may be caused by dysfunction of proteasome activities. We next analyzed the activities of the 26S proteasomes in HEK293 cells and found that FUS mutant expression decreased their activities. Upon the inhibition of proteasome activities with MG132, FUS mutant cells expanded PML-NBs. These results support the notion that decreased proteasome activities in FUS mutant cells may contribute to the inhibition of PML-NB turnover. We also observed that primary fibroblasts from an ALS patient harboring the FUS mutant R521G exhibited enlarged PML-NBs under baseline conditions and a striking impairment of PML-NB turnover following ATO exposure.

These results indicate that impaired cytoplasmic stress response, a novel gain of nuclear toxicity, or both may contribute to ALS pathogenesis. A future direction will be to

test whether enlarged PML-NBs can be identified in additional ALS patient tissues, as this pathology could potentially serve as a biomarker for the diagnosis of ALS.

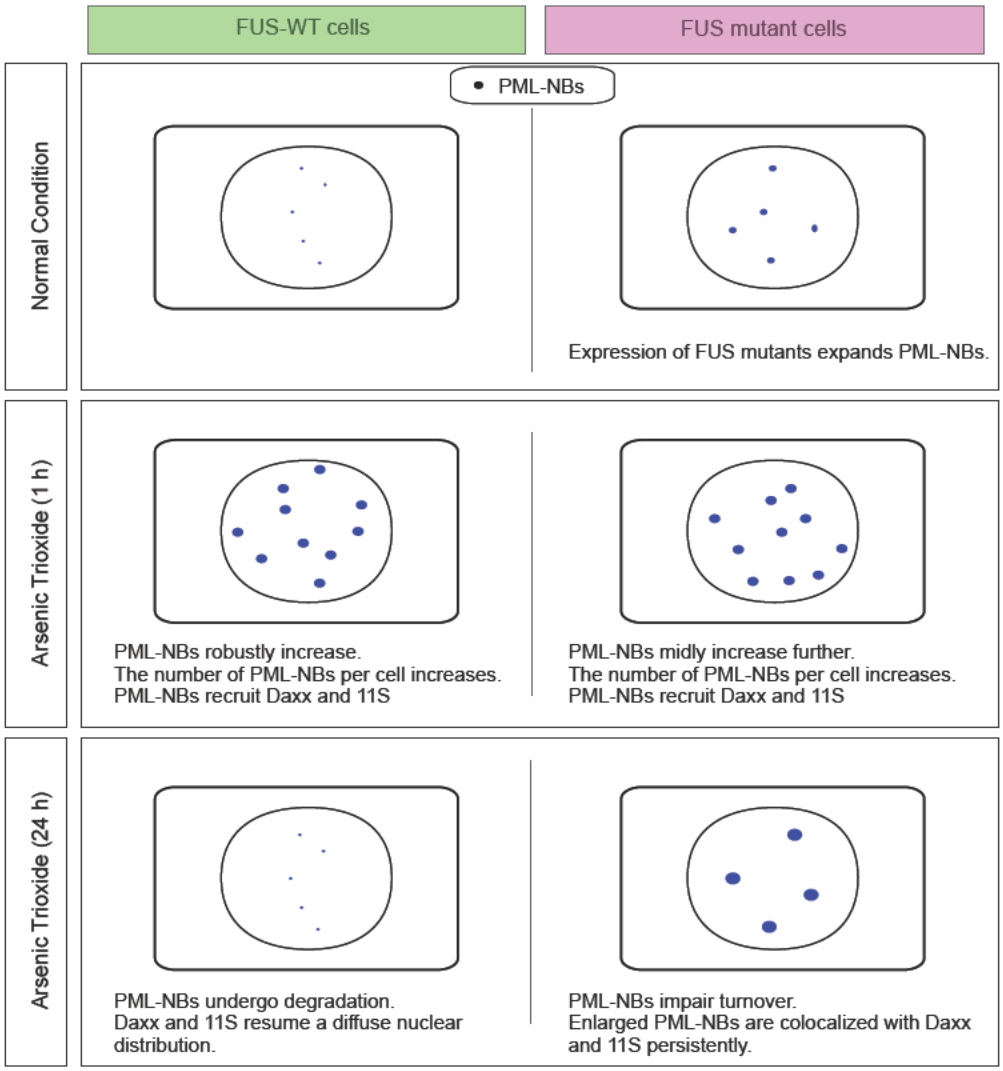

Figure 4. Expression of FUS mutants impairs the cellular stress response of PML-NBs.

The dynamic of PML-NBs in cells expressing FUS-WT (left side) and ALS-linked FUS variants (right side) are shown under different cellular conditions. (A) Under baseline conditions, WT FUS is localized primarily to the nucleus, while ALS-linked FUS mutants are prominent both in the nucleus and the cytoplasm. Expression of FUS mutants expands PML-NBs. (B) Under conditions of acute oxidative stress with arsenic trioxide, PML-NBs increase in number and size in all cell lines. PML-NBs recruit the transcriptional repressor Daxx and the 11S proteasome regulators. (C) Under prolonged oxidative stress conditions, PML-NBs in FUS WT cells undergo degradation. Daxx and 11S resume a diffuse nuclear distribution. In contrast, PML-NBs in FUS mutant cells impairs PML-NB turnover, concomitant with accumulation of Daxx and 11S into enlarged PML-NBs. Impaired stress response of PML-NBs may contribute to the pathogenesis of ALS by perturbing nuclear homeostasis.

IV.1 Stress granules, a common pathological mechanism in ALS

In chapter II, we observed that stress conditions induce mutant FUS incorporation into stress granules in both cell culture and zebrafish models of ALS (Bosco, Lemay et al. 2010). Later, many researchers found that FUS mutants are incorporated into stress granules upon insults with a variety of stressors (Dormann, Rodde et al. 2010, Kino, Washizu et al. 2011, Bentmann, Neumann et al. 2012). Moreover, other ALS-linked proteins and RNA-binding proteins such as TDP-43, profilin-1, hnRNPA1, hnRNPA2 and SMN1 are also reported to accumulate in stress granules under stress conditions (McDonald, Aulas et al. 2011, Figley, Bieri et al. 2014, Takanashi and Yamaguchi 2014), implicating a possible role for stress granule alternation or sequestration of essential RNA proteins related to RNA metabolism in ALS.

It is not clear, however, whether FUS mutants alter either the assembly or dynamics of stress granules. Recently, Baron et al. found that FUS mutant cells delay the assembly of stress granules under the oxidative condition with sodium arsenite in both HEK293 and neuronal NSC-34 cells (Baron, Kaushansky et al. 2013). Once stress granules are formed in FUS mutant cells, they become more dynamic, larger, and more abundant compared to those in control cells; this suggests the localization of mutant FUS to stress granules may impair stress response. In addition, similar observations have been reported recently in cells expressing ALS-linked mutations either in TDP-43 or profilin-1 (Figley, Bieri et al. 2014, Liu-Yesucevitz, Lin et al. 2014). These results suggest that altered stress response and impaired stress granule dynamics are common pathological events in ALS.

While most FUS mutants containing disrupted nuclear localization signal sequences are associated with stress granules under stress conditions, FUS-WT remains inside the nucleus (Bosco, Lemay et al. 2010, Dormann, Rodde et al. 2010, Gal, Zhang et al. 2011, Sun, Diaz et al. 2011). Sama et al. found that hyperosmolar stress with sorbitol enhanced translocation of FUS-WT to cytoplasm and its association into stress granules, indicating FUS-WT may also participate in stress response under certain conditions (Sama, Ward et al. 2013).

Stress granules are dynamic structures. According to the results of our monitoring stress granule assembly and disassembly in FUS mutants, stress granules are formed within 10 minutes, and dissociation occurs within minutes after stressors are removed (in chapter II). How does the reversible form of stress granules become irreversible aggregates? According to the Two Hit Hypothesis proposed by the Haass group, the first hit, caused by accumulations of FUS mutants in cytoplasm, might be the initial step for the disease process, and the second hit, caused by cellular stress, induces incorporation of mutant FUS into stress granules (Dormann and Haass 2011). Later subsequent chronic stress eventually leads to irreversible protein aggregates (Dormann and Haass 2011, Wolozin 2012). Supporting this notion, neuronal cytoplasmic inclusions in patient tissues were labeled with stress granule markers such as PABP-1, TIA-1, TIAR, and eukaryotic translation initiation factor 3 subunit (elF3), suggesting that the deposition of stress granules may initiate pathological inclusion formation in ALS (Dormann, Rodde et al. 2010, Liu-Yesucevitz, Bilgutay et al. 2010, Bentmann, Haass et al. 2013). Moreover,

while cytoplasmic localization of FUS mutants is accumulated into stress granules upon oxidative stress, FUS wild-type can interact with FUS mutants through prion-like domains, which causes sequestration into stress granules (Vance, Scotter et al. 2013). The result suggests that stress granules may serve as seeds to form inclusions (Dormann and Haass 2011, Wolozin 2012). These aggregates may have deleterious effects on neuronal cells by sequestering essential components, including mRNA and RNA-binding proteins (Wolozin 2012).

What mechanism is involved in the dissociation of stress granules after acute stress is removed? One paper suggests that autophagy may contribute to this process. The authors found that FUS(R521C)-positive stress granules are colocalized with LC3-positive autophagosomes in oxidative stress conditions (Ryu, Jun et al. 2014). Moreover, autophagic activation with rampamycin enhances the clearance of mutant FUS positive stress granules in an autophagy-dependent manner. These results also point to a potential therapeutic approach in ALS-FUS pathology (Ryu, Jun et al. 2014).

Is FUS critical to form stress granules? The depletion of TDP-43 exhibits altered stress granule dynamics including delayed formation and reduced size, suggesting that TDP-43 is essential for the formation of stress granules (McDonald, Aulas et al. 2011, Aulas, Stabile et al. 2012). Moreover, TDP-43 regulates the levels of G3BP mRNA, which is the essential component to form stress granules (McDonald, Aulas et al. 2011). In contrast to TDP-43, FUS knockdown does not affect the expression of two stress granule proteins, G3BP and TIA-1 (Aulas, Stabile et al. 2012). Moreover, the size and

number of stress granules are not altered in either HeLa and SK-N-SH cells with FUS knockdown, indicating that FUS itself is not required for stress granule assembly (Aulas, Stabile et al. 2012). Therefore, the exact role of FUS and stress granule formation in the context of the ALS condition should be investigated further.

IV.2 Abnormal sumolyation and ALS

Several stresses, including heat shock, oxidative stress, and proteasome inhibition have been known to induce protein sumolyation (Gallagher, Oeser et al. 2014), a reversible post-translational modification that can alter cellular distribution, cellular activity, and the stability of several proteins through covalent conjugation of small ubiquitin-like modifier (SUMO) proteins to target proteins (Geiss-Friedlander and Melchior 2007). Therefore, the stress-induced sumolyation of target proteins can alter their function to regulate cellular stress response. Recent analysis by chromatin immunoprecipitation assay coupled to high-throughput DNA sequencing and mRNA sequencing revealed that heat shock induced SUMO2 localization to active DNA regulatory elements which encode regulators of gene expression and the post-transcriptional modification of RNA (Seifert, Schofield et al. 2015). SUMO2 did not directly activate or inhibit transcription during the heat shock, but may help to maintain the integrity of transcription regulatory protein complexes in response to heat shock (Seifert, Schofield et al. 2015). Therefore, abnormal SUMO modification may contribute to impaired cellular stress responses.

Sumolyation also regulates chromosome segregation, nuclear architecture, and embryonic viability (Nacerddine, Lehembre et al. 2005). An enzyme cascade involving a dimeric SUMO-activating enzyme (E1), a single SUMO conjugating enzyme (E2) and a limited amount of SUMO ligase (E3) mediates sumolyation. Ubiquitin-like conjugating enzyme 9 (UBC9) is the only SUMO-conjugating enzyme in mammalian cells. A UBC9-deficient mouse model exhibited early lethality caused by chromatin-condensation and chromosome-segregation defects, indicating that sumolyation may play an essential role in genome stability (Nacerddine, Lehembre et al. 2005). In addition, these mice showed defects in nuclear organization, including disruption of nucleoli and PML-NBs. Interestingly, FUS is proposed to act like SUMO E3 ligase for Ebp1 sumoylation and to interact directly with a SUMO E2 ligase, UBC9 (Oh, Liu et al. 2010). Further study is needed to confirm whether mutant FUS causes abnormal sumolyation or altered nuclear organization by perturbing UBC9 localization or expression. Moreover, it is worth to investigate whether altered UBC9 localization or expression participates in the abnormal SUMO2/3 accumulation in FUS mutant cells observed in chapter III .

Abnormal SUMO- or PML-positive inclusions have been observed in several neurodegenerative diseases including ALS, FTD, spinocerebellar ataxia, and neuronal intranuclear inclusion disease (NIID) (Dorval and Fraser 2007, Woulfe 2007, Woulfe 2008). In chapter III, my results showed that abnormal Daxx sequestration into PML-NBs upon oxidative insult with ATO was increased in FUS mutant cells. PML mutants with sumolyation defects (K65/160/490R) are unable to recruit partner proteins such as Sp100

and Daxx, suggesting SUMO modification is a prerequisite for PML to form PML-NBs and recruit partner proteins (Zhong, Muller et al. 2000). Therefore, it is plausible that FUS mutant cells abnormally increased the accumulation of SUMO-modified proteins. In chapter III, we observed that FUS mutant cells increased accumulation of SUMO2/3-modified proteins in Triton X-100 insoluble fractions under normal growth conditions, suggesting that increased SUMO modifications may contribute to ALS-FUS pathogenesis. The evidence for abnormal SUMO modification is emerging in ALS pathogenesis (Dangoumau, Veyrat-Durebex et al. 2013). For instance, mutant SOD1 (G93C) or a splicing isoform of TDP-43 lacking the C-terminus (TDP-S6) is found in SUMO-positive inclusions in a cell culture model of ALS (Seyfried, Gozal et al. 2010, Dangoumau, Veyrat-Durebex et al. 2013). TDP-S6 forms highly insoluble nuclear inclusions conjugated with SUMO2/3 and mutant SOD1 (G93R) is conjugated with SUMO3 for increased stability, suggesting that SUMO modification can participate in aggregation of TDP-43 and SOD1 (Seyfried, Gozal et al. 2010, Niikura, Kita et al. 2014). Moreover, the impairment of excitatory amino acid transporter 2 (EAAT2) in astroglial cells is caused by the formation of a C-terminal fragment, which is conjugated with SUMO1 (CFT-SUMO).

It is still controversial whether protein sumolyation associated with neurodegenerative diseases serves to enhance protein solubility or to promote aggregate formation (Gallagher, Oeser et al. 2014). For instance, sumolyation of α-synuclein is reported to prevent α-synuclein from forming fibrils, whereas decreased sumolyation of

α-synuclein leads to increased toxicity (Krumova, Meulmeester et al. 2011). Consistent with this finding, increased sumolyation of polyQ-expanded ataxin-1 (Atxn1 82Q) enhances its solubility and promotes ubiquitin-proteasome-mediated degradation (Guo, Giasson et al. 2014). In contrast, under oxidative stress conditions, increased SUMO modification on polyQ-expanded ataxin-1 promotes its insolubility and inclusion formation (Ryu, Cho et al. 2010). Therefore, the solubility of SUMO-modified proteins depends on the nature of target proteins.

Does SUMO need to be detached before undergoing proteasome-mediated degradation in the case of SUMO modified PML-NBs? Bailey et al. found that increased free SUMO1 accumulation with ATO stimuli is detected by western blot analysis, implicating that SUMO detachment from PML-NBs is a necessary step for PML degradation (Bailey and O'Hare 2005). It is still unknown, however, which SUMO proteases participate specifically in PML-NB degradation. Six SUMO proteases are identified in mammalian cells, and each protease has a specific substrate and cellular localization (Hickey, Wilson et al. 2012). Interestingly, the depletion of SUMO protease SENP6 can enlarge the size of PML-NBs in HeLa cells along with increasing the number of PML-NBs (Hattersley, Shen et al. 2011). It would be interesting to analyze whether the expressions of FUS mutants affect SUMO protease localization or expression to cause enlargement of PML-NBs or abnormal SUMO2/3 accumulations in the Triton X-100 insoluble fractions we observed in chapter III.

In addition to the role of sumolyation in protein aggregates, SUMO modification controls several cellular events including apoptosis and transcriptional regulation (Shih, Chang et al. 2007). Although the event of Daxx accumulation into PML-NBs is not compromised on cell viability in HEK293 cells under oxidative stress conditions, Daxx accumulation is reported to regulate apoptosis (Yang, Khosravi-Far et al. 1997, Torii, Egan et al. 1999). In a SOD1-G93A transgenic mouse, Daxx accumulation in the spinal cord was increased before disease onset, suggesting that Daxx accumulation contributes to motor neuron loss (Raoul, Buhler et al. 2006). Moreover, the SUMO E3 ligase PIAS1 mediates ultraviolet (UV)-induced apoptosis by recruiting Daxx to sumolyated PIAS1 foci in HeLa cells (Sudharsan and Azuma 2012). Sumolyation of the transcriptional co-activator p300 promotes the recruitment of histone deacetylase 6 (HDAC6), leading to transcriptional repression (Girdwood, Bumpass et al. 2003). Protein de-sumolyation also regulates cellular mechanisms. Oxidative stress induces de-sumolyation of both c-fos and c-Jun, which results in a transcription activation for antioxidant proteins (Feligioni and Nistico 2013). Therefore, the balance between sumolyation and de-sumolyation is crucial to maintaining cellular homeostasis.

IV.3 PML and RNF4 for nuclear homeostasis

PML is a well-known target protein for SUMO in response to oxidative stress (Sahin, de The et al. 2014, Sahin, Ferhi et al. 2014). Moreover, PML-NBs are able to induce sumolyation of partner proteins that accumulate inside the shell of PML-NBs under the

condition of oxidative stress (Sahin, Ferhi et al. 2014). Therefore, oxidative stress-induced PML-NB formation and associated protein degradation are critical to nuclear homeostasis.

PML-NBs are the site for protein degradation in the nucleus. For example, a nucleolar protein, N4BP1, is also located in PML-NBs and undergoes SUMO-regulated polyubiquitylation and proteasomal turnover (Sharma, Murillas et al. 2010). PML-NBs work with RNF4 for sumolyated protein degradation in the nucleus. RNF4 is a poly-SUMO-specific E3 ubiquitin ligase and promotes ubiquitination of SUMO-conjugated proteins for their degradation (Lallemand-Breitenbach, Jeanne et al. 2008, Tatham, Geoffroy et al. 2008). Nuclear factor erythroid 2-related factor 2 (Nrf2), which regulates oxidative stress response, is also sumolyated and located in PML-NBs upon ATO treatment (Malloy, McIntosh et al. 2013). In addition, ATO treatment induces RNF4-mediated polyubiquitination of Nrf2 and its degradation through nuclear proteasomes. Therefore, PML-NBs are essential for regulating proteasomal turnover of target proteins.

In cultured cells without oxidative stress, PML-SUMO-RNF4 has been proposed as a nuclear protein quality control system (Guo, Giasson et al. 2014). For instance, in a cell culture model of spinocerebellar ataxias (SCAs), the pathogenic ataxin-1 protein with 82 contiguous gluatamines is targeted at PML-NBs. Interestingly, overexpression of PML is able to enhance degradation of Atxn1-82Q. The process for Atxn1-82Q protein degradation includes PML-mediated Atxn1-82Q sumolyation and RNF4-mediated ubiquitination of SUMO2-Atxn1-82Q. Consistent with this result, misfolded TDP-43 and

Huntingtin-97QP in cell nucleus exhibit sumolyation, ubiquitination, and degradations (Guo, Giasson et al. 2014). In addition, increased expression of PML by interferon beta stimulus enhances clearance of mutant ataxin-7 in a mouse model of SCA7 (Chort, Alves et al. 2013). Collectively, these results suggest that PML-SUMO-RNF4 is critical to cleaning up misfolded proteins and maintaining cellular homeostasis in cell nucleus.

In addition to its role in protein degradation, RNF4 plays a role in DNA damage response in cell culture lines and in vivo (Galanty, Belotserkovskaya et al. 2012, Guzzo, Berndsen et al. 2012, Yin, Seifert et al. 2012, Hay 2013, Vyas, Kumar et al. 2013). Decreased expression of RNF4 in cultured cells increased sensitivity to ionizing radiation (Yin, Seifert et al. 2012, Vyas, Kumar et al. 2013). Interestingly, laser micro-irradiation induced endogenous RNF4 accumulation at the site of DNA damage where phospholyated H2AX (ɣH2AX) is localized (Galanty, Belotserkovskaya et al. 2012, Yin, Seifert et al. 2012). The SUMO-interacting motif (SIM) and the RING domain of RNF4 are required for recruitment at the site of DNA damage (Yin, Seifert et al. 2012, Vyas, Kumar et al. 2013). The depletion of RNF4 expressions does not alter the recruitment of proteins required for DNA damage response, including Nijmegen breakage syndrome 1 (NBS1), mediator of DNA-damage checkpoint 1 (MDC1), RNF8, p53-binding protein 1 (53BP1), and breast cancer early-onset 1 (BRCA1) (Yin, Seifert et al. 2012). RNF4 depletion did cause a delay in their removal from the DNA damage site, however (Yin, Seifert et al. 2012). Indeed, the recruitment of Rad51 and RPA70 to ssDNA is dependent on RNF4 expression, indicating that RNF4-depleted cells may impair the 5′-to-3′

exonuclease-mediated resection from a DNA double strand break (Yin, Seifert et al. 2012). Moreover, ionizing radiation enhances sumolyation of MDC1, which serves as a platform for recruiting RNF4 at the site of DNA damage (Yin, Seifert et al. 2012). RNF4-deficient mice, whose phenotypes are similar to those of FUS knockout mice (Hicks, Singh et al. 2000, Kuroda, Sok et al. 2000), showed DNA damage and an age-dependent defect in spermatogenesis by ionizing radiation (Vyas, Kumar et al. 2013). FUS is also recruited at the site of DNA damage (Mastrocola, Kim et al. 2013, Wang, Pan et al. 2013, Rulten, Rotheray et al. 2014). We could not examine the localization or expression of RNF4 in HEK293 cells due to technical problems. Future studies should examine whether FUS mutant cells impair RNF4 expression or localization in the absence and presence of stress conditions with ionizing radiation.

PML-NBs are also believed to participate in DNA damage response. Previously, PML in SiHa cells was reported to colocalize with the DNA damage response protein TopBP1 upon exposure to ionizing radiation (Xu, Timanova-Atanasova et al. 2003). In addition, upon DNA damage, PML-NBs are able to recruit ATM and phosphorylated histone H2AX, which are not associated with PML-NBs in normal conditions (Dellaire and Bazett-Jones 2004). Therefore, PML-NBs might regulate DNA-damage response by acting as storage bins that release or accumulate many proteins linked to DNA-repair and checkpoint (Bernardi and Pandolfi 2007). Further study is needed to investigate whether FUS mutant expression alters the role of PML-NBs in DNA damage response.

IV.4 Proteasome dysfunction links to ALS

Ubiquitin-proteasome pathways account for 80-90% of protein degradation in cultured mammalian cells (Lee and Goldberg 1998), and proteasomes are present in both the cytoplasm and the nucleus. Although the 20S proteasome, the 19S proteasome regulatory complex, ubiquitin, the PA28 regulatory factor, the ubiquitin-specific protease HAUSP, and E1-E3 enzymes are present in the nucleus (von Mikecz 2006), it is still controversial whether nuclear proteins are degraded within the nucleus or transported to the cytoplasm for hydrolysis. The microinjection of fluorogenic precursor substrate Suc-LLVY-AMC into the nuclei of live HEp-2 cells showed a linear increase of nuclear fluorescence intensity over time without any change in cytoplasmic fluorescence, indicating that the nucleus has its own proteasomal activity (Rockel, Stuhlmann et al. 2005).

Protein aggregates in several neurodegenerative disease may result from an impaired protein degradation pathway (Goldberg 2003, Goldberg 2007). Proper degradation of toxic protein is critical to prevent aggregates, especially in neuronal cells because of their postmitotic and long-lived properties. Dysfunctions of this system includes impairments in ubiquitination, substrate delivery to the proteasome, or proteasome activity (McKinnon and Tabrizi 2014). Insufficient ubiquitination can be caused by depletion or reduced activity of E1, E2, or E3 enzymes. In addition, dysfunction of proteasome activity can be caused directly by disease-associated misfolded proteins or age-related decline in catalytic activity. Moreover, mitochondrial dysfunction can cause impairment of

proteasome activity through the depletion of ATP production and/or elevation of reactive oxygen species (ROS) (McKinnon and Tabrizi 2014). An age-related decline in proteasome activity may contribute to the pathogenesis of late-onset neurodegenerative disease. The age-related accumulation of ROS products causes the induction of oxidized, misfolded protein aggregation, which exacerbates the decline of proteasome activity. Interestingly, FUS-positive aggregates are hardly observed in cultured cells under basal conditions. For example, healthy cultured rat cortical neurons overexpressing FUS-R521C mutants do not form FUS-positive aggregates (Ryu, Jun et al. 2014), which are often observed in the end-stage tissues; this suggests that FUS-positive aggregate formation might be induced by environmental factors.

FUS mutant cells showed decreased activity of 26S proteasome, and this may contribute to increased nuclear p62/SQSTM1 accumulations and inhibition of PML-NB turnover (in chapter III). In addition, the pilot experiment for measuring the activities of 26S proteasomes purified from brain lysates in our hFUS-R495X transgenic mice revealed that 26S proteasome activities were decreased significantly in hFUS-R495X transgenic mice compared to hFUS-WT transgenic and nontransgenic control mice. We could not conclude what mechanism causes the reduction of 26S proteasome activity. There is cumulative evidence that FUS may have a role in the ubiquitin-proteasome system. For instance, wild-type FUS target the gene, ZNF294, or LISTERIN, which encodes an E3 ubiquitin ligase (Tan, Riley et al. 2012). Moreover, PAR-CLIP analysis in HEK293 cells expressing FUS mutants (R521G or R521H) revealed that ALS-linked

FUS mutants target the transcripts for endoplasmic reticulum and ubiquitin-proteasome-related genes (Hoell, Larsson et al. 2011). Using a stringent tandem-affinity purification method, FUS interacting proteins are identified in HEK293 cells expressing either FUS-WT or FUS-P525L (Wang, Jiang et al. 2015). Interestingly, both FUS-WT and P525L interact with components for protein degradation pathways, such as ubiquitin-like modifier-activating enzyme 1 (UBA1) and 26S proteasome non-ATPase regulatory subunit 12 (PSND12/Rpn5). While overexpression of FUS-WT or P525L in HEK293 cells and SH-SY5Y cells decreased ATP production significantly, there was no difference in ATP production levels in cells expressing WT or mutant FUS. Further study needs to be performed to investigate how FUS mutants cause the reduction of proteasome activity.

In ALS cases, the down-regulation of proteasome activity has been observed in the spinal cord tissues from sporadic ALS patients and an SOD1-G93A transgenic mouse model, concomitant with a decrease in the level of 20S β5 catalytic subunits (Kabashi, Agar et al. 2008, Kabashi, Agar et al. 2012). Moreover, altered UPS function was found in human fibroblasts from individuals harboring either UBQLN2-T487I or TDP-43-M337V mutants linked to ALS (Yang, Zhang et al. 2015). Motor neuron-specific knockouts of the proteasome subunit Rpt3 cause motor neuron degeneration and inclusion formation including TDP-43, FUS, OPTN, and ubiquilin-2, whereas knockouts of the autophagy-related protein Atg7 do not induce any motor phenotypes. This suggests that the motor neuron is sensitive in proteasome dysfunction (Tashiro, Urushitani et al. 2012). Nevertheless, others argued that autophagy is also involved in ALS pathology. For

example, inhibition of either proteasome activity using MG132 or autophagic function with 3-MA increased the expression of TDP-43 and its pathological form, TDP-25, whereas trehalose treatment to enhance autophagic function decreased the expression levels, suggesting that both autophagy and the ubiquitin-proteasome system contribute to the degradation of TDP-43 (Wang, Fan et al. 2010). Moreover, stress granules containing FUS mutants are associated with LC-II, and autophagy mediates the disassembly of stress granules (Ryu, Jun et al. 2014).

Several ALS-linked genes also participate in the ubiquitin-proteasome system. Ubiquilin-2 is a member of the ubiquilin family and plays a role in the ubiquitinated substrate delivery to the proteasome (Zhang, Yang et al. 2014). Mutations in UBQLN2 are associated with dominantly inherited X-linked ALS (Deng, Chen et al. 2011). The expression of mutant ubiquilin2 (P497H or P506T) in SH-SY5Y cells exhibits impairment of proteasomal degradation by UbG76V-GFP reporter assay, whereas over expression of wild-type ubiquilin-2 promotes the clearance of C-terminal TDP-43 fragment (261-414 aa) in human H4 cells (Cassel and Reitz 2013). Moreover, the mutations in genes encoding valosin-containing protein (VCP) or sequestosome1/p62, which regulates protein degradation through proteasome, are associated with ALS, supporting the notion that an impaired proteasome degradation system contributes to ALS pathogenies (Johnson, Mandrioli et al. 2010, Fecto, Yan et al. 2011).

In chapter III, we found that the expression levels of proteasome subunits including PA200, Rnp2, Rpt5, Rpn13 and MCP were not changed, whereas the three peptidase

activities of 26S proteasome were decreased in FUS mutant cells. The 26S proteasome is a large macromolecular machine that consists of the proteolytic core particle, the 20S proteasome is composed of 14 different subunits, and the 19S regulatory particle is composed of 19 different particles. In proliferating cells, proteasome assembly continuously occurs from inactive precursor complex (Saeki and Tanaka 2012, Gu and Enenkel 2014). Further research is needed to examine whether FUS mutant expressions alter proper proteasome assembly. Moreover, where proteasome dysfunction in FUS mutant cells occurs-in the cytoplasm, the nucleus, or both-should be analyzed.

IV.5 Intranuclear inclusions in ALS

Aggregate formation is the hallmark of several neurodegenerative disease including ALS, Alzheimer's disease, and Huntington's disease (Mukai, Isagawa et al. 2005, Blokhuis, Groen et al. 2013, Jucker and Walker 2013). Some of these conditions exhibit nuclear aggregates that contain proteasomes, p62/SQSTM1, ubiquitin, SUMO1, PML, and chaperones (Woulfe 2008). In chapter III, FUS mutant cells increased sequestration of Daxx and 11S/PA28 proteasome regulators into large PML-NBs upon oxidative insult with ATO. In addition, FUS mutant cells increased abnormal nuclear p62 accumulation (in chapter III). Therefore, it is easy to assume that enlargement of PML-NBs may serve as an initial step for intranuclear inclusion formation. Previously, ubiquitin, p62/ SQSTM1, or SUMO1-positive intranuclear inclusions were identified in patient tissues affected by FTD-ALS (Bigio, Johnson et al. 2004, Mackenzie, Baker et al. 2006,

Pikkarainen, Hartikainen et al. 2008). Recently, abnormal, dot-like p62 positive, TDP-43-negative neuronal intranuclear inclusions were found in the hippocampus and cerebellum tissues harboring C9orf72 expansion linked to FTD-ALS (Al-Sarraj, King et al. 2011). Observation of the neuronal intranuclear inclusions is rare in ALS cases, however. In 1997, eosinophillic intranuclear inclusions is the first observation in ALS (Kakita, Oyanagi et al. 1997). Seven years later, eosinophilic neuronal intranuclear inclusions labeled with PML, proteasomes, non-expanded ataxin-3, and ubiquitin were observed in ALS patients with rapid progression (Seilhean, Takahashi et al. 2004), suggesting that abnormal nuclear inclusions may participate in the pathogenesis of ALS.

FUS itself is sequestered in nuclear aggregates (Nomura, Watanabe et al. 2014). ALS patient tissues harboring FUS mutations show intranuclear inclusions containing FUS in neurons having the hypoglossal nucleus and this observation is only found in early-onset cases (Mackenzie, Ansorge et al. 2011). FUS mutant, G156E, which contains intact nuclear localization signal, is sequestrated in nuclear aggregates in rat hippocampal neurons that occur cytotoxicity (Nomura, Watanabe et al. 2014). A subset of FUS mutant (G156E) at the SYQG region linked to fALS has the ability to form amyloid-like fibrillar aggregates, which can serve as seeds triggering the accumulation of wild-type FUS into aggregated structures forming intranuclear inclusions, concomitant with decreased cell viability. Nuclear aggregation containing FUS also presents along with abnormal RNAPII sequestration in patient fibroblast cells harboring mutant FUS (H517Q or △NLS)

(Schwartz, Podell et al. 2014), suggesting that FUS nuclear aggregates may participate in ALS pathogenesis.

Proteasome dysfunction may contribute to intranuclear inclusion formation. SUMO1-positive intranuclear inclusions are enhanced in PC12 cells by treatment of the proteasome inhibitor, lactacystin (Pountney, Huang et al. 2003). Proteasome inhibition with MG132 also increased SUMO1 accumulation in the nucleus (Bailey and O'Hare 2005). Interestingly, these SUMO1 are colocalized with ubiquitin (Bailey and O'Hare 2005). Consistent with this finding, we observed that MG132 (1 μM) treatment for 24 hours increased the size of PML-NBs in FUS mutant cells. Further study is needed to examine nuclear aggregates containing PML-NBs in motor neurons from our FUS-transgenic mouse model expressing FUS-R495X.

Do intranuclear aggregates induce cellular toxicity? Some experimental results support the notion that aggregation causes cellular toxicity. PC12 cells expressing mutant atrophin-1 with expanded polyglutamine stretches enhanced the formation of SUMO1-positive intranuclear aggregates, which results in cell death. Moreover, cells expressing mutant ataxin-1, which is linked to spincerebellar ataxia 1 (SCA1) disease, increased nuclear aggregate formation, concomitant with cell death in oxidative stress conditions (Kim, Kim et al. 2003).

Nuclear inclusions sequester essential nuclear proteins, including transcription factors, components for the ubiquitin-proteasome system, and RNA-binding proteins; this sequestration may cause dysregulation in transcription, splicing, and protein

degradation in the nucleus. Therefore, nuclear dysfunction may serve as a crucial mechanism in neurodegenerative disease.

Conclusion

ALS is a progressive neurodegenerative disease characterized by loss of motor neurons in the brain and spinal cord. While mutations in FUS account for a subset of familial ALS, the mechanism by which FUS mutants cause motor neuron degeneration is still not known. The work in this dissertation demonstrates that FUS mutant expression impairs cellular stress response by (i) accumulation of mutant FUS into stress granules and (ii) inhibition of PML-NB dynamics. Abnormally enlarged PML-NBs under stress conditions may perturb nuclear homeostasis, implicating that a novel nuclear pathology specific to mutant FUS expression may contribute to ALS pathogenesis. Furthermore, FUS mutant expression leads to inhibit proteasome activity. Further analysis to reveal how FUS mutant expression alters proteasome activity will provide more evidence to understand the pathological mechanism in ALS and will contribute to the development of therapeutic approaches for this severe disease.

Appendix I:

An approach to generate an FUS-knockout zebrafish model

using zinc finger nucleases

ALS is an adult-onset neurodegenerative disease. In zebrafish, both overexpression of genes via mRNA injection and down-regulation of genes using morpholino oligonucleotides are good tools for studying the transient effects of target proteins in zebrafish embryos. However, these tools are not suitable for examining progressive degeneration in the adult stage. Therefore, we aimed to generate a transgenic zebrafish model.

To create an FUS knock-out zebrafish model, we adapted engineered zinc-finger nucleases (ZFNs). ZFNs has been used for genetic modifications in cell lines, invertebrates, and zebrafish (Meng, Noyes et al. 2008). ZFNs are a chimeric fusion between a Cys_2His_2 zinc-finger protein (ZFP) and the cleavage domain of *Fok*I endonuclease (Carroll 2011). Each ZFP can recognize distinct three-base-pairs (bp) of DNA sequences. A zinc-finger cassette forms with 3 to 6 ZFPs and recognizes 9 to 18 bp of the DNA sequences. If a pair of ZFNs is assembled properly with opposite strands of the DNA sequences with a spacer of 5- or 6-bp distance between the binding sites, *Fok*I forms dimerization to initiate nuclease activity. This cleavage activity leads to DNA double-stranded breaks at the target site. This gene disruption may be induced when the cells undergo DNA repair through non-homologous end joining (NHEJ). Alternatively, gene insertion or correction can be introduced by applying a desired DNA template; this event requires a DNA homology-direct repair system (Urnov, Rebar et al. 2010).

Our collaborator, Dr. Wolfe, helped us find possible targets of ZFNs on the genomic DNA of the zebrafish FUS. In particular, we found candidates on exon 4, 6, and 13. We

targeted regions on exon 6 of the zebrafish FUS after validating the activity of the ZFNs on each target with the yeast-based MEL1 reporter assay (Figure A1-1) (Doyon, McCammon et al. 2008). The ZFN-6-1 contained 3 ZFPs with a 6-bp spacer between the ZFP recognition regions (Figure A1-1A). The ZFN-6-2 included an additional ZFP at the right ZFN recognition site to target a total 12 bp (Figure A1-1B). Through modular assembly-based approaches, individual ZFPs were ligated into the pCS2 vector containing modified *Fok*I endonuclease. The ZFP modules and pCS6 vectors were provided by the Lawson lab (Meng, Noyes et al. 2008). RNA encoding ZFNs was generated *in vitro* using an SP6 Transcription kit (Ambion, AM1340), and different concentrations (100, 200 and 500 pg) of RNA were microinjected into one-cell-stage zebrafish embryos. The embryos were separated based on their morphology (normal or abnormal) at 30 hours post-fertilization (hpf), and DNA was extracted to validate the activities of ZFNs.

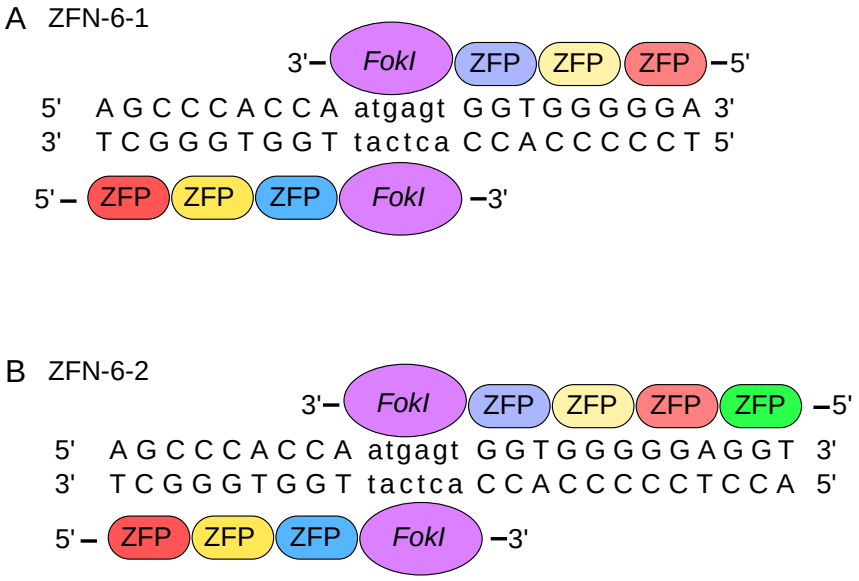

Figure A1-1. Possible targets of ZFNs were located on exon 6 of the zebrafish FUS.

(A) The ZFN-6-1 contained 3 ZFPs to target a total 9 bp. **(B)** The ZFN-6-2 included an additional ZFP at the right ZFN recognition site to target a total 12 bp. Both ZFNs contained a spacer of 6 bp distance between binding sites.

Analyzing the ZFN-mediated mutagenesis on exon 6 of the FUS gene required amplification of an ~100-bp fragment containing target regions on exon 6, followed by analysis of the PCR product via Cel-I SURVEYOR nucleases (Cel-I, SURVEYOR Mutation Detection Kit, Transgenomic) to validate the activity of the ZFNs. The Cel-I enzyme can detect any DNA mismatch generated by ZFN-mediated gene insertion or deletion. As validated by the Wolfe lab, the CelI digestion using the PCR product from the injection of active ZFNs (P-C) produced the small fragments caused by DNA mismatches (Figure A1-2). However, both candidate ZFNs on exon 6 did not exhibit any activity (Figure A1-2).

One concern raised by applying ZFNs for gene manipulation includes cytotoxicity caused by the off-target effect. Furthermore, the efficiency of target-gene mutagenesis by ZNFs is quite low (Moore, Reyon et al. 2012). In future study, other genetic modification tools such as transcription activator-like effector nucleases (TALEN) and clustered regularly interspaced short palindromic repeats (CRISPRs)/CRISPR-associated (Cas) systems, may be considered to manipulate FUS expression on zebrafish.

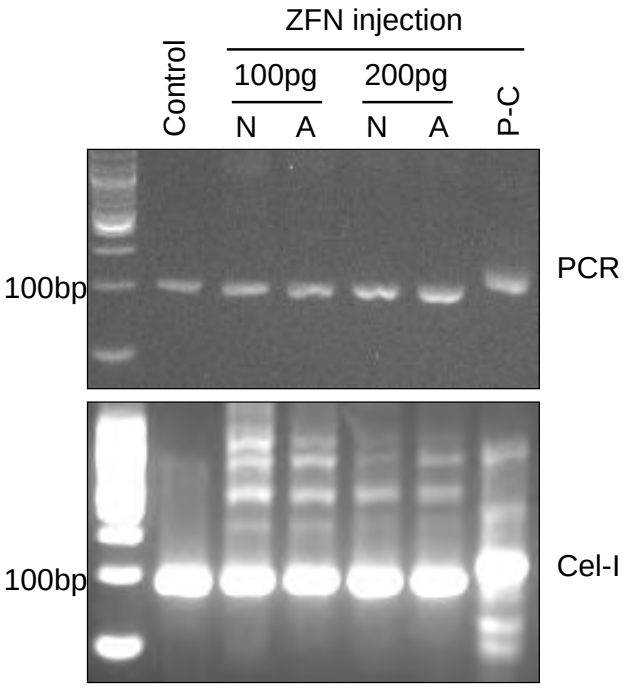

Figure A1-2. The activities of ZFNs (ZFN-6-1) were validated by Cel-I assay.

Top panel: An ~100 bp fragment containing target regions was amplified by PCR. **Bottom panel:** The PCR products were analyzed by Cel-I assay to check the mutagenesis caused by the activity of ZFNs. Control, non-injected embryos; N, normal morphology; A, abnormal morphology; P-C, active ZFNs from the Wolfe lab.

Appendix II:

A possible approach to identifying FUS interacting proteins

FUS may regulate several cellular functions, including RNA splicing, transcription, DNA damage repair, and microRNA biogenesis (Deng, Gao et al. 2014). FUS targets more than 5,500 mRNA in human brains (Lagier-Tourenne, Polymenidou et al. 2012). However, it is not clear what protein interacts directly with FUS or FUS mutants to cause motor neuron degeneration. Analysis of the interactions between FUS and partner proteins provides insights into FUS function in the context of ALS. We aimed to identify FUS-interacting proteins and validate whether FUS mutants generate new interactions or lose normal associations.

For the pilot experiment, we performed immunoprecipitation of GFP-tagged FUS using anti-GFP beads (μMACS GFP Isolation Kits, Miltenyi Biotec) in HEK293 cells expressing FUS variants (WT or R495X). Next the products were analyzed via 2D gel electrophoresis to check if FUS mutants altered normal FUS interactions with partner proteins. This initial trial revealed that many proteins were immunoprecipitated with GFP-FUS together, which might have been caused by the nonspecific interactions. Therefore, we changed the method to increase specificity and minimize false interactions.

To accomplish this, we decided to perform photo-cross-linking with an engineered aryl azide ligase, a special enzyme derived from the natural E. coli enzyme known as lipoic acid ligase (LplA) (Baruah, Puthenveetil et al. 2008). This engineered ligase catalyzes the covalent binding of a fluorinated aryl azide to an LplA acceptor peptide (LAP). The LAP is a 17-amino-acid unnatural peptide that may be fused with the protein

of interest. UV irradiation produces a reactive oxygen species that cross-links to any surrounding proteins, which may increase specificity.

We generated four constructs containing LAP and myc sequences that were conjugated with either FUS-WT or FUS-P525L (Figure A2-A). The LM1 and LM2 synthetic constructs had 12- and 7-amino-acid linkers between the myc and full length of FUS (1-526), respectively. The LM3 synthetic construct contained N-terminal truncation of FUS (225-526) with 5-amino-acid linkers. For negative control (or LAC), a lysine on the Lap peptide was substituted with alanine to inhibit the interaction with LplA, and eventually the photo-cross-linking product using the LAC construct represented non-specific interactions.

Each construct was cloned into a pcDNA5/FRT/TO/TOPO vector and transfected into FlipIn TRex HEK293 cells to generate doxycycline-inducible cell lines. After 48 hour of doxycycline induction, cells were lysed in an RIPA buffer, and the expression level of each construct was evaluated by western blotting. The expression levels of all synthetic constructs were quite low in inducible HEK293 cells. Later, we transfected these constructs transiently in HEK293 cells and found the expression levels were detectably high (Figure A2-1B). Therefore, we decided to analyze these constructs via transient transfection. We checked FUS localization and found LAP-myc tag did not perturb its normal property (Figure A2-C). LM1-FUS-WT expressed in the nucleus, and LM1-FUS-P525L showed cytoplasmic mislocalization. Interestingly, the truncation form of FUS (LM3-FUS-WT) expressed throughout the nucleus, and it even localized inside

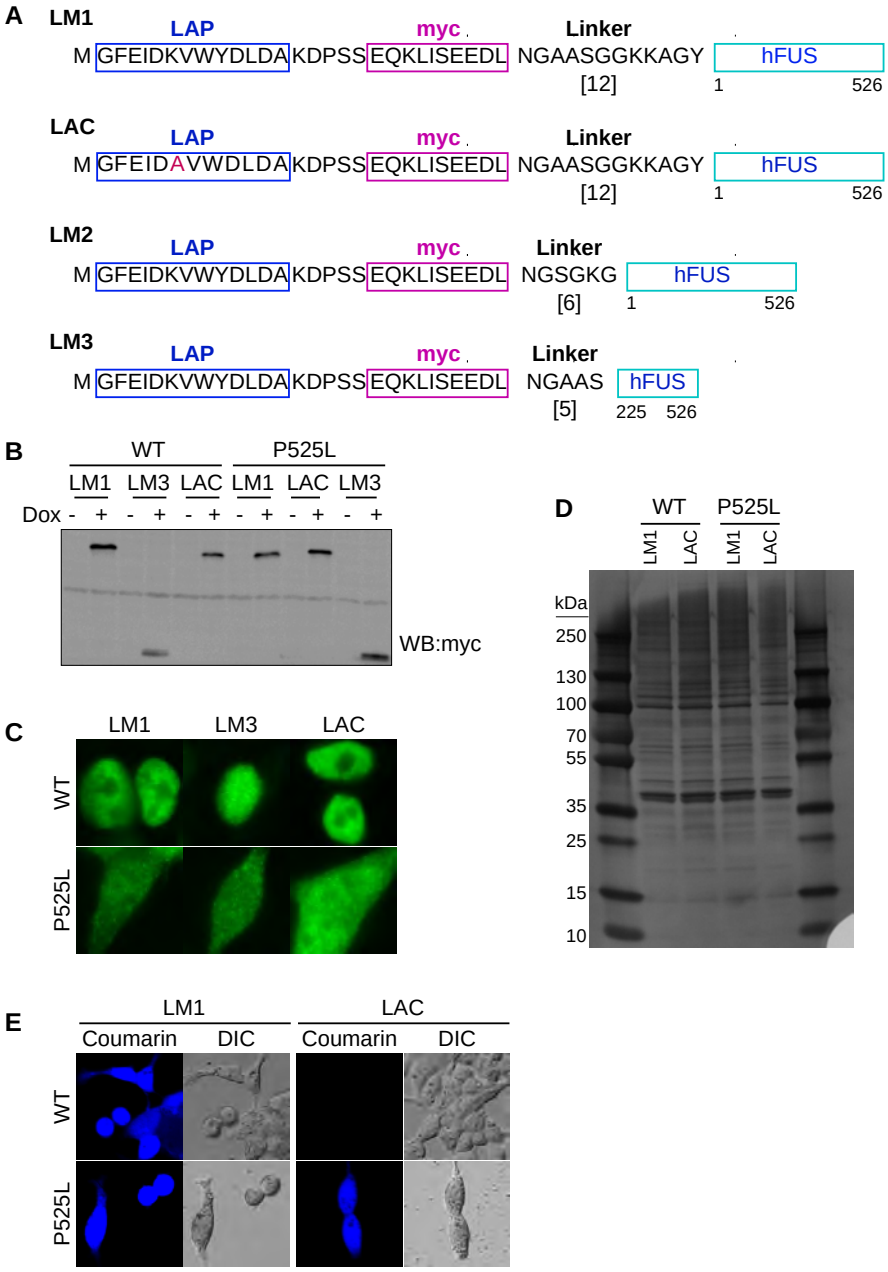

Figure A2. Constructs containing LAP-myc-FUS variants were designed and tested to identify FUS interacting proteins.

(A) Constructs containing LAP-myc-FUS variants were designed. **(B)** A western blot of cellular lysates using anti-myc antibody showed the expression of Lap-myc-FUS constructs. **(C)** Fluorescence images showed the localization of Lap-myc-FUS constructs. **(D)** A blot with silver staining showed the immunoprecipitated proteins with LM1 and LAC constructs in HEK293 cells. **(E)** Fluorescence images showed the expression of LM1 and LAC constructs. Blue signals represented the ligation activities of LM1 constructs with coumarin. The negative control (LAC) also showed the ligation activities.

the nucleolus where FUS expression is normally excluded (Figure A2-C).

Next, we tried to test photo-cross-linking after transient transfection of LM1 and LAC constructs into HEK293 cells. At 48 h after transfection, the HEK293 cells were trypsinized and collected. The cells were then incubated in the ligation buffer containing LplA, aryl azide, ATP, and magnesium acetate for 30 minutes at 37°C (Baruah, Puthenveetil et al. 2008). Photo-cross-linking was performed with 0.15 J/cm2 of 365 nm UV light using a Stratalinker (Stratagene) and the cells were immunoprecipitatied with anti-myc microbeads (Miltenyi Biotec). The immunoprecipitated product was further analyzed through silver staining after electrophoresis. Unfortunately, this trial did not result in any specific FUS interactions, producing instead lots of non-specific products. The lysis buffer had Dithiothreitol (DTT) and Tris that might have reduced and quenched reactions during aryl azide photo-activation. Therefore, several steps should be optimized, including the cell-lysis buffer, UV irradiation condition, and ligation-buffer composition.

To validate ligation affinity between LplA and LAP in our cell system, we changed the substrate from aryl azide to coumarin fluorophore, which has a fluorescence signal easily detectable by live-cell imaging (Uttamapinant, White et al. 2010). Coumarin (20 μM) was incubated for 5 minutes in HEK293 cells, overexpressing LAP-myc-FUS constructs, and was then washed out with culture media for 10 minutes to remove residual coumarin that was not ligated to LAP. We detected coumarin fluorescence signals in our cells (Figure A2-C), but the coumarin signal was also present in the cells,

expressing LAC constructs which should not conjugate with coumarin. Moreover, the cells expressing LM1-WT exhibited large amount of cytosolic coumarin expression, which FUS-WT should have expressed predominantly in the nucleus. For our next step, we should monitor a timeframe for coumarin expression and optimize the washing time to remove residual coumarin. To succeed in photo-cross-linking, we should consider several factors, including the concentration of LplA and aryl azide along with the duration and power of UV irradiation.

Recently, the groups of FUS-interacting proteins have been found in HEK293 cells using dual-tag affinity purification and mass spectrometry (Wang, Jiang et al. 2015). Wang *et al.* found that FUS interacted with proteins such as VCP/p97, PSF, UBA-1, and 26S proteasome non-ATPase regulatory subunit 12 suggesting the FUS mutant may perturb the mechanism related to energy metabolism and protein degradation pathway.

Appendix III:

The expression of p62/SQSTM1 and PML-NBs in a transgenic mouse model of ALS

Our lab developed a transgenic mouse model expressing human FUS-R495X under the control of a mouse prion promoter. FUS-R495X showed cytoplasmic translocation in the cortex and spinal cord consistent with our observations in HEK293 cells (in Chapters II and III) (Figure A3-1A). Although we observed quite a large amount of FUS-R495X expressed in cytoplasm, transgenic mice have not developed obvious motor phenotypes. However, our collaboration with the Durham lab showed that overexpression of FUS-R495X induced cytoplasmic sequestration of protein arginine methyltransferase 1 (PRMT1) in the spinal motor neurons, while the localization of PRMT1 was not altered in the neuronal cells in transgenic mice expressing FUS-WT and non-transgenic controls (Tibshirani, Tradewell et al. 2015).

In Chapter III, we observed that mutant FUS expression was associated with increased nuclear p62 foci accumulation and expanded PML-NBs in HEK293 cells. To check the relevance of these events in neuronal cells, we first examined the p62 expressions in the brain and spinal cord of a FUS-R495X transgenic mouse. The tissue lysates were generated from 5-month-old FUS-R495X transgenic mice (n=7) and non-transgenic controls (n=7). Overall, the level of p62 expression was higher in the lysates from the cortex than the spinal cord. However, we found that the level of p62 in the FUS-R495X cortex had not changed when compared to the p62 levels in the non-transgenic controls (Figure A3-1B), consistent with our results in HEK293 cells (in Chapter III). Next, we examined the localization of p62 in tissue sections from the FUS-R495X

transgenic mice. However, due to technical issues, we could not detect p62 expressions in the cortex or spinal cord sections by the immunofluorescence method.

In contrast, the levels of p62 expressions were elevated in the spinal cord lysates from a transgenic mouse model expressing SOD1-G93A (Gal, Strom et al. 2007). Moreover, p62 was co-localized with mutant SOD1 and ubiquitin in the spinal motor neurons of the SOD1-G93A transgenic mice, and overexpression of p62 induced aggregate formation of SOD1-G93A in NSC34 cells (Gal, Strom et al. 2007). Collectively, these results suggest that p62 plays a critical role in aggregation formation in ALS-SOD1. The role of p62 includes facilitation of misfolded protein degradation (Pankiv, Lamark et al. 2010, Lippai and Low 2014). Decreased activity of proteasome has been found in ALS patients' tissues and a transgenic mouse model expressing mutant SOD1 (Kabashi, Agar et al. 2008, Kabashi, Agar et al. 2012). Therefore, down regulation of proteasome activity may contribute to mutant SOD1 aggregates with p62 in a SOD1-G93A mouse model.

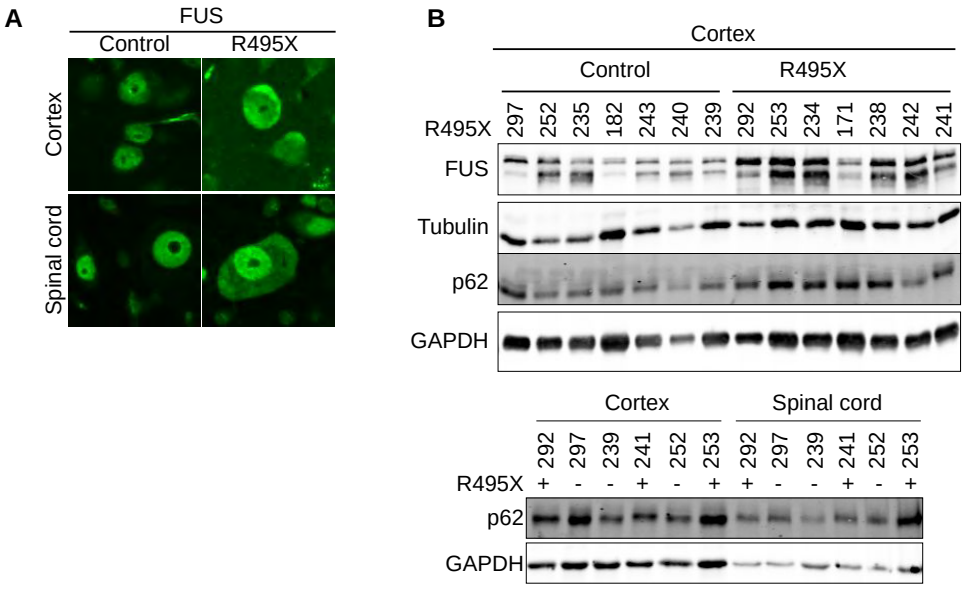

Figure A3-1. Expression of FUS-R495X showed no obvious change of p62 levels.

(A) FUS expressions were observed in the cortex and spinal cord sections. The tissue sections were stained with anti-FUS antibody (1:500, Bethyl laboratory, A300-293A) **(B)** Western blots showed the expression of FUS (1:1000, Bethyl laboratory, A300-293A) and p62 (1:1000, BD Bioscience, 610832) in tissue lysates from the cortex and spinal cord. Tubulin and GAPDH were used as a loading control.

Studies for examining PML-NBs in mouse tissues are limited. Recently, PML expression was analyzed throughout the adult brains of mice. Immunostaining analysis detected high PML expressions in the cortex and all hippocampal layers at the adult stage of mouse (2 to 3 months old) (Hall, Magalska et al. 2015). In addition, neuronal cells in the cerebral cortex expressed PML strongly, but other cell types, such as microglia, oligodendrocytes, and astrocytes, did not express PML (Hall, Magalska et al. 2015).

We were challenged to detect PML-NBs in our transgenic mouse tissue sections. By applying different methods for tissue preparation, we finally detected PML signals through a “squash” method (Figure A3-2). This method was developed to detect several nuclear bodies such as Cajal bodies, Gems, and PML-NBs in mouse tissues (Tapia, Bengoechea et al. 2012). Briefly, perfused mouse brains and spinal cords were cut into small pieces and placed on a siliconized slide, which was covered with a glass coverslip. The tissue was squashed by gently tapping on the top of the tissue pieces to dissociate cell nuclei. We stained slides with anti-PML (Millipore, 05-718, 1:200) and anti-Daxx (Santa Cruz Biotechnology, ac-7152, 1:500) antibodies. PML and Daxx expressed diffusely throughout the nucleus in the cortex and spinal cord of both the transgenic and control mice (Figure A3-2). A population of cells expressed a focal accumulation of PML and Daxx. Daxx foci frequently localized inside the nucleolus and were observed in all samples. We could not conclude whether Daxx foci were increased in an FUS transgenic mouse. Previously, increased Daxx accumulation was associated with motor neuron death

in a SOD1-G93A mouse model (Raoul, Buhler et al. 2006). Further study is required to check whether neuronal cells enhance Daxx accumulations in an FUS transgenic mouse.

Daxx was not co-localized with PML-NBs in our mouse model system (Figure A3-2). Cultured mouse fibroblasts showed localization of Daxx in PML-NBs (Tapia, Bengoechea et al. 2012). Interestingly, these PML-NBs were larger when compared with neuronal cells, suggesting that PML-NBs in neuronal cells may differ from those in fibroblast (Tapia, Bengoechea et al. 2012). Our findings suggest that PML-NBs are expressed in cortex and spinal cord of a 3-month-old FUS transgenic mouse. Our next step should be to focus on analyzing whether expression of PML-NBs is altered in FUS transgenic mice.

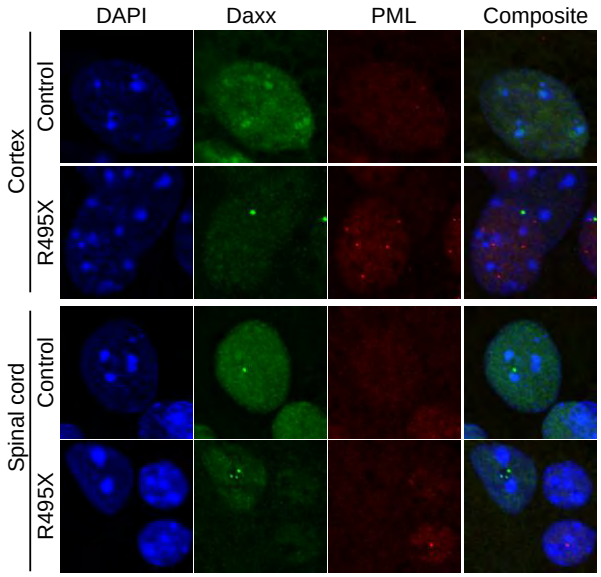

Figure A3-2. A population of cells expressed a focal accumulation of PML and Daxx. in cortex and spinal cord of a 3-month-old FUS transgenic mouse.

Confocal z-stack maximum intensity of projections showed Daxx and PML expressions in cortex and spinal cord tissues.

Bibliography

Abalkhail, H., J. Mitchell, J. Habgood, R. Orrell and J. de Belleroche (2003). "A new familial amyotrophic lateral sclerosis locus on chromosome 16q12.1-16q12.2." Am J Hum Genet 73(2): 383-389.

Ahmad, Y., F. M. Boisvert, P. Gregor, A. Cobley and A. I. Lamond (2009). "NOPdb: Nucleolar Proteome Database--2008 update." Nucleic Acids Res 37(Database issue): D181-184.

Al-Chalabi, A. and O. Hardiman (2013). "The epidemiology of ALS: a conspiracy of genes, environment and time." Nat Rev Neurol 9(11): 617-628.

Al-Sarraj, S., A. King, C. Troakes, B. Smith, S. Maekawa, I. Bodi, B. Rogelj, A. Al-Chalabi, T. Hortobagyi and C. E. Shaw (2011). "p62 positive, TDP-43 negative, neuronal cytoplasmic and intranuclear inclusions in the cerebellum and hippocampus define the pathology of C9orf72-linked FTLD and MND/ALS." Acta Neuropathol 122(6): 691-702.

Amador-Ortiz, C., W. L. Lin, Z. Ahmed, D. Personett, P. Davies, R. Duara, N. R. Graff-Radford, M. L. Hutton and D. W. Dickson (2007). "TDP-43 immunoreactivity in hippocampal sclerosis and Alzheimer's disease." Ann Neurol 61(5): 435-445.

Andersen, P. M. (2006). "Amyotrophic lateral sclerosis associated with mutations in the CuZn superoxide dismutase gene." Curr Neurol Neurosci Rep 6(1): 37-46.

Anderson, P. and N. Kedersha (2008). "Stress granules: the Tao of RNA triage." Trends Biochem Sci 33(3): 141-150.

Andersson, M. K., A. Stahlberg, Y. Arvidsson, A. Olofsson, H. Semb, G. Stenman, O. Nilsson and P. Aman (2008). "The multifunctional FUS, EWS and TAF15 proto-oncoproteins show cell type-specific expression patterns and involvement in cell spreading and stress response." BMC Cell Biol 9: 37.

Armstrong, G. A. and P. Drapeau (2013). "Loss and gain of FUS function impair neuromuscular synaptic transmission in a genetic model of ALS." Hum Mol Genet 22(21): 4282-4292.

Ascoli, C. A. and G. G. Maul (1991). "Identification of a novel nuclear domain." J Cell Biol 112(5): 785-795.

Aulas, A., S. Stabile and C. Vande Velde (2012). "Endogenous TDP-43, but not FUS, contributes to stress granule assembly via G3BP." Mol Neurodegener 7: 54.

Ayala, Y. M., P. Zago, A. D'Ambrogio, Y. F. Xu, L. Petrucelli, E. Buratti and F. E. Baralle (2008). "Structural determinants of the cellular localization and shuttling of TDP-43." J Cell Sci 121(Pt 22): 3778-3785.

Bailey, D. and P. O'Hare (2005). "Comparison of the SUMO1 and ubiquitin conjugation pathways during the inhibition of proteasome activity with evidence of SUMO1 recycling." Biochem J 392(Pt 2): 271-281.

Baker, M., I. R. Mackenzie, S. M. Pickering-Brown, J. Gass, R. Rademakers, C. Lindholm, J. Snowden, J. Adamson, A. D. Sadovnick, S. Rollinson, A. Cannon, E. Dwosh, D. Neary, S. Melquist, A. Richardson, D. Dickson, Z. Berger, J. Eriksen, T. Robinson, C. Zehr, C. A. Dickey, R. Crook, E. McGowan, D. Mann, B. Boeve, H. Feldman and M. Hutton (2006). "Mutations in progranulin cause tau-negative frontotemporal dementia linked to chromosome 17." Nature 442(7105): 916-919.

Bannwarth, S., S. Ait-El-Mkadem, A. Chaussenot, E. C. Genin, S. Lacas-Gervais, K. Fragaki, L. Berg-Alonso, Y. Kageyama, V. Serre, D. G. Moore, A. Verschueren, C. Rouzier, I. Le Ber, G. Auge, C. Cochaud, F. Lespinasse, K. N'Guyen, A. de Septenville, A. Brice, P. Yu-Wai-Man, H. Sesaki, J. Pouget and V. Paquis-Flucklinger (2014). "A mitochondrial origin for frontotemporal dementia and amyotrophic lateral sclerosis through CHCHD10 involvement." Brain 137(Pt 8): 2329-2345.

Barber, S. C., R. J. Mead and P. J. Shaw (2006). "Oxidative stress in ALS: a mechanism of neurodegeneration and a therapeutic target." Biochim Biophys Acta 1762(11-12): 1051-1067.

Barmada, S. J., G. Skibinski, E. Korb, E. J. Rao, J. Y. Wu and S. Finkbeiner (2010). "Cytoplasmic mislocalization of TDP-43 is toxic to neurons and enhanced by a mutation associated with familial amyotrophic lateral sclerosis." J Neurosci 30(2): 639-649.

Baron, D. M., L. J. Kaushansky, C. L. Ward, R. R. Sama, R. J. Chian, K. J. Boggio, A. J. Quaresma, J. A. Nickerson and D. A. Bosco (2013). "Amyotrophic lateral sclerosis-linked FUS/TLS alters stress granule assembly and dynamics." Mol Neurodegener 8: 30.

Baruah, H., S. Puthenveetil, Y. A. Choi, S. Shah and A. Y. Ting (2008). "An engineered aryl azide ligase for site-specific mapping of protein-protein interactions through photo-cross-linking." Angew Chem Int Ed Engl 47(37): 7018-7021.

Baumer, D., D. Hilton, S. M. Paine, M. R. Turner, J. Lowe, K. Talbot and O. Ansorge (2010). "Juvenile ALS with basophilic inclusions is a FUS proteinopathy with FUS mutations." Neurology 75(7): 611-618.

Belzil, V. V., P. N. Valdmanis, P. A. Dion, H. Daoud, E. Kabashi, A. Noreau, J. Gauthier, P. Hince, A. Desjarlais, J. P. Bouchard, L. Lacomblez, F. Salachas, P. F. Pradat, W. Camu, V. Meininger, N. Dupre and G. A. Rouleau (2009). "Mutations in FUS cause FALS and SALS in French and French Canadian populations." Neurology 73(15): 1176-1179.

Bennett, E. J., T. A. Shaler, B. Woodman, K. Y. Ryu, T. S. Zaitseva, C. H. Becker, G. P. Bates, H. Schulman and R. R. Kopito (2007). "Global changes to the ubiquitin system in Huntington's disease." Nature 448(7154): 704-708.

Bentmann, E., C. Haass and D. Dormann (2013). "Stress granules in neurodegeneration--lessons learnt from TAR DNA binding protein of 43 kDa and fused in sarcoma." Febs j 280(18): 4348-4370.

Bentmann, E., M. Neumann, S. Tahirovic, R. Rodde, D. Dormann and C. Haass (2012). "Requirements for stress granule recruitment of fused in sarcoma (FUS) and TAR DNA-binding protein of 43 kDa (TDP-43)." J Biol Chem 287(27): 23079-23094.

Bernardi, R. and P. P. Pandolfi (2003). "Role of PML and the PML-nuclear body in the control of programmed cell death." Oncogene 22(56): 9048-9057.

Bernardi, R. and P. P. Pandolfi (2007). "Structure, dynamics and functions of promyelocytic leukaemia nuclear bodies." Nat Rev Mol Cell Biol 8(12): 1006-1016.

Bernardi, R., A. Papa and P. P. Pandolfi (2008). "Regulation of apoptosis by PML and the PML-NBs." Oncogene 27(48): 6299-6312.

Bertolotti, A., T. Melot, J. Acker, M. Vigneron, O. Delattre and L. Tora (1998). "EWS, but not EWS-FLI-1, is associated with both TFIID and RNA polymerase II: interactions between two members of the TET family, EWS and hTAFII68, and subunits of TFIID and RNA polymerase II complexes." Mol Cell Biol 18(3): 1489-1497.

Besche, H. C. and A. L. Goldberg (2012). "Affinity purification of mammalian 26S proteasomes using an ubiquitin-like domain." Methods Mol Biol 832: 423-432.

Besche, H. C., W. Haas, S. P. Gygi and A. L. Goldberg (2009). "Isolation of mammalian 26S proteasomes and p97/VCP complexes using the ubiquitin-like domain from HHR23B reveals novel proteasome-associated proteins." Biochemistry 48(11): 2538-2549.

Bigio, E. H., N. A. Johnson, A. W. Rademaker, B. B. Fung, M. M. Mesulam, N. Siddique, L. Dellefave, J. Caliendo, S. Freeman and T. Siddique (2004). "Neuronal ubiquitinated intranuclear inclusions in familial and non-familial frontotemporal dementia of the motor neuron disease type associated with amyotrophic lateral sclerosis." J Neuropathol Exp Neurol 63(8): 801-811.

Blair, I. P., K. L. Williams, S. T. Warraich, J. C. Durnall, A. D. Thoeng, J. Manavis, P. C. Blumbergs, S. Vucic, M. C. Kiernan and G. A. Nicholson (2010). "FUS mutations in amyotrophic lateral sclerosis: clinical, pathological, neurophysiological and genetic analysis." J Neurol Neurosurg Psychiatry 81(6): 639-645.

Block, G. J., C. H. Eskiw, G. Dellaire and D. P. Bazett-Jones (2006). "Transcriptional regulation is affected by subnuclear targeting of reporter plasmids to PML nuclear bodies." Mol Cell Biol 26(23): 8814-8825.

Blokhuis, A. M., E. J. Groen, M. Koppers, L. H. van den Berg and R. J. Pasterkamp (2013). "Protein aggregation in amyotrophic lateral sclerosis." Acta Neuropathol 125(6): 777-794.

Bogdanov, A. M., E. A. Bogdanova, D. M. Chudakov, T. V. Gorodnicheva, S. Lukyanov and K. A. Lukyanov (2009). "Cell culture medium affects GFP photostability: a solution." Nat Methods 6(12): 859-860.

Bosco, D. A., N. Lemay, H. K. Ko, H. Zhou, C. Burke, T. J. Kwiatkowski, Jr., P. Sapp, D. McKenna-Yasek, R. H. Brown, Jr. and L. J. Hayward (2010). "Mutant FUS proteins that cause amyotrophic lateral sclerosis incorporate into stress granules." Hum Mol Genet 19(21): 4160-4175.

Boulon, S., B. J. Westman, S. Hutten, F. M. Boisvert and A. I. Lamond (2010). "The nucleolus under stress." Mol Cell 40(2): 216-227.

Broe, M., C. E. Shepherd, D. M. Mann, E. A. Milward, W. P. Gai, E. Thiel and G. M. Halliday (2005). "Insoluble alpha-synuclein in Alzheimer's disease without Lewy body formation." Neurotox Res 7(1-2): 69-76.

Buchan, J. R. and R. Parker (2009). "Eukaryotic stress granules: the ins and outs of translation." Mol Cell 36(6): 932-941.

Butler, K., L. A. Martinez and M. V. Tejada-Simon (2013). "Impaired cognitive function and reduced anxiety-related behavior in a promyelocytic leukemia (PML) tumor suppressor protein-deficient mouse." Genes Brain Behav 12(2): 189-202.

Calvio, C., G. Neubauer, M. Mann and A. I. Lamond (1995). "Identification of hnRNP P2 as TLS/FUS using electrospray mass spectrometry." Rna 1(7): 724-733.

Carroll, D. (2011). "Genome engineering with zinc-finger nucleases." Genetics 188(4): 773-782.

Cassel, J. A. and A. B. Reitz (2013). "Ubiquilin-2 (UBQLN2) binds with high affinity to the C-terminal region of TDP-43 and modulates TDP-43 levels in H4 cells:

characterization of inhibition by nucleic acids and 4-aminoquinolines." Biochim Biophys Acta 1834(6): 964-971.

Chio, A., A. Calvo, L. Mazzini, R. Cantello, G. Mora, C. Moglia, L. Corrado, S. D'Alfonso, E. Majounie, A. Renton, F. Pisano, I. Ossola, M. Brunetti, B. J. Traynor and G. Restagno (2012). "Extensive genetics of ALS: a population-based study in Italy." Neurology 79(19): 1983-1989.

Chio, A., G. Restagno, M. Brunetti, I. Ossola, A. Calvo, G. Mora, M. Sabatelli, M. R. Monsurro, S. Battistini, J. Mandrioli, F. Salvi, R. Spataro, J. Schymick, B. J. Traynor and V. La Bella (2009). "Two Italian kindreds with familial amyotrophic lateral sclerosis due to FUS mutation." Neurobiol Aging 30(8): 1272-1275.

Chort, A., S. Alves, M. Marinello, B. Dufresnois, J. G. Dornbierer, C. Tesson, M. Latouche, D. P. Baker, M. Barkats, K. H. El Hachimi, M. Ruberg, A. Janer, G. Stevanin, A. Brice and A. Sittler (2013). "Interferon beta induces clearance of mutant ataxin 7 and improves locomotion in SCA7 knock-in mice." Brain 136(Pt 6): 1732-1745.

Cirulli, E. T., B. N. Lasseigne, S. Petrovski, P. C. Sapp, P. A. Dion, C. S. Leblond, J. Couthouis, Y. F. Lu, Q. Wang, B. J. Krueger, Z. Ren, J. Keebler, Y. Han, S. E. Levy, B. E. Boone, J. R. Wimbish, L. L. Waite, A. L. Jones, J. P. Carulli, A. G. Day-Williams, J. F. Staropoli, W. W. Xin, A. Chesi, A. R. Raphael, D. McKenna-Yasek, J. Cady, J. M. Vianney de Jong, K. P. Kenna, B. N. Smith, S. Topp, J. Miller, A. Gkazi, A. Al-Chalabi, L. H. van den Berg, J. Veldink, V. Silani, N. Ticozzi, C. E. Shaw, R. H. Baloh, S. Appel, E. Simpson, C. Lagier-Tourenne, S. M. Pulst, S. Gibson, J. Q. Trojanowski, L. Elman, L. McCluskey, M. Grossman, N. A. Shneider, W. K. Chung, J. M. Ravits, J. D. Glass, K. B. Sims, V. M. Van Deerlin, T. Maniatis, S. D. Hayes, A. Ordureau, S. Swarup, J. Landers, F. Baas, A. S. Allen, R. S. Bedlack, J. W. Harper, A. D. Gitler, G. A. Rouleau, R. Brown, M. B. Harms, G. M. Cooper, T. Harris, R. M. Myers and D. B. Goldstein (2015). "Exome sequencing in amyotrophic lateral sclerosis identifies risk genes and pathways." Science 347(6229): 1436-1441.

Colombrita, C., E. Zennaro, C. Fallini, M. Weber, A. Sommacal, E. Buratti, V. Silani and A. Ratti (2009). "TDP-43 is recruited to stress granules in conditions of oxidative insult." J Neurochem 111(4): 1051-1061.

Condemine, W., Y. Takahashi, J. Zhu, F. Puvion-Dutilleul, S. Guegan, A. Janin and H. de The (2006). "Characterization of endogenous human promyelocytic leukemia isoforms." Cancer Res 66(12): 6192-6198.

Corrado, L., R. Del Bo, B. Castellotti, A. Ratti, C. Cereda, S. Penco, G. Soraru, Y. Carlomagno, S. Ghezzi, V. Pensato, C. Colombrita, S. Gagliardi, L. Cozzi, V. Orsetti, M. Mancuso, G. Siciliano, L. Mazzini, G. P. Comi, C. Gellera, M. Ceroni, S. D'Alfonso and

V. Silani (2010). "Mutations of FUS gene in sporadic amyotrophic lateral sclerosis." J Med Genet 47(3): 190-194.

Crozat, A., P. Aman, N. Mandahl and D. Ron (1993). "Fusion of CHOP to a novel RNA-binding protein in human myxoid liposarcoma." Nature 363(6430): 640-644.

Cudkowicz, M. E., D. McKenna-Yasek, P. E. Sapp, W. Chin, B. Geller, D. L. Hayden, D. A. Schoenfeld, B. A. Hosler, H. R. Horvitz and R. H. Brown (1997). "Epidemiology of mutations in superoxide dismutase in amyotrophic lateral sclerosis." Ann Neurol 41(2): 210-221.

Cushman, M., B. S. Johnson, O. D. King, A. D. Gitler and J. Shorter (2010). "Prion-like disorders: blurring the divide between transmissibility and infectivity." J Cell Sci 123(Pt 8): 1191-1201.

Daigle, J. G., N. A. Lanson, Jr., R. B. Smith, I. Casci, A. Maltare, J. Monaghan, C. D. Nichols, D. Kryndushkin, F. Shewmaker and U. B. Pandey (2013). "RNA-binding ability of FUS regulates neurodegeneration, cytoplasmic mislocalization and incorporation into stress granules associated with FUS carrying ALS-linked mutations." Hum Mol Genet 22(6): 1193-1205.

Damme, P. V., A. Goris, V. Race, N. Hersmus, B. Dubois, L. V. Bosch, G. Matthijs and W. Robberecht (2010). "The occurrence of mutations in FUS in a Belgian cohort of patients with familial ALS." Eur J Neurol 17(5): 754-756.

Dangoumau, A., C. Veyrat-Durebex, H. Blasco, J. Praline, P. Corcia, C. R. Andres and P. Vourc'h (2013). "Protein SUMOylation, an emerging pathway in amyotrophic lateral sclerosis." Int J Neurosci 123(6): 366-374.

Dantuma, N. P., K. Lindsten, R. Glas, M. Jellne and M. G. Masucci (2000). "Short-lived green fluorescent proteins for quantifying ubiquitin/proteasome-dependent proteolysis in living cells." Nat Biotechnol 18(5): 538-543.

de The, H., M. Le Bras and V. Lallemand-Breitenbach (2012). "The cell biology of disease: Acute promyelocytic leukemia, arsenic, and PML bodies." J Cell Biol 198(1): 11-21.

DeJesus-Hernandez, M., J. Kocerha, N. Finch, R. Crook, M. Baker, P. Desaro, A. Johnston, N. Rutherford, A. Wojtas, K. Kennelly, Z. K. Wszolek, N. Graff-Radford, K. Boylan and R. Rademakers (2010). "De novo truncating FUS gene mutation as a cause of sporadic amyotrophic lateral sclerosis." Hum Mutat 31(5): E1377-1389.

DeJesus-Hernandez, M., I. R. Mackenzie, B. F. Boeve, A. L. Boxer, M. Baker, N. J. Rutherford, A. M. Nicholson, N. A. Finch, H. Flynn, J. Adamson, N. Kouri, A. Wojtas, P.

Sengdy, G. Y. Hsiung, A. Karydas, W. W. Seeley, K. A. Josephs, G. Coppola, D. H. Geschwind, Z. K. Wszolek, H. Feldman, D. S. Knopman, R. C. Petersen, B. L. Miller, D. W. Dickson, K. B. Boylan, N. R. Graff-Radford and R. Rademakers (2011). "Expanded GGGGCC hexanucleotide repeat in noncoding region of C9ORF72 causes chromosome 9p-linked FTD and ALS." Neuron 72(2): 245-256.

Dellaire, G. and D. P. Bazett-Jones (2004). "PML nuclear bodies: dynamic sensors of DNA damage and cellular stress." Bioessays 26(9): 963-977.

Dellaire, G., R. W. Ching, K. Ahmed, F. Jalali, K. C. Tse, R. G. Bristow and D. P. Bazett-Jones (2006). "Promyelocytic leukemia nuclear bodies behave as DNA damage sensors whose response to DNA double-strand breaks is regulated by NBS1 and the kinases ATM, Chk2, and ATR." J Cell Biol 175(1): 55-66.

Deng, H., K. Gao and J. Jankovic (2014). "The role of FUS gene variants in neurodegenerative diseases." Nat Rev Neurol 10(6): 337-348.

Deng, H. X., W. Chen, S. T. Hong, K. M. Boycott, G. H. Gorrie, N. Siddique, Y. Yang, F. Fecto, Y. Shi, H. Zhai, H. Jiang, M. Hirano, E. Rampersaud, G. H. Jansen, S. Donkervoort, E. H. Bigio, B. R. Brooks, K. Ajroud, R. L. Sufit, J. L. Haines, E. Mugnaini, M. A. Pericak-Vance and T. Siddique (2011). "Mutations in UBQLN2 cause dominant X-linked juvenile and adult-onset ALS and ALS/dementia." Nature 477(7363): 211-215.

Dhar, S. K., J. Zhang, J. Gal, Y. Xu, L. Miao, B. C. Lynn, H. Zhu, E. J. Kasarskis and D. K. St Clair (2014). "FUsed in sarcoma is a novel regulator of manganese superoxide dismutase gene transcription." Antioxid Redox Signal 20(10): 1550-1566.

Dion, P. A., H. Daoud and G. A. Rouleau (2009). "Genetics of motor neuron disorders: new insights into pathogenic mechanisms." Nat Rev Genet 10(11): 769-782.

Doi, H., S. Koyano, Y. Suzuki, N. Nukina and Y. Kuroiwa (2010). "The RNA-binding protein FUS/TLS is a common aggregate-interacting protein in polyglutamine diseases." Neurosci Res 66(1): 131-133.

Dormann, D. and C. Haass (2011). "TDP-43 and FUS: a nuclear affair." Trends Neurosci 34(7): 339-348.

Dormann, D., R. Rodde, D. Edbauer, E. Bentmann, I. Fischer, A. Hruscha, M. E. Than, I. R. Mackenzie, A. Capell, B. Schmid, M. Neumann and C. Haass (2010). "ALS-associated fused in sarcoma (FUS) mutations disrupt Transportin-mediated nuclear import." Embo j 29(16): 2841-2857.

Dorval, V. and P. E. Fraser (2007). "SUMO on the road to neurodegeneration." Biochim Biophys Acta 1773(6): 694-706.

Doyon, Y., J. M. McCammon, J. C. Miller, F. Faraji, C. Ngo, G. E. Katibah, R. Amora, T. D. Hocking, L. Zhang, E. J. Rebar, P. D. Gregory, F. D. Urnov and S. L. Amacher (2008). "Heritable targeted gene disruption in zebrafish using designed zinc-finger nucleases." Nat Biotechnol 26(6): 702-708.

Dreyfuss, G., M. J. Matunis, S. Pinol-Roma and C. G. Burd (1993). "hnRNP proteins and the biogenesis of mRNA." Annu Rev Biochem 62: 289-321.

Everett, R. D. and M. K. Chelbi-Alix (2007). "PML and PML nuclear bodies: implications in antiviral defence." Biochimie 89(6-7): 819-830.

Everett, R. D., W. C. Earnshaw, A. F. Pluta, T. Sternsdorf, A. M. Ainsztein, M. Carmena, S. Ruchaud, W. L. Hsu and A. Orr (1999). "A dynamic connection between centromeres and ND10 proteins." J Cell Sci 112 (Pt 20): 3443-3454.

Fecto, F., J. Yan, S. P. Vemula, E. Liu, Y. Yang, W. Chen, J. G. Zheng, Y. Shi, N. Siddique, H. Arrat, S. Donkervoort, S. Ajroud-Driss, R. L. Sufit, S. L. Heller, H. X. Deng and T. Siddique (2011). "SQSTM1 mutations in familial and sporadic amyotrophic lateral sclerosis." Arch Neurol 68(11): 1440-1446.

Feligioni, M. and R. Nistico (2013). "SUMO: a (oxidative) stressed protein." Neuromolecular Med 15(4): 707-719.

Ferraiuolo, L., J. Kirby, A. J. Grierson, M. Sendtner and P. J. Shaw (2011). "Molecular pathways of motor neuron injury in amyotrophic lateral sclerosis." Nat Rev Neurol 7(11): 616-630.

Ferrante, R. J., S. E. Browne, L. A. Shinobu, A. C. Bowling, M. J. Baik, U. MacGarvey, N. W. Kowall, R. H. Brown, Jr. and M. F. Beal (1997). "Evidence of increased oxidative damage in both sporadic and familial amyotrophic lateral sclerosis." J Neurochem 69(5): 2064-2074.

Figley, M. D., G. Bieri, R. M. Kolaitis, J. P. Taylor and A. D. Gitler (2014). "Profilin 1 associates with stress granules and ALS-linked mutations alter stress granule dynamics." J Neurosci 34(24): 8083-8097.

Finley, D. (2009). "Recognition and processing of ubiquitin-protein conjugates by the proteasome." Annu Rev Biochem 78: 477-513.

Flanagan-Steet, H., M. A. Fox, D. Meyer and J. R. Sanes (2005). "Neuromuscular synapses can form in vivo by incorporation of initially aneural postsynaptic specializations." Development 132(20): 4471-4481.

Foran, E., A. Bogush, M. Goffredo, P. Roncaglia, S. Gustincich, P. Pasinelli and D. Trotti (2011). "Motor neuron impairment mediated by a sumoylated fragment of the glial glutamate transporter EAAT2." Glia 59(11): 1719-1731.

Fox, A. H., Y. W. Lam, A. K. Leung, C. E. Lyon, J. Andersen, M. Mann and A. I. Lamond (2002). "Paraspeckles: a novel nuclear domain." Curr Biol 12(1): 13-25.

Fox, A. H. and A. I. Lamond (2010). "Paraspeckles." Cold Spring Harb Perspect Biol 2(7): a000687.

Freischmidt, A., T. Wieland, B. Richter, W. Ruf, V. Schaeffer, K. Muller, N. Marroquin, F. Nordin, A. Hubers, P. Weydt, S. Pinto, R. Press, S. Millecamps, N. Molko, E. Bernard, C. Desnuelle, M. H. Soriani, J. Dorst, E. Graf, U. Nordstrom, M. S. Feiler, S. Putz, T. M. Boeckers, T. Meyer, A. S. Winkler, J. Winkelman, M. de Carvalho, D. R. Thal, M. Otto, T. Brannstrom, A. E. Volk, P. Kursula, K. M. Danzer, P. Lichtner, I. Dikic, T. Meitinger, A. C. Ludolph, T. M. Strom, P. M. Andersen and J. H. Weishaupt (2015). "Haploinsufficiency of TBK1 causes familial ALS and fronto-temporal dementia." Nat Neurosci 18(5): 631-636.

Fujii, R., S. Okabe, T. Urushido, K. Inoue, A. Yoshimura, T. Tachibana, T. Nishikawa, G. G. Hicks and T. Takumi (2005). "The RNA binding protein TLS is translocated to dendritic spines by mGluR5 activation and regulates spine morphology." Curr Biol 15(6): 587-593.

Fujii, R. and T. Takumi (2005). "TLS facilitates transport of mRNA encoding an actin-stabilizing protein to dendritic spines." J Cell Sci 118(Pt 24): 5755-5765.

Fujita, K., H. Ito, S. Nakano, Y. Kinoshita, R. Wate and H. Kusaka (2008). "Immunohistochemical identification of messenger RNA-related proteins in basophilic inclusions of adult-onset atypical motor neuron disease." Acta Neuropathol 116(4): 439-445.

Gajdusek, D. C. and A. M. Salazar (1982). "Amyotrophic lateral sclerosis and parkinsonian syndromes in high incidence among the Auyu and Jakai people of West New Guinea." Neurology 32(2): 107-126.

Gal, J., A. L. Strom, R. Kilty, F. Zhang and H. Zhu (2007). "p62 accumulates and enhances aggregate formation in model systems of familial amyotrophic lateral sclerosis." J Biol Chem 282(15): 11068-11077.

Gal, J., J. Zhang, D. M. Kwinter, J. Zhai, H. Jia, J. Jia and H. Zhu (2011). "Nuclear localization sequence of FUS and induction of stress granules by ALS mutants." Neurobiol Aging 32(12): 2323 e2327-2340.

Galanty, Y., R. Belotserkovskaya, J. Coates and S. P. Jackson (2012). "RNF4, a SUMO-targeted ubiquitin E3 ligase, promotes DNA double-strand break repair." Genes Dev 26(11): 1179-1195.

Gallagher, P. S., M. L. Oeser, A. C. Abraham, D. Kaganovich and R. G. Gardner (2014). "Cellular maintenance of nuclear protein homeostasis." Cell Mol Life Sci 71(10): 1865-1879.

Gardiner, M., R. Toth, F. Vandermoere, N. A. Morrice and J. Rouse (2008). "Identification and characterization of FUS/TLS as a new target of ATM." Biochem J 415(2): 297-307.

Geiss-Friedlander, R. and F. Melchior (2007). "Concepts in sumoylation: a decade on." Nat Rev Mol Cell Biol 8(12): 947-956.

Geoffroy, M. C., E. G. Jaffray, K. J. Walker and R. T. Hay (2010). "Arsenic-induced SUMO-dependent recruitment of RNF4 into PML nuclear bodies." Mol Biol Cell 21(23): 4227-4239.

Gerbino, V., M. T. Carri, M. Cozzolino and T. Achsel (2013). "Mislocalised FUS mutants stall spliceosomal snRNPs in the cytoplasm." Neurobiol Dis 55: 120-128.

Gibb, S. L., W. Boston-Howes, Z. S. Lavina, S. Gustincich, R. H. Brown, Jr., P. Pasinelli and D. Trotti (2007). "A caspase-3-cleaved fragment of the glial glutamate transporter EAAT2 is sumoylated and targeted to promyelocytic leukemia nuclear bodies in mutant SOD1-linked amyotrophic lateral sclerosis." J Biol Chem 282(44): 32480-32490.

Girdwood, D., D. Bumpass, O. A. Vaughan, A. Thain, L. A. Anderson, A. W. Snowden, E. Garcia-Wilson, N. D. Perkins and R. T. Hay (2003). "P300 transcriptional repression is mediated by SUMO modification." Mol Cell 11(4): 1043-1054.

Goldbaum, O., M. Oppermann, M. Handschuh, D. Dabir, B. Zhang, M. S. Forman, J. Q. Trojanowski, V. M. Lee and C. Richter-Landsberg (2003). "Proteasome inhibition stabilizes tau inclusions in oligodendroglial cells that occur after treatment with okadaic acid." J Neurosci 23(26): 8872-8880.

Goldberg, A. L. (2003). "Protein degradation and protection against misfolded or damaged proteins." Nature 426(6968): 895-899.

Goldberg, A. L. (2007). "On prions, proteasomes, and mad cows." N Engl J Med 357(11): 1150-1152.

Gordon, D., C. Abajian and P. Green (1998). "Consed: a graphical tool for sequence finishing." Genome Res 8(3): 195-202.

Gordon, P. H. (2013). "Amyotrophic Lateral Sclerosis: An update for 2013 Clinical Features, Pathophysiology, Management and Therapeutic Trials." Aging Dis 4(5): 295-310.

Gregory, R. I., K. P. Yan, G. Amuthan, T. Chendrimada, B. Doratotaj, N. Cooch and R. Shiekhattar (2004). "The Microprocessor complex mediates the genesis of microRNAs." Nature 432(7014): 235-240.

Groen, E. J., K. Fumoto, A. M. Blokhuis, J. Engelen-Lee, Y. Zhou, D. M. van den Heuvel, M. Koppers, F. van Diggelen, J. van Heest, J. A. Demmers, J. Kirby, P. J. Shaw, E. Aronica, W. G. Spliet, J. H. Veldink, L. H. van den Berg and R. J. Pasterkamp (2013). "ALS-associated mutations in FUS disrupt the axonal distribution and function of SMN." Hum Mol Genet 22(18): 3690-3704.

Gu, Z. C. and C. Enenkel (2014). "Proteasome assembly." Cell Mol Life Sci 71(24): 4729-4745.

Guo, L., B. I. Giasson, A. Glavis-Bloom, M. D. Brewer, J. Shorter, A. D. Gitler and X. Yang (2014). "A cellular system that degrades misfolded proteins and protects against neurodegeneration." Mol Cell 55(1): 15-30.

Guzzo, C. M., C. E. Berndsen, J. Zhu, V. Gupta, A. Datta, R. A. Greenberg, C. Wolberger and M. J. Matunis (2012). "RNF4-dependent hybrid SUMO-ubiquitin chains are signals for RAP80 and thereby mediate the recruitment of BRCA1 to sites of DNA damage." Sci Signal 5(253): ra88.

Hall, M. H., A. Magalska, M. Malinowska, B. Ruszczycki, I. Czaban, S. Patel, M. Ambrozek-Latecka, E. Zolocinska, H. Broszkiewicz, K. Parobczak, R. R. Nair, M. Rylski, R. Pawlak, C. R. Bramham and G. M. Wilczynski (2015). "Localization and regulation of PML bodies in the adult mouse brain." Brain Struct Funct.

Hattersley, N., L. Shen, E. G. Jaffray and R. T. Hay (2011). "The SUMO protease SENP6 is a direct regulator of PML nuclear bodies." Mol Biol Cell 22(1): 78-90.

Hay, R. T. (2013). "Decoding the SUMO signal." Biochem Soc Trans 41(2): 463-473.

Hetman, M. and M. Pietrzak (2012). "Emerging roles of the neuronal nucleolus." Trends Neurosci 35(5): 305-314.

Hickey, C. M., N. R. Wilson and M. Hochstrasser (2012). "Function and regulation of SUMO proteases." Nat Rev Mol Cell Biol 13(12): 755-766.

Hicks, G. G., N. Singh, A. Nashabi, S. Mai, G. Bozek, L. Klewes, D. Arapovic, E. K. White, M. J. Koury, E. M. Oltz, L. Van Kaer and H. E. Ruley (2000). "Fus deficiency in mice results in defective B-lymphocyte development and activation, high levels of chromosomal instability and perinatal death." Nat Genet 24(2): 175-179.

Hoell, J. I., E. Larsson, S. Runge, J. D. Nusbaum, S. Duggimpudi, T. A. Farazi, M. Hafner, A. Borkhardt, C. Sander and T. Tuschl (2011). "RNA targets of wild-type and mutant FET family proteins." Nat Struct Mol Biol 18(12): 1428-1431.

Hofmann, T. G. and H. Will (2003). "Body language: the function of PML nuclear bodies in apoptosis regulation." Cell Death Differ 10(12): 1290-1299.

Huang, C., J. Tong, F. Bi, Q. Wu, B. Huang, H. Zhou and X. G. Xia (2012). "Entorhinal cortical neurons are the primary targets of FUS mislocalization and ubiquitin aggregation in FUS transgenic rats." Hum Mol Genet 21(21): 4602-4614.

Huang, E. J., J. Zhang, F. Geser, J. Q. Trojanowski, J. B. Strober, D. W. Dickson, R. H. Brown, Jr., B. E. Shapiro and C. Lomen-Hoerth (2010). "Extensive FUS-immunoreactive pathology in juvenile amyotrophic lateral sclerosis with basophilic inclusions." Brain Pathol 20(6): 1069-1076.

Hutton, M., C. L. Lendon, P. Rizzu, M. Baker, S. Froelich, H. Houlden, S. Pickering-Brown, S. Chakraverty, A. Isaacs, A. Grover, J. Hackett, J. Adamson, S. Lincoln, D. Dickson, P. Davies, R. C. Petersen, M. Stevens, E. de Graaff, E. Wauters, J. van Baren, M. Hillebrand, M. Joosse, J. M. Kwon, P. Nowotny, L. K. Che, J. Norton, J. C. Morris, L. A. Reed, J. Trojanowski, H. Basun, L. Lannfelt, M. Neystat, S. Fahn, F. Dark, T. Tannenberg, P. R. Dodd, N. Hayward, J. B. Kwok, P. R. Schofield, A. Andreadis, J. Snowden, D. Craufurd, D. Neary, F. Owen, B. A. Oostra, J. Hardy, A. Goate, J. van Swieten, D. Mann, T. Lynch and P. Heutink (1998). "Association of missense and 5'-splice-site mutations in tau with the inherited dementia FTDP-17." Nature 393(6686): 702-705.

Iko, Y., T. S. Kodama, N. Kasai, T. Oyama, E. H. Morita, T. Muto, M. Okumura, R. Fujii, T. Takumi, S. Tate and K. Morikawa (2004). "Domain architectures and characterization of an RNA-binding protein, TLS." J Biol Chem 279(43): 44834-44840.

Ishigaki, S., A. Masuda, Y. Fujioka, Y. Iguchi, M. Katsuno, A. Shibata, F. Urano, G. Sobue and K. Ohno (2012). "Position-dependent FUS-RNA interactions regulate alternative splicing events and transcriptions." Sci Rep 2: 529.

Ishihara, T., Y. Ariizumi, A. Shiga, T. Kato, C. F. Tan, T. Sato, Y. Miki, M. Yokoo, T. Fujino, A. Koyama, A. Yokoseki, M. Nishizawa, A. Kakita, H. Takahashi and O. Onodera (2013). "Decreased number of Gemini of coiled bodies and U12 snRNA level in amyotrophic lateral sclerosis." Hum Mol Genet 22(20): 4136-4147.

Ishov, A. M., A. G. Sotnikov, D. Negorev, O. V. Vladimirova, N. Neff, T. Kamitani, E. T. Yeh, J. F. Strauss, 3rd and G. G. Maul (1999). "PML is critical for ND10 formation and recruits the PML-interacting protein daxx to this nuclear structure when modified by SUMO-1." J Cell Biol 147(2): 221-234.

Ito, D., M. Seki, Y. Tsunoda, H. Uchiyama and N. Suzuki (2011). "Nuclear transport impairment of amyotrophic lateral sclerosis-linked mutations in FUS/TLS." Ann Neurol 69(1): 152-162.

Janer, A., A. Werner, J. Takahashi-Fujigasaki, A. Daret, H. Fujigasaki, K. Takada, C. Duyckaerts, A. Brice, A. Dejean and A. Sittler (2010). "SUMOylation attenuates the aggregation propensity and cellular toxicity of the polyglutamine expanded ataxin-7." Hum Mol Genet 19(1): 181-195.

Jeanne, M., V. Lallemand-Breitenbach, O. Ferhi, M. Koken, M. Le Bras, S. Duffort, L. Peres, C. Berthier, H. Soilihi, B. Raught and H. de The (2010). "PML/RARA oxidation and arsenic binding initiate the antileukemia response of As2O3." Cancer Cell 18(1): 88-98.

Johnson, J. O., J. Mandrioli, M. Benatar, Y. Abramzon, V. M. Van Deerlin, J. Q. Trojanowski, J. R. Gibbs, M. Brunetti, S. Gronka, J. Wuu, J. Ding, L. McCluskey, M. Martinez-Lage, D. Falcone, D. G. Hernandez, S. Arepalli, S. Chong, J. C. Schymick, J. Rothstein, F. Landi, Y. D. Wang, A. Calvo, G. Mora, M. Sabatelli, M. R. Monsurro, S. Battistini, F. Salvi, R. Spataro, P. Sola, G. Borghero, G. Galassi, S. W. Scholz, J. P. Taylor, G. Restagno, A. Chio and B. J. Traynor (2010). "Exome sequencing reveals VCP mutations as a cause of familial ALS." Neuron 68(5): 857-864.

Johnson, J. O., E. P. Pioro, A. Boehringer, R. Chia, H. Feit, A. E. Renton, H. A. Pliner, Y. Abramzon, G. Marangi, B. J. Winborn, J. R. Gibbs, M. A. Nalls, S. Morgan, M. Shoai, J. Hardy, A. Pittman, R. W. Orrell, A. Malaspina, K. C. Sidle, P. Fratta, M. B. Harms, R. H. Baloh, A. Pestronk, C. C. Weihl, E. Rogaeva, L. Zinman, V. E. Drory, G. Borghero, G. Mora, A. Calvo, J. D. Rothstein, C. Drepper, M. Sendtner, A. B. Singleton, J. P. Taylor, M. R. Cookson, G. Restagno, M. Sabatelli, R. Bowser, A. Chio and B. J. Traynor (2014). "Mutations in the Matrin 3 gene cause familial amyotrophic lateral sclerosis." Nat Neurosci 17(5): 664-666.

Johnston, C. A., B. R. Stanton, M. R. Turner, R. Gray, A. H. Blunt, D. Butt, M. A. Ampong, C. E. Shaw, P. N. Leigh and A. Al-Chalabi (2006). "Amyotrophic lateral

sclerosis in an urban setting: a population based study of inner city London." J Neurol 253(12): 1642-1643.

Jucker, M. and L. C. Walker (2013). "Self-propagation of pathogenic protein aggregates in neurodegenerative diseases." Nature 501(7465): 45-51.

Kabashi, E., J. N. Agar, Y. Hong, D. M. Taylor, S. Minotti, D. A. Figlewicz and H. D. Durham (2008). "Proteasomes remain intact, but show early focal alteration in their composition in a mouse model of amyotrophic lateral sclerosis." J Neurochem 105(6): 2353-2366.

Kabashi, E., J. N. Agar, M. J. Strong and H. D. Durham (2012). "Impaired proteasome function in sporadic amyotrophic lateral sclerosis." Amyotroph Lateral Scler 13(4): 367-371.

Kabashi, E., V. Bercier, A. Lissouba, M. Liao, E. Brustein, G. A. Rouleau and P. Drapeau (2011). "FUS and TARDBP but not SOD1 interact in genetic models of amyotrophic lateral sclerosis." PLoS Genet 7(8): e1002214.

Kabashi, E. and H. D. Durham (2006). "Failure of protein quality control in amyotrophic lateral sclerosis." Biochim Biophys Acta 1762(11-12): 1038-1050.

Kabashi, E., P. N. Valdmanis, P. Dion, D. Spiegelman, B. J. McConkey, C. Vande Velde, J. P. Bouchard, L. Lacomblez, K. Pochigaeva, F. Salachas, P. F. Pradat, W. Camu, V. Meininger, N. Dupre and G. A. Rouleau (2008). "TARDBP mutations in individuals with sporadic and familial amyotrophic lateral sclerosis." Nat Genet 40(5): 572-574.

Kakita, A., K. Oyanagi, H. Nagai and H. Takahashi (1997). "Eosinophilic intranuclear inclusions in the hippocampal pyramidal neurons of a patient with amyotrophic lateral sclerosis." Acta Neuropathol 93(5): 532-536.

Kedersha, N. and P. Anderson (2007). "Mammalian stress granules and processing bodies." Methods Enzymol 431: 61-81.

Kedersha, N., P. Ivanov and P. Anderson (2013). "Stress granules and cell signaling: more than just a passing phase?" Trends Biochem Sci 38(10): 494-506.

Khabazian, I., J. S. Bains, D. E. Williams, J. Cheung, J. M. Wilson, B. A. Pasqualotto, S. L. Pelech, R. J. Andersen, Y. T. Wang, L. Liu, A. Nagai, S. U. Kim, U. K. Craig and C. A. Shaw (2002). "Isolation of various forms of sterol beta-D-glucoside from the seed of Cycas circinalis: neurotoxicity and implications for ALS-parkinsonism dementia complex." J Neurochem 82(3): 516-528.

Kiernan, M. C., S. Vucic, B. C. Cheah, M. R. Turner, A. Eisen, O. Hardiman, J. R. Burrell and M. C. Zoing (2011). "Amyotrophic lateral sclerosis." Lancet 377(9769): 942-955.

Kim, S. J., T. S. Kim, S. Hong, H. Rhim, I. Y. Kim and S. Kang (2003). "Oxidative stimuli affect polyglutamine aggregation and cell death in human mutant ataxin-1-expressing cells." Neurosci Lett 348(1): 21-24.

Kino, Y., C. Washizu, E. Aquilanti, M. Okuno, M. Kurosawa, M. Yamada, H. Doi and N. Nukina (2011). "Intracellular localization and splicing regulation of FUS/TLS are variably affected by amyotrophic lateral sclerosis-linked mutations." Nucleic Acids Res 39(7): 2781-2798.

Kino, Y., C. Washizu, M. Kurosawa, M. Yamada, H. Miyazaki, T. Akagi, T. Hashikawa, H. Doi, T. Takumi, G. G. Hicks, N. Hattori, T. Shimogori and N. Nukina (2015). "FUS/TLS deficiency causes behavioral and pathological abnormalities distinct from amyotrophic lateral sclerosis." Acta Neuropathol Commun 3(1): 24.

Korb, E. and S. Finkbeiner (2013). "PML in the Brain: From Development to Degeneration." Front Oncol 3: 242.

Kristiansen, M., P. Deriziotis, D. E. Dimcheff, G. S. Jackson, H. Ovaa, H. Naumann, A. R. Clarke, F. W. van Leeuwen, V. Menendez-Benito, N. P. Dantuma, J. L. Portis, J. Collinge and S. J. Tabrizi (2007). "Disease-associated prion protein oligomers inhibit the 26S proteasome." Mol Cell 26(2): 175-188.

Krumova, P., E. Meulmeester, M. Garrido, M. Tirard, H. H. Hsiao, G. Bossis, H. Urlaub, M. Zweckstetter, S. Kugler, F. Melchior, M. Bahr and J. H. Weishaupt (2011). "Sumoylation inhibits alpha-synuclein aggregation and toxicity." J Cell Biol 194(1): 49-60.

Kurki, S., L. Latonen and M. Laiho (2003). "Cellular stress and DNA damage invoke temporally distinct Mdm2, p53 and PML complexes and damage-specific nuclear relocalization." J Cell Sci 116(Pt 19): 3917-3925.

Kuroda, M., J. Sok, L. Webb, H. Baechtold, F. Urano, Y. Yin, P. Chung, D. G. de Rooij, A. Akhmedov, T. Ashley and D. Ron (2000). "Male sterility and enhanced radiation sensitivity in TLS(-/-) mice." Embo j 19(3): 453-462.

Kuzuhara, S. and Y. Kokubo (2005). "Atypical parkinsonism of Japan: amyotrophic lateral sclerosis-parkinsonism-dementia complex of the Kii peninsula of Japan (Muro disease): an update." Mov Disord 20 Suppl 12: S108-113.

Kwiatkowski, T. J., Jr., D. A. Bosco, A. L. Leclerc, E. Tamrazian, C. R. Vanderburg, C. Russ, A. Davis, J. Gilchrist, E. J. Kasarskis, T. Munsat, P. Valdmanis, G. A. Rouleau, B.

A. Hosler, P. Cortelli, P. J. de Jong, Y. Yoshinaga, J. L. Haines, M. A. Pericak-Vance, J. Yan, N. Ticozzi, T. Siddique, D. McKenna-Yasek, P. C. Sapp, H. R. Horvitz, J. E. Landers and R. H. Brown, Jr. (2009). "Mutations in the FUS/TLS gene on chromosome 16 cause familial amyotrophic lateral sclerosis." Science 323(5918): 1205-1208.

Kwon, I., S. Xiang, M. Kato, L. Wu, P. Theodoropoulos, T. Wang, J. Kim, J. Yun, Y. Xie and S. L. McKnight (2014). "Poly-dipeptides encoded by the C9orf72 repeats bind nucleoli, impede RNA biogenesis, and kill cells." Science 345(6201): 1139-1145.

Lafarga, M., I. Casafont, R. Bengoechea, O. Tapia and M. T. Berciano (2009). "Cajal's contribution to the knowledge of the neuronal cell nucleus." Chromosoma 118(4): 437-443.

Lagier-Tourenne, C. and D. W. Cleveland (2009). "Rethinking ALS: the FUS about TDP-43." Cell 136(6): 1001-1004.

Lagier-Tourenne, C., M. Polymenidou and D. W. Cleveland (2010). "TDP-43 and FUS/TLS: emerging roles in RNA processing and neurodegeneration." Hum Mol Genet 19(R1): R46-64.

Lagier-Tourenne, C., M. Polymenidou, K. R. Hutt, A. Q. Vu, M. Baughn, S. C. Huelga, K. M. Clutario, S. C. Ling, T. Y. Liang, C. Mazur, E. Wancewicz, A. S. Kim, A. Watt, S. Freier, G. G. Hicks, J. P. Donohue, L. Shiue, C. F. Bennett, J. Ravits, D. W. Cleveland and G. W. Yeo (2012). "Divergent roles of ALS-linked proteins FUS/TLS and TDP-43 intersect in processing long pre-mRNAs." Nat Neurosci 15(11): 1488-1497.

Lai, S. L., Y. Abramzon, J. C. Schymick, D. A. Stephan, T. Dunckley, A. Dillman, M. Cookson, A. Calvo, S. Battistini, F. Giannini, C. Caponnetto, G. L. Mancardi, R. Spataro, M. R. Monsurro, G. Tedeschi, K. Marinou, M. Sabatelli, A. Conte, J. Mandrioli, P. Sola, F. Salvi, I. Bartolomei, F. Lombardo, G. Mora, G. Restagno, A. Chio and B. J. Traynor (2011). "FUS mutations in sporadic amyotrophic lateral sclerosis." Neurobiol Aging 32(3): 550 e551-554.

Lallemand-Breitenbach, V. and H. de The (2010). "PML nuclear bodies." Cold Spring Harb Perspect Biol 2(5): a000661.

Lallemand-Breitenbach, V., M. Jeanne, S. Benhenda, R. Nasr, M. Lei, L. Peres, J. Zhou, J. Zhu, B. Raught and H. de The (2008). "Arsenic degrades PML or PML-RARalpha through a SUMO-triggered RNF4/ubiquitin-mediated pathway." Nat Cell Biol 10(5): 547-555.

Lallemand-Breitenbach, V., J. Zhu, Z. Chen and H. de The (2012). "Curing APL through PML/RARA degradation by As2O3." Trends Mol Med 18(1): 36-42.

Lallemand-Breitenbach, V., J. Zhu, F. Puvion, M. Koken, N. Honore, A. Doubeikovsky, E. Duprez, P. P. Pandolfi, E. Puvion, P. Freemont and H. de The (2001). "Role of promyelocytic leukemia (PML) sumolation in nuclear body formation, 11S proteasome recruitment, and As2O3-induced PML or PML/retinoic acid receptor alpha degradation." J Exp Med 193(12): 1361-1371.

Lang, E., A. Grudic, S. Pankiv, O. Bruserud, A. Simonsen, R. Bjerkvig, M. Bjoras and S. O. Boe (2012). "The arsenic-based cure of acute promyelocytic leukemia promotes cytoplasmic sequestration of PML and PML/RARA through inhibition of PML body recycling." Blood 120(4): 847-857.

Lange, A., R. E. Mills, S. E. Devine and A. H. Corbett (2008). "A PY-NLS nuclear targeting signal is required for nuclear localization and function of the Saccharomyces cerevisiae mRNA-binding protein Hrp1." J Biol Chem 283(19): 12926-12934.

Law, W. J., K. L. Cann and G. G. Hicks (2006). "TLS, EWS and TAF15: a model for transcriptional integration of gene expression." Brief Funct Genomic Proteomic 5(1): 8-14.

Lee, B. J., A. E. Cansizoglu, K. E. Suel, T. H. Louis, Z. Zhang and Y. M. Chook (2006). "Rules for nuclear localization sequence recognition by karyopherin beta 2." Cell 126(3): 543-558.

Lee, D. H. and A. L. Goldberg (1998). "Proteasome inhibitors: valuable new tools for cell biologists." Trends Cell Biol 8(10): 397-403.

Lee, E. B., V. M. Lee and J. Q. Trojanowski (2012). "Gains or losses: molecular mechanisms of TDP43-mediated neurodegeneration." Nat Rev Neurosci 13(1): 38-50.

Lemmens, R., M. J. Moore, A. Al-Chalabi, R. H. Brown, Jr. and W. Robberecht (2010). "RNA metabolism and the pathogenesis of motor neuron diseases." Trends Neurosci 33(5): 249-258.

Lerga, A., M. Hallier, L. Delva, C. Orvain, I. Gallais, J. Marie and F. Moreau-Gachelin (2001). "Identification of an RNA binding specificity for the potential splicing factor TLS." J Biol Chem 276(9): 6807-6816.

Li, H., C. Leo, J. Zhu, X. Wu, J. O'Neil, E. J. Park and J. D. Chen (2000). "Sequestration and inhibition of Daxx-mediated transcriptional repression by PML." Mol Cell Biol 20(5): 1784-1796.

Lii, C. K., A. H. Lin, S. L. Lee, H. W. Chen and T. S. Wang (2011). "Oxidative modifications of proteins by sodium arsenite in human umbilical vein endothelial cells." Environ Toxicol 26(5): 459-471.

Lillo, P. and J. R. Hodges (2009). "Frontotemporal dementia and motor neurone disease: overlapping clinic-pathological disorders." J Clin Neurosci 16(9): 1131-1135.

Ling, S. C., M. Polymenidou and D. W. Cleveland (2013). "Converging mechanisms in ALS and FTD: disrupted RNA and protein homeostasis." Neuron 79(3): 416-438.

Lippai, M. and P. Low (2014). "The role of the selective adaptor p62 and ubiquitin-like proteins in autophagy." Biomed Res Int 2014: 832704.

Liu, Q. and G. Dreyfuss (1996). "A novel nuclear structure containing the survival of motor neurons protein." EMBO J 15(14): 3555-3565.

Liu, Y. H., W. Wei, J. Yin, G. P. Liu, Q. Wang, F. Y. Cao and J. Z. Wang (2009). "Proteasome inhibition increases tau accumulation independent of phosphorylation." Neurobiol Aging 30(12): 1949-1961.

Liu-Yesucevitz, L., A. Bilgutay, Y. J. Zhang, T. Vanderweyde, A. Citro, T. Mehta, N. Zaarur, A. McKee, R. Bowser, M. Sherman, L. Petrucelli and B. Wolozin (2010). "Tar DNA binding protein-43 (TDP-43) associates with stress granules: analysis of cultured cells and pathological brain tissue." PLoS One 5(10): e13250.

Liu-Yesucevitz, L., A. Y. Lin, A. Ebata, J. Y. Boon, W. Reid, Y. F. Xu, K. Kobrin, G. J. Murphy, L. Petrucelli and B. Wolozin (2014). "ALS-linked mutations enlarge TDP-43-enriched neuronal RNA granules in the dendritic arbor." J Neurosci 34(12): 4167-4174.

Logroscino, G., B. J. Traynor, O. Hardiman, A. Chio, D. Mitchell, R. J. Swingler, A. Millul, E. Benn and E. Beghi (2010). "Incidence of amyotrophic lateral sclerosis in Europe." J Neurol Neurosurg Psychiatry 81(4): 385-390.

Loschi, M., C. C. Leishman, N. Berardone and G. L. Boccaccio (2009). "Dynein and kinesin regulate stress-granule and P-body dynamics." J Cell Sci 122(Pt 21): 3973-3982.

Mackenzie, I. R., O. Ansorge, M. Strong, J. Bilbao, L. Zinman, L. C. Ang, M. Baker, H. Stewart, A. Eisen, R. Rademakers and M. Neumann (2011). "Pathological heterogeneity in amyotrophic lateral sclerosis with FUS mutations: two distinct patterns correlating with disease severity and mutation." Acta Neuropathol 122(1): 87-98.

Mackenzie, I. R., M. Baker, G. West, J. Woulfe, N. Qadi, J. Gass, A. Cannon, J. Adamson, H. Feldman, C. Lindholm, S. Melquist, R. Pettman, A. D. Sadovnick, E. Dwosh, S. W. Whiteheart, M. Hutton and S. M. Pickering-Brown (2006). "A family with tau-negative frontotemporal dementia and neuronal intranuclear inclusions linked to chromosome 17." Brain 129(Pt 4): 853-867.

Mackenzie, I. R. and M. Neumann (2012). "FET proteins in frontotemporal dementia and amyotrophic lateral sclerosis." Brain Res 1462: 40-43.

Majounie, E., A. E. Renton, K. Mok, E. G. Dopper, A. Waite, S. Rollinson, A. Chio, G. Restagno, N. Nicolaou, J. Simon-Sanchez, J. C. van Swieten, Y. Abramzon, J. O. Johnson, M. Sendtner, R. Pamphlett, R. W. Orrell, S. Mead, K. C. Sidle, H. Houlden, J. D. Rohrer, K. E. Morrison, H. Pall, K. Talbot, O. Ansorge, D. G. Hernandez, S. Arepalli, M. Sabatelli, G. Mora, M. Corbo, F. Giannini, A. Calvo, E. Englund, G. Borghero, G. L. Floris, A. M. Remes, H. Laaksovirta, L. McCluskey, J. Q. Trojanowski, V. M. Van Deerlin, G. D. Schellenberg, M. A. Nalls, V. E. Drory, C. S. Lu, T. H. Yeh, H. Ishiura, Y. Takahashi, S. Tsuji, I. Le Ber, A. Brice, C. Drepper, N. Williams, J. Kirby, P. Shaw, J. Hardy, P. J. Tienari, P. Heutink, H. R. Morris, S. Pickering-Brown and B. J. Traynor (2012). "Frequency of the C9orf72 hexanucleotide repeat expansion in patients with amyotrophic lateral sclerosis and frontotemporal dementia: a cross-sectional study." Lancet Neurol 11(4): 323-330.

Malloy, M. T., D. J. McIntosh, T. S. Walters, A. Flores, J. S. Goodwin and I. J. Arinze (2013). "Trafficking of the transcription factor Nrf2 to promyelocytic leukemia-nuclear bodies: implications for degradation of NRF2 in the nucleus." J Biol Chem 288(20): 14569-14583.

Mao, Y. S., B. Zhang and D. L. Spector (2011). "Biogenesis and function of nuclear bodies." Trends Genet 27(8): 295-306.

Maroui, M. A., S. Kheddache-Atmane, F. El Asmi, L. Dianoux, M. Aubry and M. K. Chelbi-Alix (2012). "Requirement of PML SUMO interacting motif for RNF4- or arsenic trioxide-induced degradation of nuclear PML isoforms." PLoS One 7(9): e44949.

Maruyama, H., H. Morino, H. Ito, Y. Izumi, H. Kato, Y. Watanabe, Y. Kinoshita, M. Kamada, H. Nodera, H. Suzuki, O. Komure, S. Matsuura, K. Kobatake, N. Morimoto, K. Abe, N. Suzuki, M. Aoki, A. Kawata, T. Hirai, T. Kato, K. Ogasawara, A. Hirano, T. Takumi, H. Kusaka, K. Hagiwara, R. Kaji and H. Kawakami (2010). "Mutations of optineurin in amyotrophic lateral sclerosis." Nature 465(7295): 223-226.

Mastrocola, A. S., S. H. Kim, A. T. Trinh, L. A. Rodenkirch and R. S. Tibbetts (2013). "The RNA-binding protein fused in sarcoma (FUS) functions downstream of poly(ADP-ribose) polymerase (PARP) in response to DNA damage." J Biol Chem 288(34): 24731-24741.

Mattsson, K., K. Pokrovskaja, C. Kiss, G. Klein and L. Szekely (2001). "Proteins associated with the promyelocytic leukemia gene product (PML)-containing nuclear body move to the nucleolus upon inhibition of proteasome-dependent protein degradation." Proc Natl Acad Sci U S A 98(3): 1012-1017.

Mazroui, R., S. Di Marco, R. J. Kaufman and I. E. Gallouzi (2007). "Inhibition of the ubiquitin-proteasome system induces stress granule formation." Mol Biol Cell 18(7): 2603-2618.

McDonald, K. K., A. Aulas, L. Destroismaisons, S. Pickles, E. Beleac, W. Camu, G. A. Rouleau and C. Vande Velde (2011). "TAR DNA-binding protein 43 (TDP-43) regulates stress granule dynamics via differential regulation of G3BP and TIA-1." Hum Mol Genet 20(7): 1400-1410.

McGoldrick, P., P. I. Joyce, E. M. Fisher and L. Greensmith (2013). "Rodent models of amyotrophic lateral sclerosis." Biochim Biophys Acta 1832(9): 1421-1436.

McGuire, V., W. T. Longstreth, Jr., T. D. Koepsell and G. van Belle (1996). "Incidence of amyotrophic lateral sclerosis in three counties in western Washington state." Neurology 47(2): 571-573.

McKinnon, C. and S. J. Tabrizi (2014). "The ubiquitin-proteasome system in neurodegeneration." Antioxid Redox Signal 21(17): 2302-2321.

Mehta, P., V. Antao, W. Kaye, M. Sanchez, D. Williamson, L. Bryan, O. Muravov and K. Horton (2014). "Prevalence of amyotrophic lateral sclerosis - United States, 2010-2011." MMWR Surveill Summ 63 Suppl 7: 1-14.

Meissner, M., S. Lopato, J. Gotzmann, G. Sauermann and A. Barta (2003). "Proto-oncoprotein TLS/FUS is associated to the nuclear matrix and complexed with splicing factors PTB, SRm160, and SR proteins." Exp Cell Res 283(2): 184-195.

Meng, X., M. B. Noyes, L. J. Zhu, N. D. Lawson and S. A. Wolfe (2008). "Targeted gene inactivation in zebrafish using engineered zinc-finger nucleases." Nat Biotechnol 26(6): 695-701.

Miller, R. G., J. D. Mitchell and D. H. Moore (2012). "Riluzole for amyotrophic lateral sclerosis (ALS)/motor neuron disease (MND)." Cochrane Database Syst Rev 3: CD001447.

Miller, R. G., T. L. Munsat, M. Swash and B. R. Brooks (1999). "Consensus guidelines for the design and implementation of clinical trials in ALS. World Federation of Neurology committee on Research." J Neurol Sci 169(1-2): 2-12.

Mirzaei, H. and F. Regnier (2008). "Protein:protein aggregation induced by protein oxidation." J Chromatogr B Analyt Technol Biomed Life Sci 873(1): 8-14.

Mitchell, J. C., P. McGoldrick, C. Vance, T. Hortobagyi, J. Sreedharan, B. Rogelj, E. L. Tudor, B. N. Smith, C. Klasen, C. C. Miller, J. D. Cooper, L. Greensmith and C. E. Shaw

(2013). "Overexpression of human wild-type FUS causes progressive motor neuron degeneration in an age- and dose-dependent fashion." Acta Neuropathol 125(2): 273-288.

Moore, F. E., D. Reyon, J. D. Sander, S. A. Martinez, J. S. Blackburn, C. Khayter, C. L. Ramirez, J. K. Joung and D. M. Langenau (2012). "Improved somatic mutagenesis in zebrafish using transcription activator-like effector nucleases (TALENs)." PLoS One 7(5): e37877.

Moore, M. J. (2005). "From birth to death: the complex lives of eukaryotic mRNAs." Science 309(5740): 1514-1518.

Morlando, M., S. Dini Modigliani, G. Torrelli, A. Rosa, V. Di Carlo, E. Caffarelli and I. Bozzoni (2012). "FUS stimulates microRNA biogenesis by facilitating co-transcriptional Drosha recruitment." Embo j 31(24): 4502-4510.

Morohoshi, F., K. Arai, E. I. Takahashi, A. Tanigami and M. Ohki (1996). "Cloning and mapping of a human RBP56 gene encoding a putative RNA binding protein similar to FUS/TLS and EWS proteins." Genomics 38(1): 51-57.

Morohoshi, F., Y. Ootsuka, K. Arai, H. Ichikawa, S. Mitani, N. Munakata and M. Ohki (1998). "Genomic structure of the human RBP56/hTAFII68 and FUS/TLS genes." Gene 221(2): 191-198.

Mukai, H., T. Isagawa, E. Goyama, S. Tanaka, N. F. Bence, A. Tamura, Y. Ono and R. R. Kopito (2005). "Formation of morphologically similar globular aggregates from diverse aggregation-prone proteins in mammalian cells." Proc Natl Acad Sci U S A 102(31): 10887-10892.

Munoz, D. G., M. Neumann, H. Kusaka, O. Yokota, K. Ishihara, S. Terada, S. Kuroda and I. R. Mackenzie (2009). "FUS pathology in basophilic inclusion body disease." Acta Neuropathol 118(5): 617-627.

Murakami, T., S. P. Yang, L. Xie, T. Kawano, D. Fu, A. Mukai, C. Bohm, F. Chen, J. Robertson, H. Suzuki, G. G. Tartaglia, M. Vendruscolo, G. S. Kaminski Schierle, F. T. Chan, A. Moloney, D. Crowther, C. F. Kaminski, M. Zhen and P. St George-Hyslop (2012). "ALS mutations in FUS cause neuronal dysfunction and death in Caenorhabditis elegans by a dominant gain-of-function mechanism." Hum Mol Genet 21(1): 1-9.

Nacerddine, K., F. Lehembre, M. Bhaumik, J. Artus, M. Cohen-Tannoudji, C. Babinet, P. P. Pandolfi and A. Dejean (2005). "The SUMO pathway is essential for nuclear integrity and chromosome segregation in mice." Dev Cell 9(6): 769-779.

Nakaya, T., P. Alexiou, M. Maragkakis, A. Chang and Z. Mourelatos (2013). "FUS regulates genes coding for RNA-binding proteins in neurons by binding to their highly conserved introns." RNA 19(4): 498-509.

Neumann, M., R. Rademakers, S. Roeber, M. Baker, H. A. Kretzschmar and I. R. Mackenzie (2009). "A new subtype of frontotemporal lobar degeneration with FUS pathology." Brain 132(Pt 11): 2922-2931.

Neumann, M., S. Roeber, H. A. Kretzschmar, R. Rademakers, M. Baker and I. R. Mackenzie (2009). "Abundant FUS-immunoreactive pathology in neuronal intermediate filament inclusion disease." Acta Neuropathol 118(5): 605-616.

Neumann, M., D. M. Sampathu, L. K. Kwong, A. C. Truax, M. C. Micsenyi, T. T. Chou, J. Bruce, T. Schuck, M. Grossman, C. M. Clark, L. F. McCluskey, B. L. Miller, E. Masliah, I. R. Mackenzie, H. Feldman, W. Feiden, H. A. Kretzschmar, J. Q. Trojanowski and V. M. Lee (2006). "Ubiquitinated TDP-43 in frontotemporal lobar degeneration and amyotrophic lateral sclerosis." Science 314(5796): 130-133.

Niikura, T., Y. Kita and Y. Abe (2014). "SUMO3 modification accelerates the aggregation of ALS-linked SOD1 mutants." PLoS One 9(6): e101080.

Nishimoto, Y., D. Ito, T. Yagi, Y. Nihei, Y. Tsunoda and N. Suzuki (2010). "Characterization of alternative isoforms and inclusion body of the TAR DNA-binding protein-43." J Biol Chem 285(1): 608-619.

Nishimoto, Y., S. Nakagawa, T. Hirose, H. J. Okano, M. Takao, S. Shibata, S. Suyama, K. Kuwako, T. Imai, S. Murayama, N. Suzuki and H. Okano (2013). "The long non-coding RNA nuclear-enriched abundant transcript 1_2 induces paraspeckle formation in the motor neuron during the early phase of amyotrophic lateral sclerosis." Mol Brain 6: 31.

Nizami, Z., S. Deryusheva and J. G. Gall (2010). "The Cajal body and histone locus body." Cold Spring Harb Perspect Biol 2(7): a000653.

Nomura, T., S. Watanabe, K. Kaneko, K. Yamanaka, N. Nukina and Y. Furukawa (2014). "Intranuclear aggregation of mutant FUS/TLS as a molecular pathomechanism of amyotrophic lateral sclerosis." J Biol Chem 289(2): 1192-1202.

Oh, S. M., Z. Liu, M. Okada, S. W. Jang, X. Liu, C. B. Chan, H. Luo and K. Ye (2010). "Ebp1 sumoylation, regulated by TLS/FUS E3 ligase, is required for its anti-proliferative activity." Oncogene 29(7): 1017-1030.

Okumura, H. (2003). "Epidemiological and clinical patterns of western pacific amyotrophic lateral sclerosis (ALS) in Guam and sporadic ALS in Rochester, Minnesota,

U.S.A. and Hokkaido, Japan: a comparative study." Hokkaido Igaku Zasshi 78(3): 187-195.

Olanow, C. W., D. P. Perl, G. N. DeMartino and K. S. McNaught (2004). "Lewy-body formation is an aggresome-related process: a hypothesis." Lancet Neurol 3(8): 496-503.

Ollion, J., J. Cochennec, F. Loll, C. Escude and T. Boudier (2013). "TANGO: a generic tool for high-throughput 3D image analysis for studying nuclear organization." Bioinformatics 29(14): 1840-1841.

Orozco, D., S. Tahirovic, K. Rentzsch, B. M. Schwenk, C. Haass and D. Edbauer (2012). "Loss of fused in sarcoma (FUS) promotes pathological Tau splicing." EMBO Rep 13(8): 759-764.

Pankiv, S., T. Lamark, J. A. Bruun, A. Overvatn, G. Bjorkoy and T. Johansen (2010). "Nucleocytoplasmic shuttling of p62/SQSTM1 and its role in recruitment of nuclear polyubiquitinated proteins to promyelocytic leukemia bodies." J Biol Chem 285(8): 5941-5953.

Patten, S. A., G. A. Armstrong, A. Lissouba, E. Kabashi, J. A. Parker and P. Drapeau (2014). "Fishing for causes and cures of motor neuron disorders." Dis Model Mech 7(7): 799-809.

Pederson, T. (2011). "The nucleolus." Cold Spring Harb Perspect Biol 3(3).

Pellizzoni, L., N. Kataoka, B. Charroux and G. Dreyfuss (1998). "A novel function for SMN, the spinal muscular atrophy disease gene product, in pre-mRNA splicing." Cell 95(5): 615-624.

Pikkarainen, M., P. Hartikainen and I. Alafuzoff (2008). "Neuropathologic features of frontotemporal lobar degeneration with ubiquitin-positive inclusions visualized with ubiquitin-binding protein p62 immunohistochemistry." J Neuropathol Exp Neurol 67(4): 280-298.

Pountney, D. L., Y. Huang, R. J. Burns, E. Haan, P. D. Thompson, P. C. Blumbergs and W. P. Gai (2003). "SUMO-1 marks the nuclear inclusions in familial neuronal intranuclear inclusion disease." Exp Neurol 184(1): 436-446.

Qiu, H., S. Lee, Y. Shang, W. Y. Wang, K. F. Au, S. Kamiya, S. J. Barmada, S. Finkbeiner, H. Lui, C. E. Carlton, A. A. Tang, M. C. Oldham, H. Wang, J. Shorter, A. J. Filiano, E. D. Roberson, W. G. Tourtellotte, B. Chen, L. H. Tsai and E. J. Huang (2014). "ALS-associated mutation FUS-R521C causes DNA damage and RNA splicing defects." J Clin Invest 124(3): 981-999.

Rabbitts, T. H., A. Forster, R. Larson and P. Nathan (1993). "Fusion of the dominant negative transcription regulator CHOP with a novel gene FUS by translocation t(12;16) in malignant liposarcoma." Nat Genet 4(2): 175-180.

Raoul, C., E. Buhler, C. Sadeghi, A. Jacquier, P. Aebischer, B. Pettmann, C. E. Henderson and G. Haase (2006). "Chronic activation in presymptomatic amyotrophic lateral sclerosis (ALS) mice of a feedback loop involving Fas, Daxx, and FasL." Proc Natl Acad Sci U S A 103(15): 6007-6012.

Regad, T., C. Bellodi, P. Nicotera and P. Salomoni (2009). "The tumor suppressor Pml regulates cell fate in the developing neocortex." Nat Neurosci 12(2): 132-140.

Renton, A. E., A. Chio and B. J. Traynor (2014). "State of play in amyotrophic lateral sclerosis genetics." Nat Neurosci 17(1): 17-23.

Renton, A. E., E. Majounie, A. Waite, J. Simon-Sanchez, S. Rollinson, J. R. Gibbs, J. C. Schymick, H. Laaksovirta, J. C. van Swieten, L. Myllykangas, H. Kalimo, A. Paetau, Y. Abramzon, A. M. Remes, A. Kaganovich, S. W. Scholz, J. Duckworth, J. Ding, D. W. Harmer, D. G. Hernandez, J. O. Johnson, K. Mok, M. Ryten, D. Trabzuni, R. J. Guerreiro, R. W. Orrell, J. Neal, A. Murray, J. Pearson, I. E. Jansen, D. Sondervan, H. Seelaar, D. Blake, K. Young, N. Halliwell, J. B. Callister, G. Toulson, A. Richardson, A. Gerhard, J. Snowden, D. Mann, D. Neary, M. A. Nalls, T. Peuralinna, L. Jansson, V. M. Isoviita, A. L. Kaivorinne, M. Holtta-Vuori, E. Ikonen, R. Sulkava, M. Benatar, J. Wuu, A. Chio, G. Restagno, G. Borghero, M. Sabatelli, D. Heckerman, E. Rogaeva, L. Zinman, J. D. Rothstein, M. Sendtner, C. Drepper, E. E. Eichler, C. Alkan, Z. Abdullaev, S. D. Pack, A. Dutra, E. Pak, J. Hardy, A. Singleton, N. M. Williams, P. Heutink, S. Pickering-Brown, H. R. Morris, P. J. Tienari and B. J. Traynor (2011). "A hexanucleotide repeat expansion in C9ORF72 is the cause of chromosome 9p21-linked ALS-FTD." Neuron 72(2): 257-268.

Ringholz, G. M., S. H. Appel, M. Bradshaw, N. A. Cooke, D. M. Mosnik and P. E. Schulz (2005). "Prevalence and patterns of cognitive impairment in sporadic ALS." Neurology 65(4): 586-590.

Robberecht, W. and T. Philips (2013). "The changing scene of amyotrophic lateral sclerosis." Nat Rev Neurosci 14(4): 248-264.

Rockel, T. D., D. Stuhlmann and A. von Mikecz (2005). "Proteasomes degrade proteins in focal subdomains of the human cell nucleus." J Cell Sci 118(Pt 22): 5231-5242.

Rogelj, B., L. E. Easton, G. K. Bogu, L. W. Stanton, G. Rot, T. Curk, B. Zupan, Y. Sugimoto, M. Modic, N. Haberman, J. Tollervey, R. Fujii, T. Takumi, C. E. Shaw and J.

Ule (2012). "Widespread binding of FUS along nascent RNA regulates alternative splicing in the brain." Sci Rep 2: 603.

Rosen, D. R., T. Siddique, D. Patterson, D. A. Figlewicz, P. Sapp, A. Hentati, D. Donaldson, J. Goto, J. P. O'Regan, H. X. Deng and et al. (1993). "Mutations in Cu/Zn superoxide dismutase gene are associated with familial amyotrophic lateral sclerosis." Nature 362(6415): 59-62.

Ross, C. A. and M. A. Poirier (2004). "Protein aggregation and neurodegenerative disease." Nat Med 10 Suppl: S10-17.

Rowland, L. P. and N. A. Shneider (2001). "Amyotrophic lateral sclerosis." N Engl J Med 344(22): 1688-1700.

Ruddy, D. M., M. J. Parton, A. Al-Chalabi, C. M. Lewis, C. Vance, B. N. Smith, P. N. Leigh, J. F. Powell, T. Siddique, E. P. Meyjes, F. Baas, V. de Jong and C. E. Shaw (2003). "Two families with familial amyotrophic lateral sclerosis are linked to a novel locus on chromosome 16q." Am J Hum Genet 73(2): 390-396.

Rulten, S. L., A. Rotheray, R. L. Green, G. J. Grundy, D. A. Moore, F. Gomez-Herreros, M. Hafezparast and K. W. Caldecott (2014). "PARP-1 dependent recruitment of the amyotrophic lateral sclerosis-associated protein FUS/TLS to sites of oxidative DNA damage." Nucleic Acids Res 42(1): 307-314.

Ryu, H. H., M. H. Jun, K. J. Min, D. J. Jang, Y. S. Lee, H. K. Kim and J. A. Lee (2014). "Autophagy regulates amyotrophic lateral sclerosis-linked fused in sarcoma-positive stress granules in neurons." Neurobiol Aging 35(12): 2822-2831.

Ryu, J., S. Cho, B. C. Park and H. Lee do (2010). "Oxidative stress-enhanced SUMOylation and aggregation of ataxin-1: Implication of JNK pathway." Biochem Biophys Res Commun 393(2): 280-285.

Saeki, Y. and K. Tanaka (2012). "Assembly and function of the proteasome." Methods Mol Biol 832: 315-337.

Sahin, U., H. de The and V. Lallemand-Breitenbach (2014). "PML nuclear bodies: assembly and oxidative stress-sensitive sumoylation." Nucleus 5(6): 499-507.

Sahin, U., O. Ferhi, M. Jeanne, S. Benhenda, C. Berthier, F. Jollivet, M. Niwa-Kawakita, O. Faklaris, N. Setterblad, H. de The and V. Lallemand-Breitenbach (2014). "Oxidative stress-induced assembly of PML nuclear bodies controls sumoylation of partner proteins." J Cell Biol 204(6): 931-945.

Sama, R. R., C. L. Ward, L. J. Kaushansky, N. Lemay, S. Ishigaki, F. Urano and D. A. Bosco (2013). "FUS/TLS assembles into stress granules and is a prosurvival factor during hyperosmolar stress." J Cell Physiol 228(11): 2222-2231.

Sapp, P. C., B. A. Hosler, D. McKenna-Yasek, W. Chin, A. Gann, H. Genise, J. Gorenstein, M. Huang, W. Sailer, M. Scheffler, M. Valesky, J. L. Haines, M. Pericak-Vance, T. Siddique, H. R. Horvitz and R. H. Brown, Jr. (2003). "Identification of two novel loci for dominantly inherited familial amyotrophic lateral sclerosis." Am J Hum Genet 73(2): 397-403.

Sasayama, H., M. Shimamura, T. Tokuda, Y. Azuma, T. Yoshida, T. Mizuno, M. Nakagawa, N. Fujikake, Y. Nagai and M. Yamaguchi (2012). "Knockdown of the Drosophila fused in sarcoma (FUS) homologue causes deficient locomotive behavior and shortening of motoneuron terminal branches." PLoS One 7(6): e39483.

Schindelin, J., I. Arganda-Carreras, E. Frise, V. Kaynig, M. Longair, T. Pietzsch, S. Preibisch, C. Rueden, S. Saalfeld, B. Schmid, J. Y. Tinevez, D. J. White, V. Hartenstein, K. Eliceiri, P. Tomancak and A. Cardona (2012). "Fiji: an open-source platform for biological-image analysis." Nat Methods 9(7): 676-682.

Schwartz, J. C., C. C. Ebmeier, E. R. Podell, J. Heimiller, D. J. Taatjes and T. R. Cech (2012). "FUS binds the CTD of RNA polymerase II and regulates its phosphorylation at Ser2." Genes Dev 26(24): 2690-2695.

Schwartz, J. C., E. R. Podell, S. S. Han, J. D. Berry, K. C. Eggan and T. R. Cech (2014). "FUS is sequestered in nuclear aggregates in ALS patient fibroblasts." Mol Biol Cell 25(17): 2571-2578.

Schwartz, J. C., X. Wang, E. R. Podell and T. R. Cech (2013). "RNA seeds higher-order assembly of FUS protein." Cell Rep 5(4): 918-925.

Seifert, A., P. Schofield, G. J. Barton and R. T. Hay (2015). "Proteotoxic stress reprograms the chromatin landscape of SUMO modification." Sci Signal 8(384): rs7.

Seilhean, D., J. Takahashi, K. H. El Hachimi, H. Fujigasaki, A. S. Lebre, V. Biancalana, A. Durr, F. Salachas, J. Hogenhuis, H. de The, J. J. Hauw, V. Meininger, A. Brice and C. Duyckaerts (2004). "Amyotrophic lateral sclerosis with neuronal intranuclear protein inclusions." Acta Neuropathol 108(1): 81-87.

Sephton, C. F., A. A. Tang, A. Kulkarni, J. West, M. Brooks, J. J. Stubblefield, Y. Liu, M. Q. Zhang, C. B. Green, K. M. Huber, E. J. Huang, J. Herz and G. Yu (2014). "Activity-dependent FUS dysregulation disrupts synaptic homeostasis." Proc Natl Acad Sci U S A.

Seyfried, N. T., Y. M. Gozal, E. B. Dammer, Q. Xia, D. M. Duong, D. Cheng, J. J. Lah, A. I. Levey and J. Peng (2010). "Multiplex SILAC analysis of a cellular TDP-43 proteinopathy model reveals protein inclusions associated with SUMOylation and diverse polyubiquitin chains." Mol Cell Proteomics 9(4): 705-718.

Sharma, P., R. Murillas, H. Zhang and M. R. Kuehn (2010). "N4BP1 is a newly identified nucleolar protein that undergoes SUMO-regulated polyubiquitylation and proteasomal turnover at promyelocytic leukemia nuclear bodies." J Cell Sci 123(Pt 8): 1227-1234.

Shelkovnikova, T. A., O. M. Peters, A. V. Deykin, N. Connor-Robson, H. Robinson, A. A. Ustyugov, S. O. Bachurin, T. G. Ermolkevich, I. L. Goldman, E. R. Sadchikova, E. A. Kovrazhkina, V. I. Skvortsova, S. C. Ling, S. Da Cruz, P. A. Parone, V. L. Buchman and N. N. Ninkina (2013). "Fused in sarcoma (FUS) protein lacking nuclear localization signal (NLS) and major RNA binding motifs triggers proteinopathy and severe motor phenotype in transgenic mice." J Biol Chem 288(35): 25266-25274.

Shelkovnikova, T. A., H. K. Robinson, C. Troakes, N. Ninkina and V. L. Buchman (2014). "Compromised paraspeckle formation as a pathogenic factor in FUSopathies." Hum Mol Genet 23(9): 2298-2312.

Shih, H. M., C. C. Chang, H. Y. Kuo and D. Y. Lin (2007). "Daxx mediates SUMO-dependent transcriptional control and subnuclear compartmentalization." Biochem Soc Trans 35(Pt 6): 1397-1400.

Sierra Bello, O., J. Gonzalez, F. Capani and G. E. Barreto (2012). "In silico docking reveals possible Riluzole binding sites on Nav1.6 sodium channel: implications for amyotrophic lateral sclerosis therapy." J Theor Biol 315: 53-63.

Sorokin, A. V., E. R. Kim and L. P. Ovchinnikov (2007). "Nucleocytoplasmic transport of proteins." Biochemistry (Mosc) 72(13): 1439-1457.

Spector, D. L. and A. I. Lamond (2011). "Nuclear speckles." Cold Spring Harb Perspect Biol 3(2).

Sreedharan, J., I. P. Blair, V. B. Tripathi, X. Hu, C. Vance, B. Rogelj, S. Ackerley, J. C. Durnall, K. L. Williams, E. Buratti, F. Baralle, J. de Belleroche, J. D. Mitchell, P. N. Leigh, A. Al-Chalabi, C. C. Miller, G. Nicholson and C. E. Shaw (2008). "TDP-43 mutations in familial and sporadic amyotrophic lateral sclerosis." Science 319(5870): 1668-1672.

Stevenson, A., D. M. Yates, C. Manser, K. J. De Vos, A. Vagnoni, P. N. Leigh, D. M. McLoughlin and C. C. Miller (2009). "Riluzole protects against glutamate-induced slowing of neurofilament axonal transport." Neurosci Lett 454(2): 161-164.

Sudharsan, R. and Y. Azuma (2012). "The SUMO ligase PIAS1 regulates UV-induced apoptosis by recruiting Daxx to SUMOylated foci." J Cell Sci 125(Pt 23): 5819-5829.

Sun, S., S. C. Ling, J. Qiu, C. P. Albuquerque, Y. Zhou, S. Tokunaga, H. Li, H. Qiu, A. Bui, G. W. Yeo, E. J. Huang, K. Eggan, H. Zhou, X. D. Fu, C. Lagier-Tourenne and D. W. Cleveland (2015). "ALS-causative mutations in FUS/TLS confer gain and loss of function by altered association with SMN and U1-snRNP." Nat Commun 6: 6171.

Sun, Z., Z. Diaz, X. Fang, M. P. Hart, A. Chesi, J. Shorter and A. D. Gitler (2011). "Molecular determinants and genetic modifiers of aggregation and toxicity for the ALS disease protein FUS/TLS." PLoS Biol 9(4): e1000614.

Takahashi, Y., V. Lallemand-Breitenbach, J. Zhu and H. de The (2004). "PML nuclear bodies and apoptosis." Oncogene 23(16): 2819-2824.

Takanashi, K. and A. Yamaguchi (2014). "Aggregation of ALS-linked FUS mutant sequesters RNA binding proteins and impairs RNA granules formation." Biochem Biophys Res Commun 452(3): 600-607.

Tan, A. Y. and J. L. Manley (2009). "The TET family of proteins: functions and roles in disease." J Mol Cell Biol 1(2): 82-92.

Tan, A. Y. and J. L. Manley (2010). "TLS inhibits RNA polymerase III transcription." Mol Cell Biol 30(1): 186-196.

Tan, A. Y., T. R. Riley, T. Coady, H. J. Bussemaker and J. L. Manley (2012). "TLS/FUS (translocated in liposarcoma/fused in sarcoma) regulates target gene transcription via single-stranded DNA response elements." Proc Natl Acad Sci U S A 109(16): 6030-6035.

Tapia, O., R. Bengoechea, A. Palanca, R. Arteaga, J. F. Val-Bernal, E. F. Tizzano, M. T. Berciano and M. Lafarga (2012). "Reorganization of Cajal bodies and nucleolar targeting of coilin in motor neurons of type I spinal muscular atrophy." Histochem Cell Biol.

Tashiro, Y., M. Urushitani, H. Inoue, M. Koike, Y. Uchiyama, M. Komatsu, K. Tanaka, M. Yamazaki, M. Abe, H. Misawa, K. Sakimura, H. Ito and R. Takahashi (2012). "Motor neuron-specific disruption of proteasomes, but not autophagy, replicates amyotrophic lateral sclerosis." J Biol Chem 287(51): 42984-42994.

Tatham, M. H., M. C. Geoffroy, L. Shen, A. Plechanovova, N. Hattersley, E. G. Jaffray, J. J. Palvimo and R. T. Hay (2008). "RNF4 is a poly-SUMO-specific E3 ubiquitin ligase required for arsenic-induced PML degradation." Nat Cell Biol 10(5): 538-546.

Thomas, M. G., L. J. Martinez Tosar, M. A. Desbats, C. C. Leishman and G. L. Boccaccio (2009). "Mammalian Staufen 1 is recruited to stress granules and impairs their assembly." J Cell Sci 122(Pt 4): 563-573.

Tibshirani, M., M. L. Tradewell, K. R. Mattina, S. Minotti, W. Yang, H. Zhou, M. J. Strong, L. J. Hayward and H. D. Durham (2015). "Cytoplasmic sequestration of FUS/ TLS associated with ALS alters histone marks through loss of nuclear protein arginine methyltransferase 1." Hum Mol Genet 24(3): 773-786.

Ticozzi, N., V. Silani, A. L. LeClerc, P. Keagle, C. Gellera, A. Ratti, F. Taroni, T. J. Kwiatkowski, Jr., D. M. McKenna-Yasek, P. C. Sapp, R. H. Brown, Jr. and J. E. Landers (2009). "Analysis of FUS gene mutation in familial amyotrophic lateral sclerosis within an Italian cohort." Neurology 73(15): 1180-1185.

Torii, S., D. A. Egan, R. A. Evans and J. C. Reed (1999). "Human Daxx regulates Fas-induced apoptosis from nuclear PML oncogenic domains (PODs)." EMBO J 18(21): 6037-6049.

Urnov, F. D., E. J. Rebar, M. C. Holmes, H. S. Zhang and P. D. Gregory (2010). "Genome editing with engineered zinc finger nucleases." Nat Rev Genet 11(9): 636-646.

Uttamapinant, C., K. A. White, H. Baruah, S. Thompson, M. Fernandez-Suarez, S. Puthenveetil and A. Y. Ting (2010). "A fluorophore ligase for site-specific protein labeling inside living cells." Proc Natl Acad Sci U S A 107(24): 10914-10919.

van Blitterswijk, M. and J. E. Landers (2010). "RNA processing pathways in amyotrophic lateral sclerosis." Neurogenetics 11(3): 275-290.

Van Langenhove, T., J. van der Zee, K. Sleegers, S. Engelborghs, R. Vandenberghe, I. Gijselinck, M. Van den Broeck, M. Mattheijssens, K. Peeters, P. P. De Deyn, M. Cruts and C. Van Broeckhoven (2010). "Genetic contribution of FUS to frontotemporal lobar degeneration." Neurology 74(5): 366-371.

Van Langenhove, T., J. van der Zee and C. Van Broeckhoven (2012). "The molecular basis of the frontotemporal lobar degeneration-amyotrophic lateral sclerosis spectrum." Ann Med 44(8): 817-828.

Vance, C., B. Rogelj, T. Hortobagyi, K. J. De Vos, A. L. Nishimura, J. Sreedharan, X. Hu, B. Smith, D. Ruddy, P. Wright, J. Ganesalingam, K. L. Williams, V. Tripathi, S. Al-Saraj, A. Al-Chalabi, P. N. Leigh, I. P. Blair, G. Nicholson, J. de Belleroche, J. M. Gallo, C. C. Miller and C. E. Shaw (2009). "Mutations in FUS, an RNA processing protein, cause familial amyotrophic lateral sclerosis type 6." Science 323(5918): 1208-1211.

Vance, C., E. L. Scotter, A. L. Nishimura, C. Troakes, J. C. Mitchell, C. Kathe, H. Urwin, C. Manser, C. C. Miller, T. Hortobagyi, M. Dragunow, B. Rogelj and C. E. Shaw (2013). "ALS mutant FUS disrupts nuclear localization and sequesters wild-type FUS within cytoplasmic stress granules." Hum Mol Genet 22(13): 2676-2688.

Verbeeck, C., Q. Deng, M. Dejesus-Hernandez, G. Taylor, C. Ceballos-Diaz, J. Kocerha, T. Golde, P. Das, R. Rademakers, D. W. Dickson and T. Kukar (2012). "Expression of Fused in sarcoma mutations in mice recapitulates the neuropathology of FUS proteinopathies and provides insight into disease pathogenesis." Mol Neurodegener 7: 53.

Vernier, M., V. Bourdeau, M. F. Gaumont-Leclerc, O. Moiseeva, V. Begin, F. Saad, A. M. Mes-Masson and G. Ferbeyre (2011). "Regulation of E2Fs and senescence by PML nuclear bodies." Genes Dev 25(1): 41-50.

von Mikecz, A. (2006). "The nuclear ubiquitin-proteasome system." J Cell Sci 119(Pt 10): 1977-1984.

Vyas, R., R. Kumar, F. Clermont, A. Helfricht, P. Kalev, P. Sotiropoulou, I. A. Hendriks, E. Radaelli, T. Hochepied, C. Blanpain, A. Sablina, H. van Attikum, J. V. Olsen, A. G. Jochemsen, A. C. Vertegaal and J. C. Marine (2013). "RNF4 is required for DNA double-strand break repair in vivo." Cell Death Differ 20(3): 490-502.

Wang, I. F., L. S. Wu and C. K. Shen (2008). "TDP-43: an emerging new player in neurodegenerative diseases." Trends Mol Med 14(11): 479-485.

Wang, T., X. Jiang, G. Chen and J. Xu (2015). "Interaction of amyotrophic lateral sclerosis/frontotemporal lobar degeneration-associated fused-in-sarcoma with proteins involved in metabolic and protein degradation pathways." Neurobiol Aging 36(1): 527-535.

Wang, W. Y., L. Pan, S. C. Su, E. J. Quinn, M. Sasaki, J. C. Jimenez, I. R. Mackenzie, E. J. Huang and L. H. Tsai (2013). "Interaction of FUS and HDAC1 regulates DNA damage response and repair in neurons." Nat Neurosci 16(10): 1383-1391.

Wang, X., S. Arai, X. Song, D. Reichart, K. Du, G. Pascual, P. Tempst, M. G. Rosenfeld, C. K. Glass and R. Kurokawa (2008). "Induced ncRNAs allosterically modify RNA-binding proteins in cis to inhibit transcription." Nature 454(7200): 126-130.

Wang, X., H. Fan, Z. Ying, B. Li, H. Wang and G. Wang (2010). "Degradation of TDP-43 and its pathogenic form by autophagy and the ubiquitin-proteasome system." Neurosci Lett 469(1): 112-116.

Wegorzewska, I., S. Bell, N. J. Cairns, T. M. Miller and R. H. Baloh (2009). "TDP-43 mutant transgenic mice develop features of ALS and frontotemporal lobar degeneration." Proc Natl Acad Sci U S A 106(44): 18809-18814.

Wolozin, B. (2012). "Regulated protein aggregation: stress granules and neurodegeneration." Mol Neurodegener 7: 56.

Woulfe, J. (2008). "Nuclear bodies in neurodegenerative disease." Biochim Biophys Acta 1783(11): 2195-2206.

Woulfe, J. M. (2007). "Abnormalities of the nucleus and nuclear inclusions in neurodegenerative disease: a work in progress." Neuropathol Appl Neurobiol 33(1): 2-42.

Wu, C. H., C. Fallini, N. Ticozzi, P. J. Keagle, P. C. Sapp, K. Piotrowska, P. Lowe, M. Koppers, D. McKenna-Yasek, D. M. Baron, J. E. Kost, P. Gonzalez-Perez, A. D. Fox, J. Adams, F. Taroni, C. Tiloca, A. L. Leclerc, S. C. Chafe, D. Mangroo, M. J. Moore, J. A. Zitzewitz, Z. S. Xu, L. H. van den Berg, J. D. Glass, G. Siciliano, E. T. Cirulli, D. B. Goldstein, F. Salachas, V. Meininger, W. Rossoll, A. Ratti, C. Gellera, D. A. Bosco, G. J. Bassell, V. Silani, V. E. Drory, R. H. Brown, Jr. and J. E. Landers (2012). "Mutations in the profilin 1 gene cause familial amyotrophic lateral sclerosis." Nature 488(7412): 499-503.

Xia, R., Y. Liu, L. Yang, J. Gal, H. Zhu and J. Jia (2012). "Motor neuron apoptosis and neuromuscular junction perturbation are prominent features in a Drosophila model of Fus-mediated ALS." Mol Neurodegener 7: 10.

Xu, Z. X., A. Timanova-Atanasova, R. X. Zhao and K. S. Chang (2003). "PML colocalizes with and stabilizes the DNA damage response protein TopBP1." Mol Cell Biol 23(12): 4247-4256.

Yamazaki, T., S. Chen, Y. Yu, B. Yan, T. C. Haertlein, M. A. Carrasco, J. C. Tapia, B. Zhai, R. Das, M. Lalancette-Hebert, A. Sharma, S. Chandran, G. Sullivan, A. L. Nishimura, C. E. Shaw, S. P. Gygi, N. A. Shneider, T. Maniatis and R. Reed (2012). "FUS-SMN protein interactions link the motor neuron diseases ALS and SMA." Cell Rep 2(4): 799-806.

Yang, S., K. Y. Zhang, R. Kariawasam, M. Bax, J. A. Fifita, L. Ooi, J. J. Yerbury, G. A. Nicholson and I. P. Blair (2015). "Evaluation of Skin Fibroblasts from Amyotrophic Lateral Sclerosis Patients for the Rapid Study of Pathological Features." Neurotox Res 28(2): 138-146.

Yang, X., R. Khosravi-Far, H. Y. Chang and D. Baltimore (1997). "Daxx, a novel Fas-binding protein that activates JNK and apoptosis." Cell 89(7): 1067-1076.

Yin, Y., A. Seifert, J. S. Chua, J. F. Maure, F. Golebiowski and R. T. Hay (2012). "SUMO-targeted ubiquitin E3 ligase RNF4 is required for the response of human cells to DNA damage." Genes Dev 26(11): 1196-1208.

Yoshida, I., A. Monji, K. Tashiro, K. Nakamura, R. Inoue and S. Kanba (2006). "Depletion of intracellular Ca2+ store itself may be a major factor in thapsigargin-induced ER stress and apoptosis in PC12 cells." Neurochem Int 48(8): 696-702.

Yu, Y., B. Chi, W. Xia, J. Gangopadhyay, T. Yamazaki, M. E. Winkelbauer-Hurt, S. Yin, Y. Eliasse, E. Adams, C. E. Shaw and R. Reed (2015). "U1 snRNP is mislocalized in ALS patient fibroblasts bearing NLS mutations in FUS and is required for motor neuron outgrowth in zebrafish." Nucleic Acids Res 43(6): 3208-3218.

Yu, Y. and R. Reed (2015). "FUS functions in coupling transcription to splicing by mediating an interaction between RNAP II and U1 snRNP." Proc Natl Acad Sci U S A 112(28): 8608-8613.

Zakaryan, R. P. and H. Gehring (2006). "Identification and characterization of the nuclear localization/retention signal in the EWS proto-oncoprotein." J Mol Biol 363(1): 27-38.

Zhang, K. Y., S. Yang, S. T. Warraich and I. P. Blair (2014). "Ubiquilin 2: a component of the ubiquitin-proteasome system with an emerging role in neurodegeneration." Int J Biochem Cell Biol 50: 123-126.

Zhong, S., S. Muller, S. Ronchetti, P. S. Freemont, A. Dejean and P. P. Pandolfi (2000). "Role of SUMO-1-modified PML in nuclear body formation." Blood 95(9): 2748-2752.

Zhong, S., P. Salomoni, S. Ronchetti, A. Guo, D. Ruggero and P. P. Pandolfi (2000). "Promyelocytic leukemia protein (PML) and Daxx participate in a novel nuclear pathway for apoptosis." J Exp Med 191(4): 631-640.

Zimber, A., Q. D. Nguyen and C. Gespach (2004). "Nuclear bodies and compartments: functional roles and cellular signalling in health and disease." Cell Signal 16(10): 1085-1104.

Zinszner, H., R. Albalat and D. Ron (1994). "A novel effector domain from the RNA-binding protein TLS or EWS is required for oncogenic transformation by CHOP." Genes Dev 8(21): 2513-2526.

Zinszner, H., J. Sok, D. Immanuel, Y. Yin and D. Ron (1997). "TLS (FUS) binds RNA in vivo and engages in nucleo-cytoplasmic shuttling." J Cell Sci 110 (Pt 15): 1741-1750.